

General Disclaimer

One or more of the Following Statements may affect this Document

- This document has been reproduced from the best copy furnished by the organizational source. It is being released in the interest of making available as much information as possible.
- This document may contain data, which exceeds the sheet parameters. It was furnished in this condition by the organizational source and is the best copy available.
- This document may contain tone-on-tone or color graphs, charts and/or pictures, which have been reproduced in black and white.
- This document is paginated as submitted by the original source.
- Portions of this document are not fully legible due to the historical nature of some of the material. However, it is the best reproduction available from the original submission.

20987-TR2

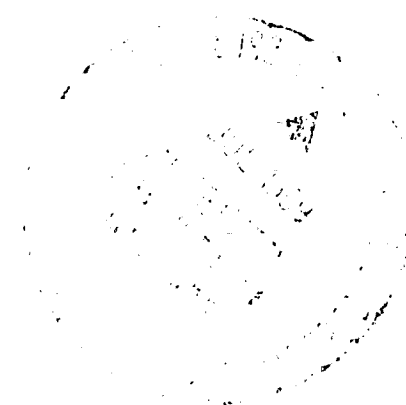
COMPUTER RECOMMENDATIONS FOR AN AUTOMATIC APPROACH AND LANDING SYSTEM FOR V/STOL AIRCRAFT

VOLUME II: EQUATIONS

By Harry T. Gaines, Robert J. Kell, Avery A. Morgan,
Leo J. Mueller, James R. Peterson, Edward R. Rang,
J. Patrick Redmond and E. David Skelley

June 1968

Distribution of this report is provided in the interest of information exchange and should not be construed as endorsement by NASA of the material presented. Responsibility for the contents resides in the organization that prepared it.



Prepared under Contract No. NAS 12-615 by
HONEYWELL INC.
Aerospace and Defense Group
Minneapolis, Minnesota and St. Petersburg, Florida

Electronics Research Center

NATIONAL AERONAUTICS AND SPACE ADMINISTRATION

FACILITY FORM 902	<u>N 69 - 3 0 9 8 5</u>	_____
	<small>(ACCESSION NUMBER)</small>	<small>(THRU)</small>
	<u>166</u>	_____
	<small>(PAGES)</small>	<small>(CODE)</small>
	<u>CR-86174</u>	<u>02</u>
	<small>(NASA CR OR TMX OR AD NUMBER)</small>	<small>(CATEGORY)</small>

FOREWORD

This computer recommendation report is submitted in accordance with Contract NAS 12-615 with the NASA Electronics Research Center (ERC), Cambridge, Massachusetts. Specifically, this report is intended to satisfy item 7C2 of Phase II, Part II of the contract statement of work.

This report is published in two volumes:

Volume I - Computer Recommendations

Volume II - Equations

Volume I contains an analysis of candidate computers for use in the Automatic Approach and Landing System (AALS) plus a recommendation of suitable computers. This volume defines a baseline AALS which is representative, in terms of complexity, of systems appropriate to the NASA-ERC flight evaluation program. Review and agreement on these equations was accomplished at NASA-ERC during a technical coordination meeting on 23, 24 May 1968.

CONTENTS

	Page
SUMMARY	1
SYSTEM DESIGN AND FUNCTIONAL REQUIREMENTS	3
NAVIGATION	10
1. Accelerometer Bias and Scale Factor Computation	10
2. Accelerometer Bias and Scale Factor Compensation	11
3. Accelerometer Cross-Axis Compensation	11
4. Accelerometer Nonlinearity Compensation	12
5. Angular Environmental Compensation	12
6. Accelerometer-to-Body Axis Transformation	13
7. Angular Increment, Rate and Acceleration Computation	14
8. Gyro Drift Computation	15
9. Gyro Drift Compensation	16
10. Gyro-to-Body Axis Transformation	16
11. Attitude Matrix Algorithm	17
12. Attitude Matrix Orthonormalization	18
13. Velocity Increment Resolution	20
14. Inertial Position, Velocity Computation	21
15. Gravity Computations	22
16. Geographic Computer	23
17. Euler Angle Computation	25
18. Preflight Attitude Alignment	26
19. Guidance Input Calculations	29
Description of Variables for Radar Input	31
UPDATE	33
Radar Position Calculation	33
Loran C Computation	36
Loran C Computation Definitions	39
GUIDANCE	41
Requirements	41
Approach Pattern	41
First Checkpoint	45
Time to Bank	46
Off-Course Displacement	48
Straight-In Approach	49
Vertical Control	50
Altitude Select	50
Speed Control	51
Final Approach	51
Flare	54
Go-Around	55
Block Diagrams	56

CONTENTS (Continued)

	Page
FLIGHT CONTROL	59
Scope	59
System Description	59
Difference Equations	64
Sampling Frequency	65
Bit Weight	65
Alternate Inner-Loop Stabilization	66
Filters	66
Plant Dynamics	66
Optimal Control	67
Conclusions	67
DISPLAYS	68
Design Considerations	68
Display Formats	70
Candidate Parameters	70
"Eight-Ball" Display	74
Baseline System	76
DOWN LINK	77
APPENDIX A - ANALOG RATE GYRO RECOMMENDATION	79
APPENDIX B - NAVIGATION UPDATE INTERFACES	81
APPENDIX C - BASELINE AALS AUTOMATIC FLIGHT CONTROL SYSTEM EQUATIONS	89
APPENDIX D - QUADRATIC OPTIMAL CONTROL FOR THE NASA LRC YHC-1A HELICOPTER	131
APPENDIX E - BASELINE DISPLAY EQUATIONS	145
APPENDIX F - DOWN LINK DESCRIPTION	155
APPENDIX G - NEW TECHNOLOGY	159
REFERENCES	161

ILLUSTRATIONS

Figure		Page
1	Baseline Automatic Approach and Landing System Functions	4
2	Automatic Approach and Landing System Simplified Signal Flow Diagram	7
3	Rectangular Approach Pattern	43
4	Straight-in Approach Pattern	49
5	Final Approach Flight Profile	52
6	Typical Performance Chart	56
7	Heading	56
8	Altitude Control	57
9	Airspeed Control	57
10	Glide Path	58
11	Flare	58
12	AFCS Pitch Axis - Hover	60
13	AFCS Pitch Axis - 100 Knots	61
14	Input/Output, Attitude Rate Damper, and Attitude/Heading/Altitude Hold Modes	62
15	Input/Output Velocity Command Modes	63
16	Example Quickened PPI Format	71
17	Example Predictor PPI Format	72

COMPUTER RECOMMENDATIONS FOR AN
AUTOMATIC APPROACH AND LANDING
SYSTEM FOR V/STOL AIRCRAFT

VOLUME II: EQUATIONS

By Harry T. Gaines, Robert J. Kell,
Avery A. Morgan, Leo J. Mueller,
James R. Peterson, Edward R. Rang,
J. Patrick Redmond and E. David Skelley

SUMMARY

A preliminary automatic approach and landing system (AALS) definition has been completed. It is considered to be a configuration typical of that which would be suitable for V/STOL use. It is designed specifically for the designated flight test vehicle, the NASA/LRC YHC-1A helicopter, and is intended to have sufficient flexibility to evaluate a variety of technology concepts.

Design details and requirements are discussed. Included are functional and mode requirements for navigation, guidance, control, and displays, and an evaluation of analog attitude rate gyros for an alternate analog inner-loop stabilization mechanization.

Results given are in terms of applicable equation and computation requirements for each subsystem. Navigation computations are based on the use of a strap-down inertial reference unit.

Attitude rate output from the single-axis gyros is in the form of pulse-rate; accelerometer output is frequency modulated. Position update methods are included. Linear control laws are used to obtain automatic control equations. Tustin's method is used to obtain the difference equations to be used in programming the digital computer. Several levels of operation or modes are defined, including both attitude control and velocity command control.

Guidance requirements are established and guidance laws are defined for the generalized V/STOL approach situation. Numerical values selected for each of the various parameters are based on the designated flight test vehicle. Guidance equations include the derivation of velocity commands. The baseline guidance subsystem is discussed relative to optimum path control.

Display requirements suitable to the baseline AALS also are defined. Display needs for both manual and automatic control are included. Display equations defined are suitable to a CRT-type display mechanization. (Display generation such as symbols, etc., was not part of the task.)

A "down link" (or telemetry system) is considered as part of the instrumentation. The discussion included herein is based entirely on information supplied by NASA/ERC.

Conclusions and recommendations are made as part of each subsystem discussion. All are pertinent to continued AALS development. Particular emphasis is placed on areas where simplifications might be made.

SYSTEM DESIGN AND FUNCTIONAL REQUIREMENTS

As treated herein, the V/STOL automatic approach and landing system includes the functions of:

- Navigation: Determination of aircraft position
- Guidance: Computation of desired path to destination
- Control: Closed-loop automatic flight control modes
- Display: Generation of typical AALS display functions

Functional requirements are limited to those specifically applicable to the automatic approach and landing problem. Specific constraints on the design and mechanization are:

- Designed for the YHC-1A helicopter
- Use of strapped-down sensors for navigation
- Use of strapped-down gyros for stability augmentation
- Use of available air data sensors
- Use of existing electrical input servo system
- Use of existing electric stick installation
- Use of GSN-5 and Loran-C to update navigation subsystem
- Use of display functions suitable to CRT-type display
- Use of an all-digital mechanization
- Inclusion of an alternate analog inner-loop stabilization system.

To obtain a system definition adequate for computer sizing purposes, a specific baseline system design was established. Figure 1 is a functional block diagram of the baseline system. Inputs are provided by the navigational up-link receiver, strapped-down sensors, air data and radar sensors, electric stick, rate gyros, and a pilot's stick control panel (PSCP). Outputs from the system will be navigation and system control information on the PSCP, guidance information and aircraft flight data to the display mechanization, and automatic flight control commands. Table 1 summarizes system input/output signals.

Computation for navigation, guidance, control, and displays will be performed in the central digital computer. Mechanization and signal flow is shown in a simplified manner in Figure 2.

Additional mechanization needs are included in Figure 2. A radar altimeter (sensor block) is required for guidance. Both on-board and telemetry instrumentation are needed for flight test. An analog attitude rate gyro and

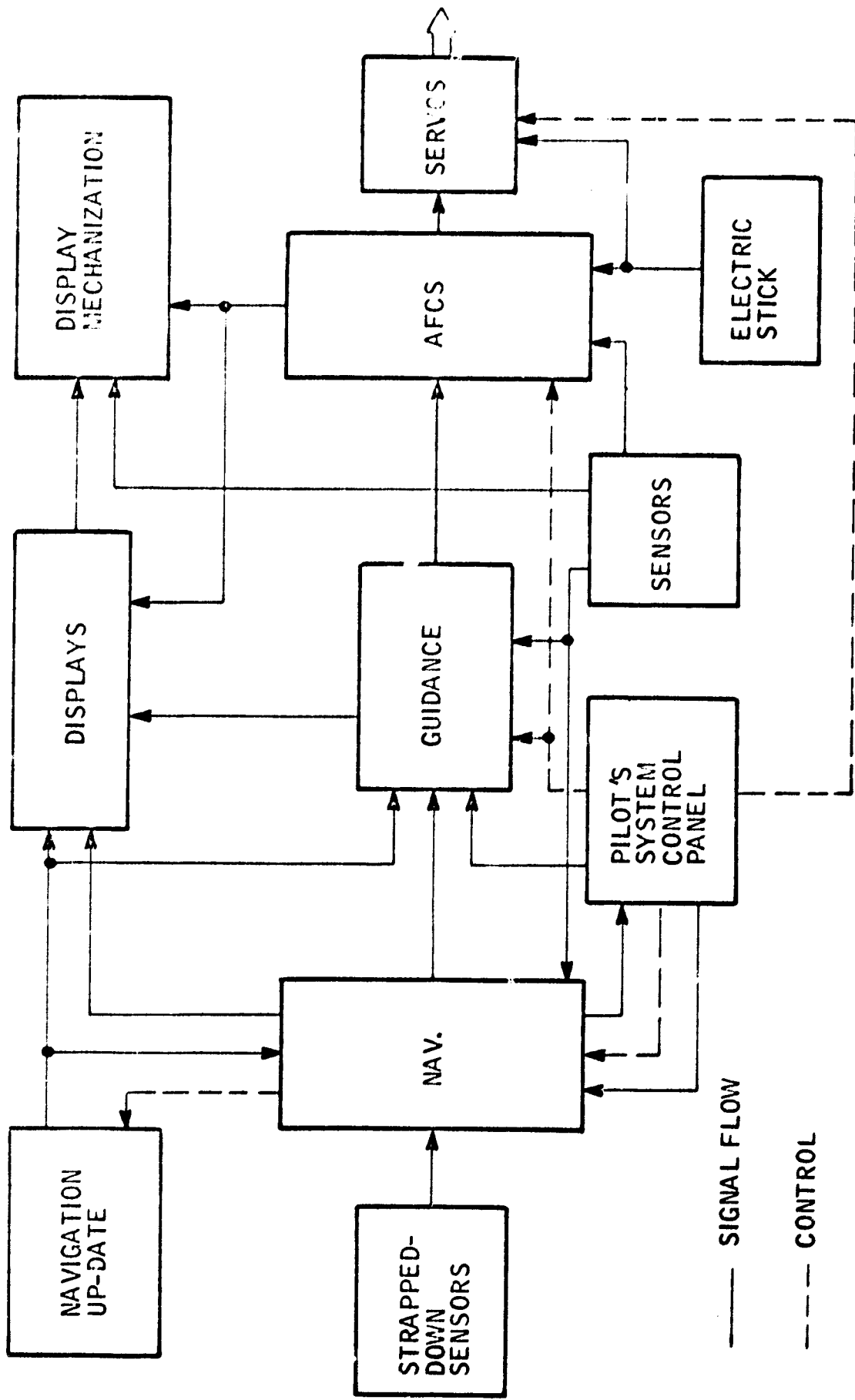


Figure 1. Baseline Automatic Approach and Landing System Functions

TABLE I
AUTOMATIC APPROACH AND LANDING SYSTEM
INPUT/OUTPUT SIGNAL DESCRIPTION

Term	In/Out	Description	Units	Accuracy	Range	Resolution	Sample rate per second	Min. num dynamic range	Type	Used by/Source
H_1	O	Bearing to specified location	deg		160 con't	0.1	16	1800	digital (D/A)	guidance
F_G	I	Pilot selected glide angle	deg	0.05	0 to 20	0.01	NA	2000	BCD code wheels	guidance
CSN 5 cont	O	Clock pulses to digital command system	---	---	---	---	---	---	(20) 10 pulse pulses	navigation
Δh	O	Altitude command error	ft		±200	0.5	8	400	digital (D/A)	displays
h_H	I	Barometric altitude	ft	1	1000 to 15000	10R/15	8	18000	analog (A/D)	sensor
h_{Co}	I	Command altitude	ft			1	NA	18000	BCD code wheels	PSCP
$h_{\dot{h}}$	O	Altitude rate command	ft/sec		±80	0.1	16	1200	digital	displays
h_P	I	Pilot selected hover altitude	ft		-1000, +10000	1	NA	11000	BCD code wheels	PSCP
h_{HYH}	O	Altitude from altitude sensing system	ft		-1000 to 15000	0.1	32	18000	digital (D/A)	pitch autopilot
h_{HYH}	O	Altitude rate from altitude sensing system	ft/sec		+80, -100	0.1	32	1800	digital (D/A)	pitch autopilot
h_{NAV}	O	Altitude above sea level	ft	10/1.0	-1000 to 18000	1	32	18000	digital	navigation
h_{NAV_o}	I	Pilot setting of initial altitude	ft		↓	↓	NA	↓	BCD code wheels	navigation
$h_{NAV_{cp}}$	I	Pilot setting of checkpoint altitude	ft		↓	↓	↓	↓	BCD code wheels	navigation
h_{NAV_L}	I	Pilot setting of landing site altitude	ft		↓	↓	↓	↓	BCD code wheels	navigation
h_R	I	Radar altimeter altitude	ft		-20 to +200	0.5	32	440	analog	sensor
$h_{\dot{R}}$	O	Radar altimeter altitude rate	ft/sec		±80	0.1	32	1200	analog	sensor
L_g	O	Longitude	deg		2	0.1 sec	64	10000	digital	navigation
L_{g_o}	I	Pilot setting of initial longitude	deg		↓	↓	NA	↓	BCD code wheels	navigation
$L_{g_{cp}}$	I	Pilot setting of checkpoint longitude	deg		↓	↓	NA	↓	BCD code wheels	navigation
L_{g_L}	I	Pilot setting of landing site longitude	deg		↓	↓	↓	↓	BCD code wheels	navigation
L_l	O	Latitude	deg		↓	↓	64	↓	digital	navigation
L_{l_o}	I	Pilot setting of initial latitude	deg		↓	↓	NA	↓	BCD code wheels	navigation
$L_{l_{cp}}$	I	Pilot setting of checkpoint latitude	deg		↓	↓	NA	↓	BCD code wheels	navigation
L_{l_L}	I	Pilot setting of landing site latitude	deg		↓	↓	NA	↓	BCD code wheels	navigation
Mode logic	I	From pilot's system control panel (PSCP)	---	---	↓	↓	---	---	18 diodes	PSCP
R_{Co}	O	Range to turn	ft	±10	0 to 12000	5	8	24000	digital (D/A)	guidance
ΔR_H	O	Horizontal range	ft	±10	0 to 12000	5	8	24000	digital (D/A)	guidance
t	I	Time	sec	0.01	---	0.01	each update	---	digital	navigation
t_{Co}	O	Time to turn	sec	0.1	0 to 2000	0.1	16	20000	digital (D/A)	guidance
u	I	Sum of incremental changes in x-axis velocity	ft/sec		-100, +300	0.1	1024	4000	digital ctr	navigation
\bar{u}_{AP}	I	Pilot setting of airspeed command	ft/sec		↓	0.1	NA	4000	digital (D/A)	PSCP
\bar{u}_D	O	Forward velocity command	ft/sec		↓	0.1	8	4000	digital (D/A)	displays
v	I	Sum of incremental changes in y-axis velocity	ft/sec		±100	0.1	1024	2000	digital ctr	navigation
v_G	O	Ground speed	ft/sec	1	0 to 300	0.1	8	3000	digital (D/A)	navigation

TABLE I
AUTOMATIC APPROACH AND LANDING SYSTEM
INPUT/OUTPUT SIGNAL DESCRIPTION (CONCLUDED)

Term	In/out	Description	Units	Accuracy	Range	Resolution	Sample rate per second	Minimum dynamic range	Type	Used by/source			
V _{IAS}	I	Indicated air speed	ft/sec		0 to 300	0.1	32	3000	analog (A/D)	pitch autopilot			
V _w	O	Local wind speed	ft/sec		0 to 100	0.2	8	500	digital (D/A)	displays			
w	I	Sum of incremental changes in z-axis velocity	ft/sec		+60, -100	0.1	1024	1600	digital ctr.	navigation			
X	I	Update downrange distance to landing point	ft	10/2%	12000 to 160000	10	8	15000	digital	navigation			
X _Q	O	Predicted downrange position	ft	10/1%	0 to 12000	1					16	12000	digital (D/A)
Y	I	Update cross-range distance to landing point	ft	10/2%	±12000 to ±15000	2	8	15000	digital	navigation			
Y _Q	O	Predicted cross-range position	ft	10/1%	0 to ±12000	1					16	24000	digital (D/A)
Y _D	O	Lateral velocity command	ft/sec		±100	0.1	16	1000	digital (D/A)	displays			
Z	I	Update altitude above landing point	ft	1	0 to 7500	1	8	7500	digital	navigation			
V _y	I	Ground wind speed	ft/sec		0 to 100	0.2	NA	500	digital	navigation			
β	I	Vehicle sideslip angle	deg		±50	0.1	32	500	analog (A/D)	pitch autopilot			
γ _w	I	Ground wind direction	deg		360 con't.	0.1	NA	3600	digital	navigation			
γ	I	Desired landing approach angle w. r. t. true north	deg	1	360 con't	0.1	NA	3600	digital	navigation			
θ _{cp}	I	Pilot-selected checkpoint bearing	deg		360 con't	0.1	NA	3600	BCD code wheels	PSCP			
δ _{L/C}	O	Total longitudinal differential collective	in.		2.6	0.0007	32	4000	digital (D/A)	pitch autopilot			
δ _{HC}	O	Cyclic yaw command	in.		2	0.0005	32	4000	digital (D/A)	lateral autopilot			
δ _{RC}	O	Cyclic roll command	in.		3	0.0008							
ε _{COL}	I	Electric collective stick	in.		13.8	0.014					1000	analog (A/D)	collective autopilot
ε _L	I	Electric stick input--pitch	in.		±6.1	0.012					1000	analog (A/D)	pitch autopilot
ε _R	I	Electric pedal input--yaw	in.		±2.6	0.005	1000	analog (A/D)	lateral autopilot				
ε _S	I	Electric stick input--roll	in.		±6.7	0.013	32	1000	analog (A/D)	lateral autopilot			
θ	I	Sum of incremental changes in pitch	deg		±46 $\overline{\text{sec}}$	12 $\overline{\text{sec}}$	1024	8	digital ctr.	navigation			
θ	O	Vehicle elevation angle w. r. t. local horizontal	deg	0.5	±35	0.06	32	1170	digital (D/A)	navigation			
θ _{COLc}	O	Collective command	in.		3.3	0.0009	32	4000	digital (D/A)	collective autopilot			
φ	I	Sum of incremental changes in roll	deg		±47 $\overline{\text{sec}}$	12 $\overline{\text{sec}}$	1024	8	digital ctr.	navigation			
φ	O	Vehicle roll angle	deg	0.5	±50	0.06	32	1670	digital (D/A)	navigation			
ψ	I	Sum of incremental changes in yaw	deg		±46 $\overline{\text{sec}}$	12 $\overline{\text{sec}}$	1024	8	digital ctr.	navigation			
ψ	O	Vehicle heading w. r. t. true north	deg	1	360 con't	0.1	16	3600	digital	navigation			
ε _ψ	O	Checkpoint heading error	deg		20	0.01	16	2000	digital	guidance			
ψ _c	I	Pilot-selected heading	deg		360 con't	0.1	NA	3600	BCD code wheels	PSCP			
ψ _D	O	Heading command	deg		360 con't	0.1	8	3600	digital (D/A)	displays			
Mode logic	I	Stick force switches	---	---	---	---	---	---	8 discretes	electric stick			
Mode logic	I	Beep trim	---	---	---	---	---	---	4 discretes	electric stick			

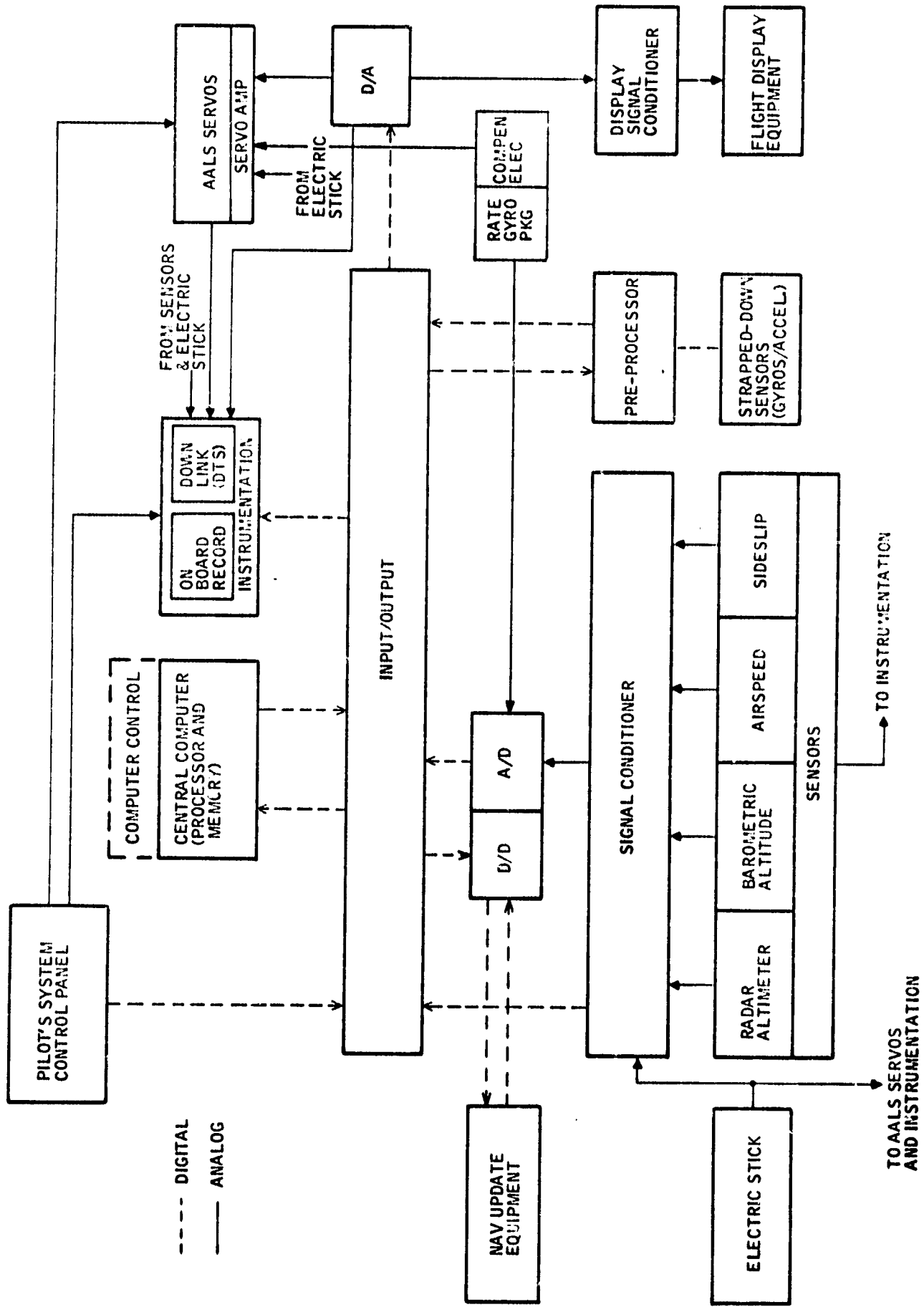


Figure 2. Automatic Approach and Landing System Simplified Signal Flow Diagram

analog compensation is included for the alternate inner-loop stabilization mechanization. (Appendix A contains an analog rate gyro recommendation.) Since both the strapped-down gyros and accelerometers output a pulse rate signal form, a method of converting to a whole word digital format is needed; this is labeled a "preprocessor". A "signal conditioner" is included to provide electrical signal matching between system input (sensor output, etc.) and computer subsystem input.

Complete in-flight control is provided by the PSCP. The baseline system definition includes the following functions in the panel:

- Navigation
 - Alignment start
 - Navigation engaged
 - Automatic update on/off
 - Initial position input (latitude, longitude, altitude)
 - Manual update input (latitude, longitude, altitude)
 - Automatic update (GSN-5/Loran-C)
 - Landing location input (latitude, longitude, altitude)
 - Readout of current position or any input
- Guidance
 - Guidance mode selection
 - Input of pilot selectable quantities
 - Readout of selected input
- Control
 - Electric stick on/off
 - Stability augmentation on/off
 - Attitude hold engage
 - Velocity command engage
 - Automatic guidance engage
 - Mode status
- System Status
 - Power on
 - Instrumentation
 - On-board on
 - Telemetry on
 - Computer ready
 - Servos aligned

Baseline panel functions are defined as a result of subsystem requirements (input, control, and status indication).

Because of the need for safety-of-flight assurance, system design is based on use of a safety pilot. The YHC-1A is normally dual-control. The right side has an electric stick installed for AALS evaluation pilot use. Normal controls exist on the left side for use by the safety pilot. Whenever the electric stick is activated (or automatic control modes are engaged), the left hand stick will follow all control motions. The safety pilot will be able to use the motion of his stick as a primary indication of safe automatic control system performance. Emergency electric stick and automatic control disengagement is provided to both pilots with switches mounted on each stick. Electric stick status (on/off) presented to the safety pilot will help provide control coordination between the pilots.

Baseline AALS requirements are given as part of each subsystem discussion in the sections that follow. Prior to further development, firm system requirements should be established in terms of both performance and mechanization.

Ground support concepts and equipment requirements also must be established to assure a compatible system mechanization.

NAVIGATION

This section describes inertial navigation equations. Navigation simply means maintaining a knowledge of vehicle position, velocity, and attitude based on the output of the inertial sensors, accelerometers and gyros, and altimeter. These equations were adapted largely from material supplied by NASA-ERC. Although useful to the baseline definition, considerable simplification can probably be made for flight test use.

The navigation equations are divided into 19 computation sections. Each section describes the equations and the frequency and precision with which they should be evaluated, and lists explanatory and critical remarks where appropriate. An attempt is made to keep the notation consistent with the material supplied by NASA-ERC, insofar as possible.

The calculations described by these equations begin (logically) after introduction into the computer of all initial conditions, constants, inertial sensor pulse counts, and the altimeter output. They carry the calculations through the point of computing the values of the position, velocity, and attitude variables.

1. Accelerometer Bias and Scale Factor Computation

$$K_{0i} = K_{0i} + \Delta K_{0i} \Delta t$$

$$K_{1i} = K_{1i} + \Delta K_{1i} \Delta t$$

Input: K_{0i} = accelerometer bias

K_{1i} = accelerometer scale factor

Constants: $\Delta K_{0i} = \left(DR_{K_0} \right)_i$ bias rate (constant)

$\Delta K_{1i} = \left(DR_{\Delta K_i / K_1} \right)_i$ scale factor rate (constant)

Output: K_{0i} = accelerometer bias

K_{1i} = accelerometer scale factor

Frequency: Very slow; Δt could be as large as several seconds

Precision: 20-bit accuracy

2. Accelerometer Bias and Scale Factor Compensation

$$C'_{0i} = C_{0i}/K_{1i} - K_{0i}$$

where $i = 1, 2, 3$.

Input: C_{0i} $i = 1, 2, 3$ = uncompensated acceleration
 K_{0i} $i = 1, 2, 3$ = bias (from 1)
 K_{1i} $i = 1, 2, 3$ = scale factor (from 1)

Output: C'_{0i} $i = 1, 2, 3$ = compensated acceleration

Frequency: 128 times per second

Precision: 20-bit accuracy

3. Accelerometer Cross-Axis Compensation

$$Q_1 = C'_{01} - K_{41} C'_{02} - K_{61} C'_{03}$$

$$Q_2 = -K_{62} C'_{01} + C'_{02} - K_{42} C'_{03}$$

$$Q_3 = -K_{43} C'_{01} - K_{63} C'_{02} + C'_{03}$$

Input: C'_{0i} $i=1, 2, 3$ = uncompensated acceleration (from 2)

Constants: K_{4i}, K_{6i} = cross-axis compensation constants

Output: Q_i $i=1, 2, 3$ = compensated acceleration

Frequency: 128 times per second

Precision: 20-bit accuracy. Since the K's are small, single-precision products should suffice.

4. Accelerometer Nonlinearity Compensation

$$\Delta v_i = Q_i [1 - Q_i (K_{2i} + Q_i K'_{3i})] \Delta t_c$$

where $i = 1, 2, 3$.

Input: Q_i $i=1, 2, 3$ = uncompensated acceleration (from 3)
 Constants: K_{2i} $i=1, 2, 3$ = nonlinear compensation constants
 $K'_{3i} = K_{3i} - 2K_{2i}^2$ = nonlinear compensation constants
 Output: Δv_i = incremental velocity (accelerometer axis components)

Frequency: 128 times per second

Precision: 20 bits. Since both constants are small, single-precision products should suffice.

5. Angular Environmental Compensation

$$\Delta v_{c1} = \Delta v_1 - [\Delta \hat{\theta}_1 \Delta \hat{\theta}_2 p_2 - (\Delta \hat{\theta}_2^2 + \Delta \hat{\theta}_2^2) p_1 - \Delta \hat{\theta}_1 \Delta \hat{\theta}_2 p_3] / \Delta t + \Delta \omega_2 p_3 + \Delta \omega_3 p_2$$

$$\Delta v_{c2} = \Delta v_2 - [\Delta \hat{\theta}_3 \Delta \hat{\theta}_2 p_3 + \Delta \hat{\theta}_1 \Delta \hat{\theta}_2 p_1 - (\Delta \hat{\theta}_3^2 + \Delta \hat{\theta}_1^2) p_2] / \Delta t + \Delta \omega_3 p_1 + \Delta \omega_1 p_3$$

$$\Delta v_{c3} = \Delta v_3 - [\Delta \hat{\theta}_1 \Delta \hat{\theta}_3 p_1 + \Delta \hat{\theta}_2 \Delta \hat{\theta}_3 p_2 - (\Delta \hat{\theta}_1^2 + \Delta \hat{\theta}_2^2) p_3] / \Delta t - \Delta \omega_1 p_2 + \Delta \omega_2 p_1$$

Input: Δv_i $i=1, 2, 3$ = uncompensated velocity increment (from 4)
 $\Delta \hat{\theta}_i$ $i=1, 2, 3$ = angular increment (from 7)
 $\Delta \omega_i$ $i=1, 2, 3$ = angular velocity increment (from 7)
 Constants: p_i $i=1, 2, 3$ = accelerometer offset constants
 Output: Δv_{ci} $i=1, 2, 3$ = compensated velocity increments

Frequency: 128 times per second

Precision: 20 bits. Since compensation will be small, single-precision products should suffice.

Remarks: These are the equations supplied by ERC. If all three accelerometers are assumed offset from the vehicle-fixed reference point, then nine constants should be used; p_1, p_2, p_3 of the first equation describing the location of the first accelerometer; p_1, p_2, p_3 of the second equation describing the location of the second accelerometer; p_1, p_2, p_3 of the third equation describing the location of the third accelerometer. Since selection of the reference point is entirely arbitrary, one of the equations can be completely eliminated by choosing it to be the c. g. of the sensitive element of one of the accelerometers. Depending on the relative location of the accelerometers in the block and the orientation of the block relative to the body axes, up to four of the remaining six constants may be eliminated by judicious choice.

6. Accelerometer-to-Body Axis Transformation

$$\underline{\Delta v_c^A} = \begin{bmatrix} \Delta v_{c1} \\ \Delta v_{c2} \\ \Delta v_{c3} \end{bmatrix} = \text{velocity increment in accelerometer axes (from 5)}$$

$$\text{Constants: } T^{BA} = T^{BM_A} T^{M_A A_M} = \text{accelerometer-to-body axis transformation matrix}$$

$$\underline{\Delta v_c^B} = \begin{bmatrix} \Delta v_{c1}^B \\ \Delta v_{c2}^B \\ \Delta v_{c3}^B \end{bmatrix} = \text{velocity increment in body axes}$$

Frequency: 128 times per second

Precision: 20 bits

Remarks: Assuming the accelerometer axes to be nominally aligned with the body axes, equations of the form of section 3 may be used. In point of fact, these calculations could be accomplished in section 3 by suitably redefining the constants used there and this section completely eliminated.

7. Angular Increment, Rate and Acceleration Computation

$$\Delta \hat{\theta}_i = \sum_{k=1}^8 (\Delta \theta_i)_k$$

$$\omega_i(t) = \sum_{k=1}^8 W_{1k} (\Delta \theta_i)_k$$

$$\omega_i(t+\Delta t) = \sum_{k=1}^8 W_{2k} (\Delta \theta_i)_k$$

$$\Delta \omega_i = \omega_i(t+\Delta t) - \omega_i(t)$$

Input: $(\Delta \theta_i)_k$ $k=1, 2, \dots, 8$ = angular increment over 1/1024 sec

Constants: W_{1k}, W_{2k} , $k=1, 2, \dots, 8$ = rate filter weights (constants)

Output: $\Delta \hat{\theta}_i$ = angular increments over 1/128 sec

$\omega_i(t), \omega_i(t+\Delta t)$ = angular rate at beginning and end of 1/128-sec interval

$\Delta \omega_i$ = angular acceleration over 1/128-sec interval (times Δt)

Frequency: 128 times per second

Precision: 24 bits for ω . Only about 8 bits for $\Delta \hat{\theta}$.

Remarks: It is felt that calculation of the rates is not only unnecessary but error producing. See section 11.

8. Gyro Drift Computation

$$\begin{bmatrix} D_1 \\ D_2 \\ D_3 \end{bmatrix} = \begin{bmatrix} R_1 \\ R_2 \\ R_3 \end{bmatrix} + \begin{bmatrix} B_{11} & -B_{31} & B_{21} \\ B_{22} & B_{12} & -B_{32} \\ B_{23} & B_{33} & B_{13} \end{bmatrix} \begin{bmatrix} C'_{01} \\ C'_{02} \\ C'_{03} \end{bmatrix} + \begin{bmatrix} 0 & -M'_{31} & M'_{21} \\ M'_{22} & 0 & -M'_{32} \\ M'_{23} & M'_{33} & 0 \end{bmatrix} \begin{bmatrix} \Delta\hat{\theta}_1 \\ \Delta\hat{\theta}_2 \\ \Delta\hat{\theta}_3 \end{bmatrix} + \begin{bmatrix} J'_1 & 0 & 0 \\ 0 & J'_2 & 0 \\ 0 & 0 & J'_3 \end{bmatrix} \begin{bmatrix} \Delta\omega_1 \\ \Delta\omega_2 \\ \Delta\omega_3 \end{bmatrix} + \begin{bmatrix} C_{11} & -C_{31} & 0 \\ 0 & C_{12} & C_{32} \\ 0 & C_{33} & C_{13} \end{bmatrix} \begin{bmatrix} C'_{01}{}^2 \\ C'_{02}{}^2 \\ C'_{03}{}^2 \end{bmatrix} + \begin{bmatrix} -C_{51} & 0 & -C_{41} \\ -C_{42} & -C_{52} & 0 \\ C_{43} & 0 & C_{53} \end{bmatrix} \begin{bmatrix} C'_{02} & C'_{03} \\ C_{03} & C'_{01} \\ C_{01} & C'_{02} \end{bmatrix} + \begin{bmatrix} Q'_{11} & Q'_{31} & 0 \\ 0 & Q'_{12} & Q'_{32} \\ 0 & Q'_{33} & Q'_{11} \end{bmatrix} \begin{bmatrix} \Delta\hat{\theta}_1{}^2 \\ \Delta\hat{\theta}_2{}^2 \\ \Delta\hat{\theta}_3{}^2 \end{bmatrix} + \begin{bmatrix} 0 & 0 & -Q'_{41} \\ -Q'_{42} & 0 & 0 \\ Q'_{43} & 0 & 0 \end{bmatrix} \begin{bmatrix} \Delta\hat{\theta}_2 & \Delta\hat{\theta}_3 \\ \Delta\hat{\theta}_3 & \Delta\hat{\theta}_1 \\ \Delta\hat{\theta}_1 & \Delta\hat{\theta}_2 \end{bmatrix}$$

Input: C'_{0i} = acceleration (from 2)
 $\Delta\hat{\theta}_i$ = angular increment (from 7)
 $\Delta\omega_i$ = angular acceleration (from 7)

Constants: $B_{1i}, B_{2i}, B_{3i}, M'_{2i} = M_{2i}/\Delta t, M'_{3i} = M_{3i}/\Delta t$
 $J'_i = J_i/\Delta t, C_{1i}, C_{3i}, C_{4i}, C_{5i}, Q'_{1i} = Q_{1i}/\Delta t^2$
 $Q'_{3i} = Q_{3i}/\Delta t^2, Q'_{4i} = Q_{4i}/\Delta t^2$

Output: $D_i, i=1, 2, 3$ = gyro drift rate

Frequency: 128 times per second

Precision: 10 bits

9. Gyro Drift Compensation

$$\omega_{ci}(t) = \omega_i(t) - D_i$$

$$\omega_{ci}(t+\Delta t) = \omega_i(t+\Delta t) - D_i$$

where $i=1, 2, 3$.

Input: $\omega_i(t), \omega_i(t+\Delta t)$ = uncompensated angular velocity (from 7)

D_i = gyro drift rate (from 8)

Output: $\omega_{ci}(t)$ = compensated angular velocity

Frequency: 128 times per second

Precision: 24 bits

Remarks: It is felt that gyro drift compensation could be performed at 1/4 to 1/8 of the above frequency with no loss of accuracy. This is based only on the assumption of gross rates of no more than 60 deg/sec and vibration that causes reasonable drift rates (say 10 deg/hr). The pulse counts and their products on which the compensation is based can be accumulated over a longer period than indicated above, and the compensation can be calculated and applied at the angular level rather than the angular rate level.

10. Gyro-to-Body Axis Transformation

$$\underline{\omega}^B(t) = T^{BG} \underline{\omega}^G(t)$$

$$\underline{\omega}^B(t+\Delta t) = T^{BG} \underline{\omega}^G(t+\Delta t)$$

Input: $\underline{\omega}^G(t) = \begin{bmatrix} \omega_{c1}(t) \\ \omega_{c2}(t) \\ \omega_{c3}(t) \end{bmatrix}$ } angular velocity in gyro input axis frame

$\underline{\omega}^G(t+\Delta t) = \begin{bmatrix} \omega_{c1}(t+\Delta t) \\ \omega_{c2}(t+\Delta t) \\ \omega_{c3}(t+\Delta t) \end{bmatrix}$ }

Constants: T^{BG} = gyro axis-to-body axis transformation matrix

Output: $\underline{\omega^B(t)}$ = $\begin{bmatrix} \omega_1 \\ \omega_2 \\ \omega_3 \end{bmatrix}$ } angular velocity in body axes

$\underline{\omega^B(t+\Delta t)}$ = $\begin{bmatrix} \omega_1' \\ \omega_2' \\ \omega_3' \end{bmatrix}$ }

Precision: 24 bits

Remarks: Assuming the gyro axes are nominally aligned with the body axes, this function can be accomplished by suitably redefining the constants in the third term of the equation of section 8, and this calculation eliminated entirely.

11. Attitude Matrix Algorithm

$$\text{TEMP} = \begin{bmatrix} -\Delta t[\omega_2\omega_2' + \omega_3\omega_3'] & -(\omega_3 + \omega_3') + \Delta t\omega_2\omega_1' & (\omega_2 + \omega_2') + \Delta t\omega_3\omega_1' \\ (\omega_3 + \omega_3') + \Delta t\omega_1\omega_2' & -\Delta t[\omega_3\omega_3' + \omega_1\omega_1'] & -(\omega_1 + \omega_1') + \Delta t\omega_3\omega_2' \\ -(\omega_2 + \omega_2') + \Delta t\omega_1\omega_3' & (\omega_1 + \omega_1') + \Delta t\omega_2\omega_3' & -\Delta t[\omega_1\omega_1' + \omega_2\omega_2'] \end{bmatrix}$$

$$\text{TEMP} = \frac{1}{2} \Delta t T^{IB}(\text{TEMP})$$

$$T^{IB} = T^{IB} + \text{TEMP}$$

Input: T^{IB} = body-to-inertial transformation matrix, last value (from 11 or 12)

$\underline{\omega^B(t)}$ = $\begin{bmatrix} \omega_1 \\ \omega_2 \\ \omega_3 \end{bmatrix}$ } angular velocity at beginning and end of interval (from 10)

$\underline{\omega^B(t+\Delta t)}$ = $\begin{bmatrix} \omega_1' \\ \omega_2' \\ \omega_3' \end{bmatrix}$ }

Output: T^{IB} = body-to-inertial transformation matrix, new value

Frequency: 128 times per second

Precision: 24 bits

Remarks: It is strongly felt that basing the attitude algorithm on numerical integration of the numerically differentiated output of integrating devices (pulse rebalanced gyros) is not only unnecessarily complicated but a potential source of serious error. The basic truncation error of this algorithm is no better (and is in fact slightly worse) than that of the conventional second-order attitude algorithm described by

$$T = T + T [\Delta\Theta - 1/2 \Delta\Theta^2],$$

$$\Delta\Theta = -\Delta\Theta^T = \begin{bmatrix} 0 & -\Delta\hat{\theta}_3 & \Delta\hat{\theta}_2 \\ \cdot & 0 & -\Delta\hat{\theta}_1 \\ \cdot & \cdot & 0 \end{bmatrix}$$

This algorithm has, in addition, the inevitable error associated with differentiating quantized data by whatever method. Rate errors that are acceptable for compensation or control can easily be accumulated into attitude errors that are entirely unacceptable. The more severe the angular environment, the more serious the problem. The derivation of rates is not necessary for maintaining attitude reference and is therefore not desirable for that purpose.

12. Attitude Matrix Orthonormalization

$$\begin{bmatrix} \text{TEMP}_{11} \\ \text{TEMP}_{12} \\ \text{TEMP}_{13} \end{bmatrix} = \begin{bmatrix} T_{22}^{IB} & T_{33}^{IB} & -T_{23}^{IB} & T_{32}^{IB} \\ T_{23}^{IB} & T_{31}^{IB} & -T_{21}^{IB} & T_{33}^{IB} \\ T_{21}^{IB} & T_{32}^{IB} & -T_{22}^{IB} & T_{31}^{IB} \end{bmatrix}$$

$$\begin{bmatrix} \text{TEMP}_{21} \\ \text{TEMP}_{22} \\ \text{TEMP}_{23} \end{bmatrix} = \begin{bmatrix} T_{32}^{IB} & T_{13}^{IB} & -T_{32}^{IB} & T_{11}^{IB} \\ T_{33}^{IB} & T_{11}^{IB} & -T_{31}^{IB} & T_{13}^{IB} \\ T_{31}^{IB} & T_{12}^{IB} & -T_{32}^{IB} & T_{11}^{IB} \end{bmatrix}$$

$$\begin{bmatrix} \text{TEMP}_{31} \\ \text{TEMP}_{32} \\ \text{TEMP}_{33} \end{bmatrix} = \begin{bmatrix} T_{12}^{\text{IB}} & T_{23}^{\text{IB}} & - & T_{13}^{\text{IB}} & T_{22}^{\text{IB}} \\ T_{13}^{\text{IB}} & T_{21}^{\text{IB}} & - & T_{11}^{\text{IB}} & T_{23}^{\text{IB}} \\ T_{11}^{\text{IB}} & T_{22}^{\text{IB}} & - & T_{12}^{\text{IB}} & T_{21}^{\text{IB}} \end{bmatrix}$$

$$\text{TEMP} = 1/2 [T^{\text{IB}} + \text{TEMP}]$$

$$\begin{bmatrix} T_{i1}^{\text{IB}} \\ T_{i2}^{\text{IB}} \\ T_{i3}^{\text{IB}} \end{bmatrix} = \begin{bmatrix} \text{TEMP}_{i1} \\ \text{TEMP}_{i2} \\ \text{TEMP}_{i3} \end{bmatrix} + 1/2 (1 - \text{TEMP}_{i1}^2 - \text{TEMP}_{i2}^2 - \text{TEMP}_{i3}^2) \cdot \begin{bmatrix} \text{TEMP}_{i1} \\ \text{TEMP}_{i2} \\ \text{TEMP}_{i3} \end{bmatrix}$$

where $i=1, 2, 3$.

Input: T^{IB} = body-to-inertial transformation matrix (from 11)

Output: T^{IB} = body-to-inertial transformation matrix (from 11)

Frequency: 16 times per second

Precision: 24 bits

Remarks: Since the second term of the last equation is a small correction, single-precision products will suffice for that equation.

The frequency of 16 times per second is much higher than necessary. Orthonormalization once every several seconds should be entirely sufficient.

The final equation above results from replacing the inverse of a square root of a quantity nominally unity by the first-order Taylor series of this function. Use of a first-order expansion is justified by the fact that the orthonormalization algorithm itself is first order. It is of interest to note that all three rows have the same scale factor error (to within first-order terms).

It can be shown that any nonsingular matrix T can be expressed as

$$T = (I + \phi)R$$

where ϕ is symmetric and R is a rotation matrix, the one closest to T in the sense of least squares. Applying the first three equations of this orthonormalization algorithm to T produces

$$TEMP = [1 + 1/2 \text{tr}(\phi)] R + 1/4 \Psi R$$

where Ψ is a symmetric matrix depending on ϕ only and second-order in ϕ . It is given in tensor notation by

$$\Psi_{ij} = \epsilon_{imn} \epsilon_{jrs} \phi_{mr} \phi_{ns}$$

so that, for example,

$$\Psi_{11} = 2(\phi_{22} \phi_{33} - \phi_{23}^2)$$

and

$$\Psi_{12} = 2(\phi_{23} \phi_{12} - \phi_{21} \phi_{33})$$

13. Velocity Increment Resolution

$$\underline{\Delta v}^I = T^{IB} \underline{\Delta v}^B$$

Input:

$$\underline{\Delta v}^B = \begin{bmatrix} \Delta v_{c1}^B \\ \Delta v_{c2}^B \\ \Delta v_{c3}^B \end{bmatrix} = \text{velocity increment in body axes (from 6)}$$

$$T^{IB} = \text{body-to-inertial transformation matrix (from 11 or 12)}$$

Output:

$$\underline{\Delta v}^I = \begin{bmatrix} \Delta v_1^I \\ \Delta v_2^I \\ \Delta v_3^I \end{bmatrix} = \text{velocity increment in inertial axes}$$

Frequency: 128 times per second

Precision: 20 bits

Remarks: Better error characteristics result if the time intervals over which Δv^B is accumulated and T^{IB} is updated are staggered. In that way, the incremental velocity is transformed by the matrix associated with the midpoint of the interval over which it was accumulated.

14. Inertial Position, Velocity Computation

$$r_i = r_i + 1/2 \Delta t v_i$$

$$v_i = v_i + \Delta t G_i + \Delta v_i^I$$

$$r_i = r_i + 1/2 \Delta t v_i$$

where $i=1, 2, 3$

Input: r_i = inertial cartesian components of position

v_i = inertial cartesian components of inertial velocity

G_i = components of gravitational acceleration (from 15)

Δv_i^J = inertial components of incremental velocity (from 13)

Output: r_i

v_i

Frequency: 64 times per second

Precision: 30 to 32 bits

Remarks: Updating position twice with first-order formulas is equivalent to updating it with second-order formulas.

Performing basic navigation in inertial coordinates has the disadvantage of a large dynamic range for the state variables and more complicated output transformations. Navigating in local vertical coordinates should be considered as an alternative.

15. Gravity Computations

$$r_o = r_e + (r_{ee}) (S2)$$

$$r_G = r_o + h_a$$

$$RI = 1/r_G$$

$$RI2 = (RI) (RI)$$

$$RI3 = (RI2) (RI)$$

$$P_o = (G) (RI3)$$

$$\lambda_o = (KJ) (RI2)$$

$$\mu_o = (5) (S2)$$

$$P_{xy} = 1 + \lambda_o (1 - \mu_o)$$

$$P_z = P_{xy} + (2) (\lambda_o)$$

$$\text{Temp} = (P_o) (P_{xy})$$

$$G_1 = (\text{Temp}) (r_1)$$

$$G_2 = (\text{Temp}) (r_2)$$

$$G_3 = (P_o) (P_z) (r_3)$$

Input: r_i = inertial position (from 14)
 h_a = altitude above geoid (from altimeter)
 $S2$ = square of sine of latitude (from 17)

Constants: r_e = equatorial radius
 r_{ee} = geoid flattening parameter
 G, KJ = gravitational parameters

Output: G_i = gravitational acceleration components
 r_o = local earth radius
 r_G = gravitational radius (based on position and altimeter)

Frequency: 16 times per second

Precision: 19 to 24 bits

Remarks: These equations embody one approach to the problem of altitude divergence control. By basing gravity on the altimeter value of altitude rather than the inertial value of altitude, the vertical channel is given the same characteristics as the horizontal channels, that is, conditional stability and the Schuler frequency.

An alternative approach which should be considered is to treat the altimeter data as augmentation in the same way that radar or Loran data is treated. Gravity is based on the inertial position, but the altimeter altitude and the inertial altitude are compared. The discrepancy is fed back at the acceleration level for restoring and at the velocity level for damping. This approach has the advantage that a stable filter can be designed which takes altimeter error characteristics into consideration.

16. Geographic Computer

$$\begin{aligned}R^2_{xy} &= r_1^2 + r_2^2 \\r_{xy} &= 1/2 (r_{xy} + R^2_{xy}/r_{xy}) \\\tan \lambda &= r_2/r_1 \\\tan L_g &= r_3/r_{xy} \\D &= (2e) r_3 r_{xy}/R^2_{xy} \\\lambda &= \tan^{-1}(\tan \lambda) \\L_g &= \tan^{-1}(\tan L_g) \\L_t &= L_g + D \\\dot{\lambda} &= \lambda + \lambda_0 - \omega_e t \\h &= r - r_0 \\\dot{\lambda} &= (r_1 v_2 - r_2 v_1)/R^2_{xy} \\\dot{\lambda} &= \dot{\lambda} - \omega_e \\v &= (r_1 v_1 + r_2 v_2 + r_3 v_3)/r \\\dot{L}_g &= (v_3/r_{xy}) - (v/r) (\tan L_g)\end{aligned}$$

$$\begin{aligned}\dot{D} &= (2e) \dot{L}_g [1 - 2(S2)] \\ \dot{L}_t &= \dot{L}_g + \dot{D} \\ \dot{h} &= v\end{aligned}$$

Input: r_i = inertial position (from 14)
 v_i = inertial velocity (from 14)
 r = magnitude of position vector (from 17)
 $R2$ = square of r (from 17)
 $r_{xy} = \sqrt{r_1^2 + r_2^2}$ (from 16)
 $S2$ = square of sine of latitude (from 17)
 t = time

Constants: $(2e)$ = geoid flattening parameter
 ω_e = earth angular velocity
 t_o = reference longitude

Output: r_{xy}
 t = longitude
 L_t = geodetic latitude
 h = inertial altitude from geoid
 \dot{h} = altitude rate
 L_g = geocentric latitude
 \dot{L}_g = geocentric latitude rate
 \dot{L}_t = geodetic latitude rate

Frequency: 16 times per second

Precision: requirements unknown

Remarks: Precision requirements are governed principally by resolution requirements of guidance and display functions.

The second equation embodies a method of bypassing the extraction of a square root.

17. Euler Angle Computation

$$R^2 = \sum_{i=1}^3 r_i^2$$

$$r = 1/2 \left(r + \frac{R^2}{r} \right)$$

$$W_i = r_i/r, \text{ where } i=1, 2, 3$$

$$S^2 = W_3^2$$

$$\cos L = 1/2 \left(\cos L + \frac{1 - S^2}{\cos L} \right)$$

$$V_i = W_i/\cos L, \text{ where } i=1, 2$$

$$U_i = W_3 V_i, \text{ where } i=1, 2$$

$$\eta_j = T_{ij}^{IB} W_i, \text{ where } i=1, 2, 3 \text{ and } j=1, 2, 3$$

$$\cos \theta \sin \psi = -T_{11}^{IB} V_2 + T_{21}^{IB} V_1$$

$$\cos \theta \cos \psi = -T_{11}^{IB} U_1 - T_{21}^{IB} U_2 + T_{31}^{IB} \cos L$$

$$\theta = \sin^{-1} \left(\eta_1 \right) \quad -90^\circ < \theta < +90^\circ$$

$$\phi = \tan^{-1} \left(\frac{\eta_2}{\eta_3} \right) \quad -90^\circ < \phi < +90^\circ$$

$$\psi = \tan^{-1} \left(\frac{\cos \theta \sin \psi}{\cos \theta \cos \psi} \right) \quad 0 \leq \psi \leq 360^\circ$$

Input:

r_i = inertial position (from 14)

T^{IB} = attitude matrix (from 11)

r = magnitude of position vector (from 17)

$\cos L$ = cosine of (geocentric) latitude (from 17)

Output: θ = elevation angle
 ϕ = roll angle
 ψ = azimuth angle
S2 = square of sine of latitude
R2 = square of r
r = magnitude of position vector
cos L = cosine of latitude

Frequency: Roll, elevation, 32 times per second
Azimuth, 16 times per second

Precision: 16 to 18 bits

Remarks: The second equation bypasses the extraction of a square root. Similarly, the fifth equation calculates a cosine as the square root of the square of the cosine.

If navigation were performed in local vertical coordinates, the attitude algorithm would be arranged to produce the body-to-local vertical transformation which would then contain all the desired attitude information.

18. Preflight Attitude Alignment

The alignment scheme outlined here is self-contained. A scheme using optical input for azimuth alignment would entail a more complicated interface with the computer and would involve somewhat more calculation. It would, however, reduce alignment error and probably require less time to accomplish. In spite of these facts, the scheme below is recommended for the first stages of AALS development.

The scheme consists of two parts, an initial alignment and a final alignment. During the initial alignment, body motion is ignored and sensor data is collected on which a body-to-local vertical transformation is based. During the final alignment, body motion is accounted for by attempting to maintain attitude reference to the local vertical. Level error is detected by measuring the acceleration in the nominally level channels, and azimuth error is detected by measuring the vehicle's secular rotation rate about the nominally east direction, the strap-down form of gyro compassing.

Initial alignment. -

- 1) Sum $\Delta\theta'$ s and $\Delta V'$ s over time t_1 :

$$\begin{aligned}V_i &= V_i + \Delta V_i^B \\ \theta_i &= \theta_i + \Delta\theta_i^B\end{aligned} \quad i=1, 2, 3$$

- 2) When complete, compute

$$\begin{aligned}g_i &= V_i/t_1 \\ \omega_i &= \theta_i/t_1\end{aligned} \quad i=1, 2, 3$$

- 3) Compute direction cosine matrix, T:

$$T_{3i} = -k_g g_i \quad i=1, 2, 3$$

$$T_{2i} = \omega_{(i+1)} T_{3(i+2)} - \omega_{(i+2)} T_{3(i+1)} \quad i=1, 2, 3$$

$$T_{2i} = k_\omega T_{2i} \quad i=1, 2, 3$$

$$T_{1i} = T_{2(i+1)} T_{3(i+2)} - T_{2(i+2)} T_{3(i+1)} \quad i=1, 2, 3$$

Orthonormalize T. - This procedure is described in section 12.

Final alignment. -

- 1) Initialize $k=0$.
- 2) Update T with gyros as when navigating.
- 3) Maintain local vertical over a Δt time by computing

$$\left\{ \begin{array}{l} \theta_E = 0 \\ \theta_N = \omega_N \cdot \Delta t \\ \theta_D = \omega_D \Delta t \\ \\ \phi = \begin{bmatrix} 0 & -\phi_D & \phi_E \\ \phi_D & 0 & -\phi_N \\ -\phi_E & \phi_N & 0 \end{bmatrix} \\ \\ T = T - \phi T \end{array} \right.$$

4) Sum ΔV 's in local vertical

$$\left\{ \begin{array}{l} V_N = V_N + \sum_j T_{1j} \Delta V_j^B \\ \\ V_E = V_E + \sum_j T_{2j} \Delta V_j^B \end{array} \right.$$

5) Every t_2 seconds compute:

$$\left\{ \begin{array}{l} \theta_E = \sum_j T_{3j} T_{1j} \\ k = k + 1 \\ Y_1 = Y_1 + \theta_E \\ Y_2 = Y_2 + k\theta_E \\ Y_3 = Y_3 + V_N \\ Y_4 = Y_4 + kV_N \\ Y_5 = Y_5 + V_E \\ Y_6 = Y_6 + kV_E \end{array} \right.$$

6) When $k=n$, compute:

$$\begin{cases} \varphi_D = k_{D1} (k_{D2} Y_2 - Y_1) \\ \varphi_E = k_{V1} (k_{V2} Y_4 - Y_3) \\ \varphi_N = k_{V1} (k_{V2} Y_6 - Y_5) \end{cases}$$

7) Correct the alignment

$$T = T - \delta T$$

8) Convert to space stable

$$T = T^{IV} T$$

9) Initialize position, velocity, orthonormalize and navigate.

Remarks: The equations involving the running index k , $k=1, 2, \dots, n$, produce the least-squares estimate of the (assumed constant) horizontal acceleration and angular rate about East.

T^{LV} is the precalculated local vertical-to-inertial transformation based on the vehicle position.

19. Guidance Input Calculations

$$S_{IE} = S_{IE} + \Delta t \omega_e C_{IE}$$

$$C_{IE} = C_{IE} - \Delta t \omega_e S_{IE}$$

$$r_1' = C_{IE} r_1 + S_{IE} r_2$$

$$r_2' = -S_{IE} r_1 + C_{IE} r_2$$

$$\Delta r_1 = r_1' - R_1$$

$$\Delta r_2 = r_2' - R_2$$

$$\Delta r_3 = r_3' - R_3$$

$$\begin{pmatrix} N_A \\ E_A \\ h_{UD} \end{pmatrix} = \begin{pmatrix} T^{RN, E} \end{pmatrix} \begin{pmatrix} \Delta r_1 \\ \Delta r_2 \\ \Delta r_3 \end{pmatrix}$$

$$v_{R1} = v_1 + \omega_e r_2$$

$$v_{R2} = v_2 - \omega_e r_1$$

$$v_{R1}' = C_{IE} v_{R1} + S_{IE} v_{R2}$$

$$v_{R2}' = -S_{IE} v_{R1} + C_{IE} v_{R2}$$

$$\begin{pmatrix} \bar{u}_G \\ \bar{v}_G \\ h_{UD} \end{pmatrix} = \begin{pmatrix} T^{RA, E} \end{pmatrix} \begin{pmatrix} v_{R1}' \\ v_{R2}' \\ v_{R3}' \end{pmatrix}$$

$$V = \frac{1}{2} \left[V + \frac{(\bar{u}_G)^2 + (\bar{v}_G)^2}{V} \right]$$

Input: S_{IE} = sine (inertial-to-earth-fixed equatorial coordinate system angle)
 C_{IE} = cosine (inertial-to-earth-fixed equatorial coordinate system angle)
 $\left. \begin{matrix} r_1 \\ r_2 \\ r_3 \end{matrix} \right\}$ = inertial position coordinates
 $\left. \begin{matrix} v_1 \\ v_2 \\ v_3 \end{matrix} \right\}$ = inertial velocity coordinates

ω_c = earth angular velocity

$\left. \begin{array}{l} R_1 \\ R_2 \end{array} \right\}$ = radar position in earth-fixed coordinates

$\left. \begin{array}{l} R_3 \\ T_{RN, E} \\ T_{RA, E} \end{array} \right\}$ = Transformation from earth-fixed equatorial to radar local vertical north, and down-range coordinate systems

Output: N_A

E_A

h_{UD}

\bar{u}_G

\bar{v}_G

\dot{h}_{UD}

V = ground speed

Frequency : 2 times per second

Precision: 12 to 30 bits

Remarks: The first two equations are used to bypass calculation of high precision sin/cos and should occasionally be replaced by actual sin/cos calculations. Similarly, the last equation bypasses the extraction of a square root.

Description of Variables for Radar Input

$\left. \begin{array}{l} m_x \\ m_y \\ m_z \end{array} \right\}$ = radar position measurements

r_o = local earth radius

t_r = time associated with radar measurement

Constants:

C_R } = cosine and sine of azimuth of radar coordinates

S_R }

l_{t_r} = radar latitude

L_{g_0} = initial longitude

m_x^p }

m_y^p } = previous radar position measurements

m_z^p }

t_r^p = time of previous radar measurement

L_r = vehicle latitude derived from radar

l_{g_r} = vehicle longitude derived from radar

UPDATE

This section contains preliminary equations for updating the inertial navigator by means of external data. Two sets of equations are presented as typical of the kind of external data which might be available. The first set is based on the reception of position data of the form available from a GSN-5 radar receiver. The second set is based on the reception of time difference data of the form available from a Loran receiver.

Preliminary interface data for VORTAC, GSN-5, Loran-C, and DECCA navigation aids are given in Appendix B.

In addition to the data itself, the computer needs an indication of when valid data is available.

Radar Position Calculation

$$h_r = m_x$$

$$Y_r = (m_y) C_r + (m_z) S_r$$

$$Z_r = (m_z) C_r - (m_y) S_r$$

$$L_r = \iota t_r + Y_r/r_o$$

$$\iota_r = Z_r/r_o$$

$$r_r = r_o + h_r$$

$$r_K = r_r \cos L_r$$

$$\iota_{g_r} = L_{g_o} + \iota_r + \omega_e t_r$$

$$r_{r1} = r_K \sin \iota_{g_r}$$

$$r_{r2} = r_K \cos \iota_{g_r}$$

$$r_{r3} = r_r \sin L_r$$

Input: m_x, m_y, m_z, r_o, t_r

Output: r_{r1}, r_{r2}, r_{r3}

Constants: $C_r, S_r, t_{t_r}, Lg_o, \omega_e$

Timing: 1 per second

Radar position extrapolation. -

$$\Delta t = t - t^p$$

$$\Delta m_x = m_x - m_x^p$$

$$\Delta m_y = m_y - m_y^p$$

$$\Delta m_z = m_z - m_z^p$$

If

$$(|\Delta m_x| + |\Delta m_y| + |\Delta m_z| < \epsilon^2)$$

$$t^p = t$$

$$m_x^p = m_x$$

$$m_y^p = m_y$$

$$m_z^p = m_z$$

$$\Delta r_r = \Delta m_x$$

$$\Delta Y_r = (\Delta m_y) C_r + (\Delta m_z) S_r$$

$$\Delta Z_r = (\Delta m_z) C_r - (\Delta m_y) S_r$$

$$\Delta L_r = \Delta Y_r / r_o$$

$$\Delta t_{g_r} = \omega_e (\Delta t) + \Delta Z_r / r_o$$

$$\Delta \cos L_r = -\Delta L_r \sin L_r$$

$$\Delta \sin L_r = \Delta L_r \cos L_r$$

$$\Delta \cos \iota g_r = -\Delta \iota g_r \sin \iota g_r$$

$$\Delta \sin \iota g_r = \Delta \iota g_r \cos \iota g_r$$

$$\Delta r_K = \Delta r_r (\cos L_r) + r_r (\Delta \cos L_r)$$

$$r_{r1} = r_{r1} + \Delta r_K (\sin \iota g_r) + r_K (\Delta \sin \iota g_r)$$

$$r_{r2} = r_{r2} + \Delta r_K (\cos \iota g_r) + r_K (\Delta \cos \iota g_r)$$

$$r_{r3} = r_{r3} + \Delta r_r (\sin L_r) + r_r (\Delta \sin L_r)$$

$$\sin L_r = \sin L_r + \Delta \sin L_r$$

$$\cos L_r = \cos L_r + \Delta \cos L_r$$

$$\sin \iota g_r = \sin \iota g_r + \Delta \sin \iota g_r$$

$$\cos \iota g_r = \cos \iota g_r + \Delta \cos \iota g_r$$

$$r_K = r_K + \Delta r_K$$

$$r_r = r_r + \Delta r_r$$

Input: $m_x, m_y, m_z, r_o, t, m_x^p, m_y^p, m_z^p, t^p, \sin L_r, \cos L_r,$
 $\sin \iota g_r, \cos \iota g_r, r_r, r_K, r_{r1}, r_{r2}, r_{r3}$

Output: $r_{r1}, r_{r2}, r_{r3}, m_x^p, m_y^p, m_z^p, t^p, r_r, r_K, \sin L_r, \cos L_r,$
 $\sin \iota g_r, \cos \iota g_r$

Constants: $C_r, S_r, \iota t_r, Lg_o, \omega_e$

Timing: 16 per second

Radar and inertial combining. -

$$i = 1, 2, 3$$

$$\Delta t_r = t - t_r$$

$$\Delta r_i = r_{ri} - r_i + \dot{r}_i \Delta t_r$$

If

$$\left(\sum_{i=1, 2, 3} |\Delta r_i| < \epsilon^2 \right)$$

$$\Delta t_{rp} = t_r - t_{rp}$$

$$\dot{r}_{ri} = (r_{ri} - r_{ri}^p) / \Delta t_{rp}$$

$$\Delta \dot{r}_i = \dot{r}_{ri} - \dot{r}_i$$

$$r_i = r_i + k_r \Delta r_i$$

$$\dot{r}_i = \dot{r}_i + k_r^{\cdot} \Delta \dot{r}_i$$

Inputs: $r_i, \dot{r}_i, r_{ri}, \dot{r}_{ri}, t, t_r, t_{rp}, r_{ri}^p, k_r, k_r^{\cdot}$

Outputs: r_i, \dot{r}_i

Constants: ϵ^2

Radar and inertial combining definitions. -

- t = present time
- t_r = time at which radar data was obtained
- r_{ri} = components of radar-derived position in inertial coordinates
- t_{rp} = time of previous radar data
- r_{ri}^p = components of previous radar position
- k_r, k_r^{\cdot} = combining gains either constant or slowly varying constants (generation equations are unknown)

Loran Computation

$$R_e = R_{e0} - \text{Ref}(U_3)(U_3)$$

$$\cos \sigma_1 = U_i U_{1i}$$

$$\Delta U_{1i} = U_i - U_{1i}$$

$$\text{TEMP} = U_i \Delta U_{1i}$$

$$\sin^2 \sigma_1 = \text{TEMP} (2 - \text{TEMP})$$

$$\sin \sigma_1 = \frac{1}{2} (\sin \sigma_1 + \sin^2 \sigma_1 / \sin \sigma_1)$$

$$\sigma_1 = \sin \sigma_1 \left[1 + \sin^2 \sigma_1 \left(\frac{1}{6} + \sin^2 \sigma_1 \left[\frac{3}{40} + \left(\frac{15}{336} \right) \sin^2 \sigma_1 \right] \right) \right]$$

$$A_1 = U_3 + U_{13}$$

$$A_2 = U_3 - U_{13}$$

$$A_{12} = (A_1)(A_1)$$

$$A_{22} = (A_2)(A_2)$$

$$A_3 = \sigma_1 + \sin \sigma_1$$

$$A_4 = \sigma_1 - \sin \sigma_1$$

$$A_5 = 1 + \cos \sigma_1$$

$$A_6 = 1 - \cos \sigma_1$$

$$A_7 = (A_3)(A_{12})$$

$$A_8 = (A_4)(A_{22})$$

$$\delta \sigma_1 = \left(\frac{f}{4} \right) (-A_7/A_5 - A_8/A_6)$$

$$R_1 = R_e (\sigma_1 + \delta \sigma_1) + \frac{h}{2} \sigma_1$$

Repeat bracketed equations for second station, obtaining R_2 , $\sin \sigma_2$, R_3 and $\sin \sigma_3$.

$$T_{c2} = K_{c1} (R_2 - R_1) + K_{c2}$$

$$T_{c3} = K_{c3} (R_3 - R_1) + K_{c4}$$

$$\Delta T_2 = T_{c2} - T_{m2}$$

$$\Delta T_3 = T_{c3} - T_{m3}$$

$$B_{i1} = -R_{i1} \sin \sigma_1 \quad i = 1, 2, 3$$

$$B_{i2} = -R_{i2} \sin \sigma_2 \quad i = 1, 2, 3$$

$$B_{i3} = -R_{i3} \sin \sigma_3 \quad i = 1, 2, 3$$

$$UTB_i = U_j B_{ji} \quad i = 1, 2, 3 \quad j = 1, 2, 3$$

$$TEMP = UTB_1 + UTB_2 + UTB_3$$

$$UTB_i = UTB_i / TEMP \quad i = 2, 3$$

$$BS_i = B_{i1} + B_{i2} + B_{i3} \quad i = 1, 2, 3$$

$$D_{ij} = B_{ij} - BS_i UTB_j \quad i = 1, 2, 3 \quad j = 2, 3$$

$$E_i = K_o \Delta T_i \quad i = 2, 3$$

$$\Delta U_i = D_{ij} E_j \quad i = 1, 2, 3 \quad j = 2, 3$$

$$U_i = U_i + \Delta U_i$$

$$U^2 = U_i U_i$$

$$\Delta \left(\frac{1}{U} \right) = \frac{1}{2} (1 - U^2)$$

$$U_i = U_i + \Delta \left(\frac{1}{U} \right) U_i$$

$$\phi' = \omega_e (t - t_{pr})$$

$$t_{pr} = t$$

$$\begin{aligned} \sin \phi &= \sin \phi + \phi' \cos \phi \\ \cos \phi &= \cos \phi - \phi' \sin \phi \\ v_1 &= U_1 \cos \phi + U_2 \sin \phi \\ v_2 &= U_2 \cos \phi - U_1 \sin \phi \\ r_{L1} &= r_G v_1 \\ r_{L2} &= r_G v_2 \\ r_{L3} &= r_G U_3 \end{aligned}$$

The Loran position can now be combined with the inertial position as in the radar description.

Input: h, T_{m2}, T_{m3}, r_G

Outputs: r_{L1}, r_{L2}, r_{L3}

Constants: station-dependent ($U_{ij}, R_{ij}, K_{c1}, K_{c2}, K_{c3}, K_{c4}$)
nonstation-dependent ($R_{eo}, R_{ef}, K_o, f/4$)

Loran Computation Definitions

- U_i = direction cosines of vehicle in earth-fixed cartesian frame referred to here as the Loran frame
- U_{ij} = direction cosines of the i th station in the Loran frame, where station 1 is the master and stations 2 and 3 are the slaves
- σ_i = the spherical range angles to the three stations
- R_i = the ranges to the stations
- R_e = earth radius corrected for flattening
- f = flattening correction coefficient in the oblateness compensation equations
- K_{c1}, K_{c3} = coefficients to convert range to time

- K_{c2}, K_{c4} = coefficients to account for fixed time delays
- K_o = coefficient to convert time to range angle
- RI_{ij} = elements of matrix which is inverse of matrix whose elements are U_{ij} . These elements are station-dependent stored constants.
- r_{Li} = Loran-derived position components in the inertial frame

GUIDANCE

Requirements

Definition of guidance laws appropriate to the NASA/ERC AALS must recognize many factors. These factors include aircraft flight capability, pilot manual control capability, environmental constraints such as imposed by geography, air traffic, buildings, etc., and operational needs such as minimizing flight time and fuel required.

There is probably no area that requires more pilot judgement than the landing phase. The word judgement implies an intelligent choice and assumes an optimum response. When the same functions are proposed in an automatic control system, the terms are often misused.

Any automatic control system that is to duplicate pilot functions must do so in a reasonably optimum manner. But what is an optimum manner? A pilot weighs many factors and then acts in the most optimum manner. A control system only weighs the factors that are built into the system and then only in a fixed manner. There is no judgement as such in a control system and the result is always predictable.

Optimum must be built in, and every possible choice must be included. The only reason systems can be called automatic now is that the choices have been greatly reduced and the weighting factor is constant. Most of the time this is adequate.

The automatic guidance system devised as the AALS baseline is also restricted. The choices have been reduced to the point where they will fit physically (as logic statements) into a digital computer. The weighting factors are constant for the most part and the results are predictable. By providing suitable displays, we still rely on the pilot for judgement to reset the automatic system. The pilot is still the most optimum controller.

Guidance laws are defined herein which are suitable for use in CRT-type displays, as well as in closed-loop automatic modes. Detailed discussions of the various computations required are included.

Approach Pattern

The guidance system as defined for the baseline AALS has the following features:

- **Rectangular approach pattern**
- **Automatic glideslope**
- **Standard turns**
- **Automatic flare**

A rectangular approach pattern was selected for the automatic guidance system. The rectangular pattern is orientated so that the landings are made into the wind. A bearing to the nearest checkpoint is computed after the guidance system is activated and when the helicopter is within the radar range. Altitude, position, speed, and heading are controlled to fly the desired path. Suitable anticipation is provided to initiate turns prior to reaching the checkpoints. Bank angles are limited to avoid stalling at the lower approach speeds.

Final approach is started at a distance of about two miles from the landing site. Speed is reduced and a constant altitude (selected by pilot) is maintained. The glideslope path (glide angle is selected by pilot) is computed on the basis of relative wind and typical helicopter performance. Speed is gradually reduced after glide-path intercept, but sufficient airspeed is maintained to avoid control problems normally associated with helicopters at low speeds.

The helicopter begins a vertical descent at an altitude preselected by the pilot. Radar altimeter signals are used during the final flare to provide the precise control needed. The system is flexible enough so that only minor changes are necessary to evaluate alternate approaches. The automatic system has been patterned after a typical pilot approach so that the entire system can be maintained or interrupted by the pilot at any time. This feature should also simplify the display system to make it more nearly like the actual flight situation.

Several approach paths were considered for this system. A spiral path in which the helicopter descends vertically in a circular path was one of those considered. At first, this spiral descent looks promising because it is conservative of airspace in the vicinity of the landing site. However, the spiral path is extremely difficult to fly for a V/STOL since the V/STOL has more cross coupling and flies closer to the stall point. The spiral descent also involves precise control in all six degrees of freedom and would be difficult to display. Extended flight in a spiral approach without visual reference is also conducive to air sickness.

A curvilinear path tangent to the straight-line final approach was also considered. The curvilinear path can be described by a suitable mathematical expression and could be modified to provide numerous interception points. This system was discarded because of the severe requirements on bank angle. If an intercept is made close to the touchdown area, the curvilinear path is too short and requires very high bank angles. The short distance also requires high decelerations in order to enter the final glide path with the proper speed.

The rectangular pattern offered the most flexibility, safety, and simplicity of all those considered. It even provides the opportunity for a straight-in approach if the vehicle is making an intercept in the proper area. This approach is shown in Figure 3, with both a left-hand and right-hand approach shown. The pattern is dimensioned such that the final and downwind legs are 12,000-foot segments. The (N, E) origin is at the landing site.

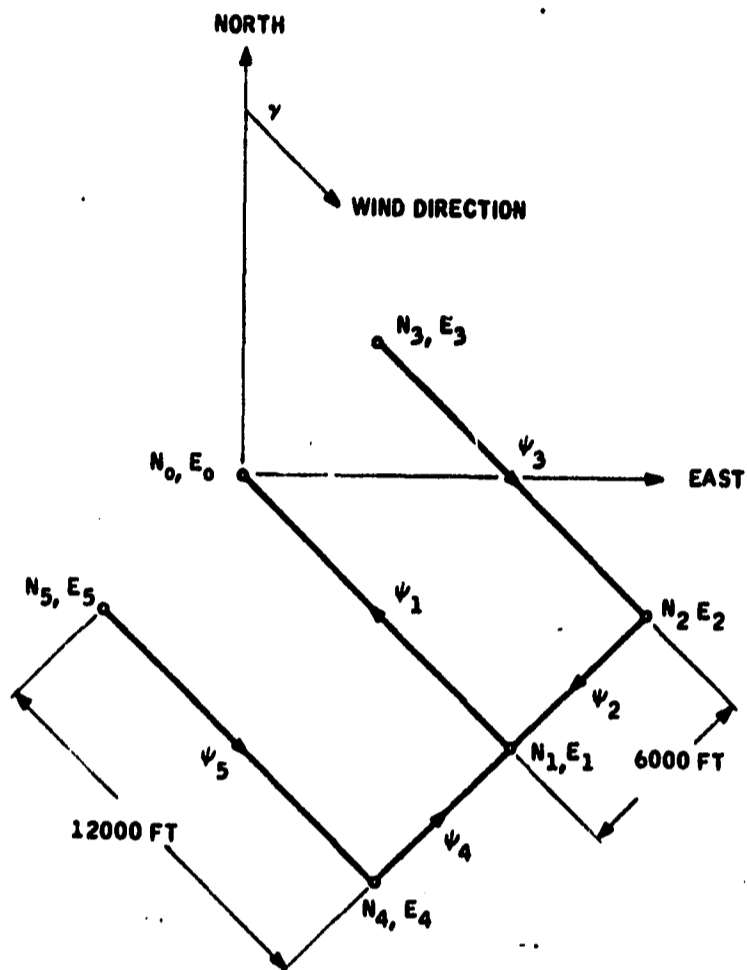


Figure 3. Rectangular Approach Pattern

The cross-course legs are 6000 feet, with the relative orientation in a north and east direction. The checkpoints at the corners are labeled, as are the headings between checkpoints. These checkpoints retain this identification regardless of which wind orientation is used. Wind direction as referenced to north determines the orientation of the final approach, cross-course, and down-wind legs. These dimensions are defined to be compatible with the test helicopter. The north and east coordinate system was chosen to conform to typical flight headings and navigation. Unfortunately, this is contrary to the practice of trigonometry, where angles are measured counterclockwise. The additional logic required to convert from one system to another is small, and it is better to stay in a coordinate system familiar to the pilot.

The coordinates are determined by the following equations:

- North coordinates in feet

$$N_0 = 0$$

$$N_1 = 12000 \cos \gamma$$

$$N_2 = [12000 \cos \gamma + 6000 \sin \gamma]$$

$$N_3 = + 6000 \sin \gamma$$

$$N_4 = [12000 \cos \gamma - 6000 \sin \gamma]$$

$$N_5 = - 6000 \sin \gamma$$

• East coordinates in feet

$$E_0 = 0$$

$$E_1 = 12000 \sin \gamma$$

$$E_2 = [12000 \sin \gamma - 6000 \cos \gamma]$$

$$E_3 = - 6000 \cos \gamma$$

$$E_4 = [12000 \sin \gamma + 6000 \cos \gamma]$$

$$E_5 = + 6000 \cos \gamma$$

where ψ_1 = approach direction, and

$$\gamma = \psi_1 + 180$$

These coordinates are stored in the computer and will be available for heading computations and other functions.

A sine and cosine routine will be used in the computer. This routine measures angles positive from a positive "X"-axis in a counterclockwise manner. The guidance system has angles measured clockwise from north. The additional logic will take the form of:

If $0 < \gamma < 90$	first quadrant sine + cosine +
$90 < \gamma < 180$	fourth quadrant sine - cosine +
$180 < \gamma < 270$	third quadrant sine - cosine -
$270 < \gamma < 360$	second quadrant sine + cosine -

The quadrant identifies the sign of the term.

The (γ) angles must also be identified in a different manner:

first quadrant use	$90 - \gamma$
fourth quadrant use	$[360 - \gamma] + 90$
third quadrant	$[360 - \gamma] + 90$
second quadrant use	$[360 - \gamma] + 90$

First Checkpoint

The helicopter's present location in terms of north and east coordinates from the landing site is designated as N_A and E_A . These coordinates are available at all times from the navigation system.

A groundrule was established not to permit guidance engagement when the helicopter is within five miles of touchdown point. This would prevent unusual maneuvering to get on the desired flight path. Again, should this prove to be a problem, additional logic can be added to permit engagements under five miles. The logic would direct the helicopter to a more distant checkpoint to avoid large bank angles. With this five-mile limit, the present location from the landing site is computed:

$$d = \sqrt{N_A^2 + E_A^2}$$

If this distance d is less than five miles, the system will not engage. The nearest checkpoint is determined by computing the distance to all checkpoints in the rectangular pattern:

$$d = \sqrt{(N_A - N_5)^2 + (E_A - E_5)^2}$$

The checkpoint with the smallest distance is the closest checkpoint. This checkpoint will then determine the desired course from the present location. All bearings are with respect to north and measured clockwise from north:

$$\Delta B = \tan^{-1} \left[\frac{E_i - E_A}{N_i - N_A} \right]$$

where "i" refers to the nearest checkpoint. This bearing should be expressed with respect to north for the display and for the guidance. To determine the quadrant and bearing, the following logic is used:

If $E_i - E_A$ is	If $N_i - N_A$ is	Then the bearing is:
+	+	ΔB_i
+	-	$180 - \Delta B_i$
-	-	$180 + \Delta B_i$
-	+	$360 - \Delta B_i$

The heading from checkpoint to checkpoint is also determined prior to the first intercept. Since the direction of the wind is known, the respective headings are computed by:

$$\psi_1 = \gamma - 180$$

$$\psi_3 = \psi_1 - 180$$

$$\psi_4 = \gamma - 90$$

$$\psi_5 = \psi_3$$

$$\psi_2 = \gamma + 90$$

Again, these are stored for future reference such as the bank-angle command. Prior to the time the helicopter reaches the first intercept, some logic must determine whether a left or a right bank is needed to pick up the first heading:

If $[\Delta B_i - \psi_3]$ is positive, use left bank

If $[\Delta B_i - \psi_3]$ is negative, use right bank

It was assumed in these expressions that the heading ψ_3 was the next heading. If the helicopter had been approaching N_2, E_2 , the heading would have been ψ_2 , and so on.

Time to Bank

Prior to arriving at the checkpoint, the helicopter must start a bank. The distance to the checkpoint is continuously being computed. As the helicopter approaches the checkpoint, the time to the landing pattern corner is:

$$t = \frac{R_i}{V_G} = \frac{[(N_i - N_A)^2 + (E_i - E_A)^2]^{1/2}}{V_G}$$

where R_i = range to checkpoint

V_G = ground velocity

N_i = coordinate checkpoint

N_A = present coordinate

The actual bank is initiated when the time computed previously is equal to the time necessary to complete one half the turn (see following sketch):



$$t_{360} = \frac{2\pi R}{V_G}$$

$$t_{\Delta\psi} = \frac{2\pi R}{V_G} \left(\frac{\Delta\psi}{360} \right)$$

The heading change for one half the turn is:

$$\Delta\psi = \frac{\psi_i - B_i}{2}$$

Also

$$R = \frac{V_G^2}{g \tan \phi}$$

The bank angle ϕ is held constant at 20 degrees to avoid stalling the helicopter:

$$t (\text{turn}) = \frac{2\pi V_G}{g \tan \phi} \left(\frac{\psi_i - B_i}{2} \right) \left(\frac{1}{360} \right)$$

The turn is held for an equal period of time before control is relinquished to the heading mode. To avoid abrupt bank angle commands, a two-second first-order lag is added to the 20-degree bank command.

An alternate to "time to turn" to initiate a turn to new course would be a "distance to checkpoint" computation.

The equation to accomplish this is easily obtained by using the previous equation for "time to turn" and combining with the present velocity:

$$t(\text{turn}) = \frac{2\pi V_G}{g \tan \phi} \left(\frac{\psi_1 - B_i}{2} \right) \frac{1}{360}$$

$$d = V_G t$$

$$d = V_G \left(\frac{2\pi V_G}{g \tan \phi} \right) \left(\frac{\psi_1 - B_i}{2} \right) \frac{1}{360}$$

When the distance to the checkpoint is the same as the "distance to turn" the bank will be initiated.

Off-Course Displacement

The off-course displacement is needed to hold proper ground track. Below some airspeed between 30 and 80 knots, the transition speed, the system controls to lateral velocity error. Under these conditions, the off-course displacement must be converted to the required lateral velocity error. The desired and actual position are continually computed and may be used to obtain the lateral displacement. First the equations of the present ground track are completed.

$$\frac{N - N_1}{E - E_1} = \frac{N_2 - N_1}{E_2 - E_1}$$

where N_1 , E_1 , and N_2 , E_2 are end points on the track. This will result in an equation of the form:

$$AE + BN + C = 0$$

Here, the A, B, and C are constants.

The perpendicular distance ΔY to course is:

$$\Delta Y = \frac{AE_A + BN_A + C}{\pm \sqrt{A^2 + B^2}}$$

where E_A , N_A are the present location.

The end points or checkpoints are selected on the basis of the present helicopter location. After the helicopter has passed a checkpoint, an "event marker" keeps a record of what leg is presently being flown.

Straight-In Approach

There are times where it may be expedient to have a straight-in approach. This should only be possible if this is the shortest path to the landing site. This is the same reasoning the pilot would use.

On this basis, consider Figure 4:

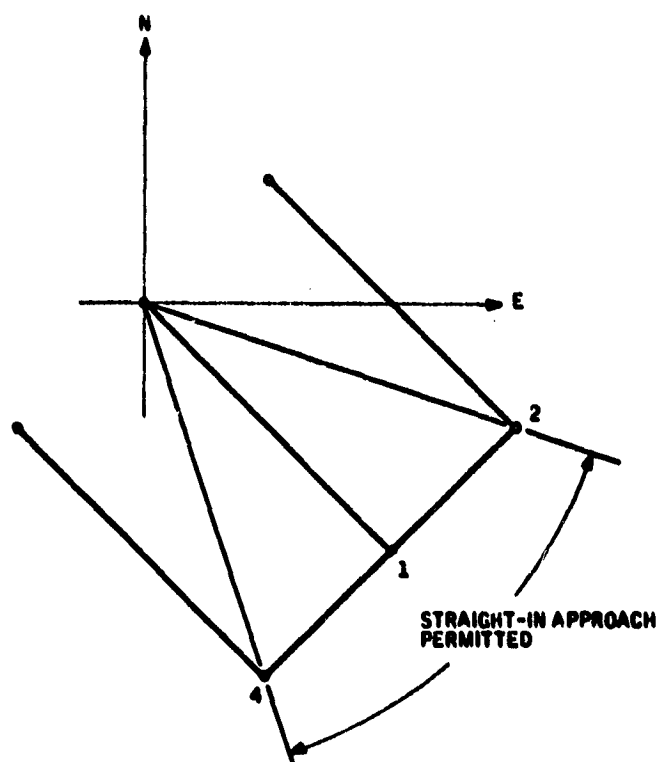


Figure 4. Straight-in Approach Pattern

By drawing a line from the landing site through checkpoints 2 and 4, a feasible straight-in approach area is defined. The included angle is 53.12 degrees or ± 26.56 from the final approach direction ψ_1 .

The actual heading at the time of interrogation is called ψ_A so that the difference between the true bearing to the landing site and the final approach direction must be within ± 26.56 degrees:

$$+26.56 < \psi_1 - \psi_A < -26.56$$

Under these conditions, the logic will always cause the helicopter to fly to checkpoint one (the final approach) even though it may be closer to checkpoint 4 or 2.

Vertical Control

The altitude control is used to provide the proper vertical guidance. The control equation needed can be expressed as:

$$\Delta h = \left[\frac{1}{T_1 S} \right] \left[\pm 8 T_1 \right]$$

where $\Delta h = h - h_{c_0}$

h = present altitude

h_{c_0} = pilot-selected approach altitude

T_1 = integrator time constant

± 8 = 8 ft/sec maximum descent rate (selected as a desirable and comfortable descent rate)

The pilot may select the command altitude h_{c_0} for the downwind and crosswind legs.

Altitude Select

A nominal 800 feet is held on the approach pattern. Since the pilot can select the altitude, certain limits must be applied.

The "event marker" is used to identify the checkpoint that is being approached. The event marker determines the logic:

h (selected) \leq 1500 feet on downwind leg

h (selected) \leq 1000 feet on base leg

h (selected) \leq 800 feet on final approach

Once the pilot selects an altitude, the altitude is reduced on each leg until 800 feet is reached on final approach. For example, assume the pilot selected 1500 feet on the downwind leg:

$$\Delta h = 1500 - 1000$$

The 1000 feet is the desired altitude on the base leg. If the pilot had selected 1000 feet, this altitude would be retained until the base leg. The "event marker" also determines the descent rate to command the final altitude.

Speed Control

It is assumed that a 100-knot speed is used on the downwind leg. This is adequate for suitable control and within the capabilities of the helicopter. If the helicopter is flying at a higher speed, the velocity is reduced through the following equation:

$$\bar{u}_c = \left[\frac{\pm 3.3 \text{ ft/sec}^2}{K} \right] \left[\frac{K}{S} \right] \left[\bar{u}_p - \bar{u}_c \right]$$

where \bar{u}_c = commanded airspeed

K = control gain

± 3.3 = constant deceleration

\bar{u}_p = pilot-selected speed

Final Approach

The final approach distance has been selected as 12,000 feet to be compatible with the helicopter characteristics of the flight test vehicle. This permits adequate distance for deceleration and also descent to 800 feet if the helicopter is at some other altitude. After a short period of level flight, a nominal six-degree glide path is intercepted and followed to the landing site. Glide-path angle is selected by the pilot.

Various research agencies have conducted tests with slopes of 6, 9, and 12 degrees. The recommendations favor the 6- and 7-degree slopes. The steeper angles (12 degrees and more) are very difficult to follow since forward speed and sink rate have to be adjusted rapidly. Also, depending on the forward speed, the steeper angles are too close to the autorotation speed. To keep on these steep paths, the helicopter has to fly very near the autorotation speed or "vortex ring" speed. The vortex-ring speed is when the downwash velocity is equal to the descent rate. This region creates severe roughness and wide variations in descent rate.

The rate of descent will vary as the helicopter flies the glide path. Descent rates are limited by the vortex ring, autorotation, flare capabilities and forward speed. Sufficient altitude must be available so that the helicopter can flare to the final touchdown without exceeding the "g" limits.

During this descent the helicopter is operating near or in the region of the back side of the power-required curve. This means that a decrease in forward velocity means an increase in power required. This also means the autopilot will control rate of descent almost entirely by power changes.

The final approach is nominally started at an altitude of 800 feet and a speed of 100 knots. The checkpoint on the final approach is 12,000 feet from the landing site. The 800-foot altitude is maintained while the speed is reduced to 50 knots. At a distance of about 8000 feet from the landing site, the helicopter will intercept the six-degree glide path. It will descend along the path as it decreases the speed to 25 knots. At an altitude of 100 feet it will continue to decrease the speed to almost zero. At a pilot-selected altitude above the landing site (about six feet), the helicopter will make a vertical descent to touchdown. This is summarized in Figure 5:

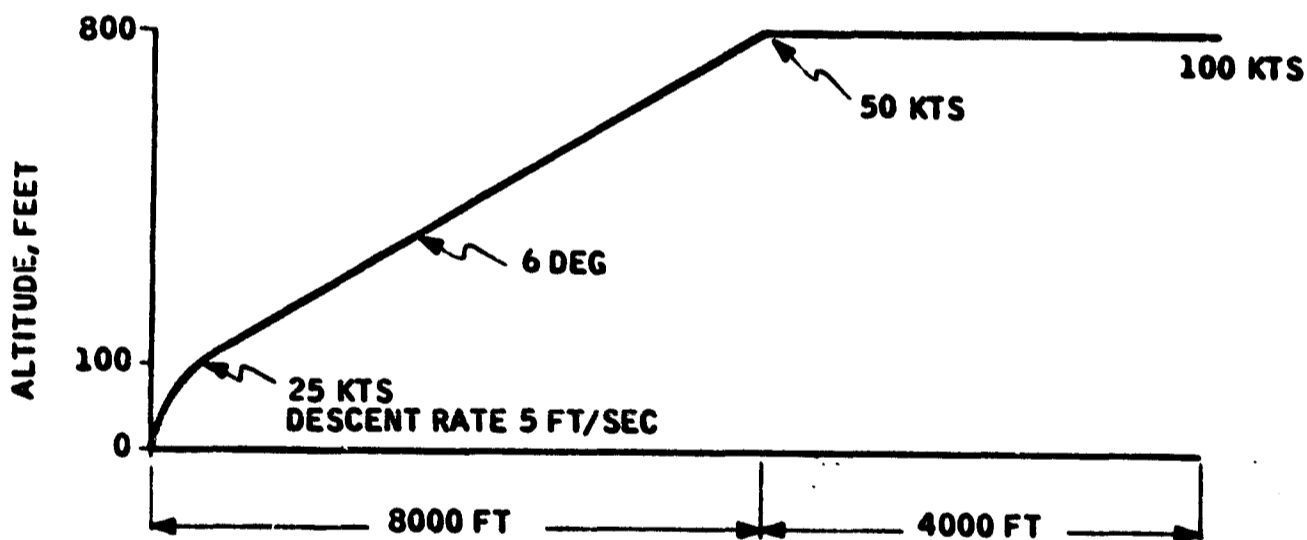


Figure 5. Final Approach Flight Profile

Altitude less than 800 feet should not normally be considered for the approach, since certain minimum altitudes are recommended over congested areas. The 800 to 1000 feet altitudes are ideal from the standpoint of the approach. With such an altitude there is some margin for small variations in approach speed, overshoot on the initial entry to the glide path, and some time for update of the inertial reference.

On the final approach, speed is reduced to 50 knots. The equation is then:

$$\bar{u}_c = \left[\frac{[\pm 3.3 \text{ ft/sec}^2]}{K} \right] \left[\frac{K}{S} \right] [85 - \bar{u}_c]$$

where 85 ft/sec = 50 knots. A switch must be made from airspeed to inertial speed. It is assumed that inertial speed is introduced gradually so that upon transfer there is no transient.

In manual systems, pilots have had difficulty in capturing the glide path. Generally, the overshoot is large since the pilot has insufficient warning that the glideslope intercept is near. With the inertial system some warning should be available so that a descent rate command can be given prior to the intercept. The lead time will depend on the glide path chosen. The effective angle of the glide path in turn will depend on the wind velocity.

To provide proper anticipation of the glide path, a high-passed descent rate command is used. This command is initiated about 1.5 seconds prior to glide-path intercept. The exact time depends on system response, magnitude of the step, the high-pass time constant, and other factors:

$$t = \frac{\pi R}{60 V}$$

where R = radius of maneuver

$$R = \frac{V^2}{A_n}$$

$$A_n = 0.1 g = 3.2 \text{ ft/sec}^2$$

The descent rate is 8 ft/sec nominal:

$$\dot{h}_{\text{input}} = \left[\frac{-8 \text{ ft}}{\text{sec}} \right] \left[\frac{20S}{1 + 20S} \right]$$

At a time "t" a step input of 8 ft/sec through a 20-second high pass should provide the proper anticipation for glidepath intercept and control. The range is simply:

$$R = \frac{800}{\tan E_g}$$

where E_g = glideslope angle.

To follow the glideslope, the system requires an appropriate altitude rate as a command input:

$$\dot{h} = V \tan E_g$$

where $E_g = 6$ degrees
 $V =$ true ground speed
 $\dot{h} =$ altitude rate

After the glide-path intercept, the speed is reduced to 25 knots by the following command:

$$\bar{u}_c = \left[\frac{[\pm 3.3 \text{ ft/sec}^2]}{K} \right] \left[\frac{K}{S} \right] [42 - \bar{u}_c]$$

where $42 \text{ ft/sec} = 25 \text{ knots}$.

Flare

The final flare is assumed to start at an altitude of about 100 feet. At this point the rate of descent and forward speed have been reduced to small values. The final 100 feet is sufficient to flare to a landing without exceeding any "g" limit and is reasonably comfortable for passengers. The last 100 feet may also be used to correct for some deviation in fore and aft position. It is definitely preferable to have a slight forward speed at touchdown, since there is less chance for sideslip. (The helicopter has more directional stability although very small.)

At this time, the radar altimeter is used to provide the necessary altitude (accurately). The required deceleration is 0.25g if the speed is 25 knots at 100 feet. The descent rate is 6 ft/sec or less. The equation:

$$\bar{u}_c = \left[\frac{-12 \text{ ft/sec}^2}{K} \right] \left[\frac{K}{S} \right] [0 - \bar{u}_c]$$

will reduce forward speed to zero. At an altitude of about 6 feet, as measured by the radar altimeter, the wings-level command is given. Altitude rate is then commanded:

$$\dot{h}_c = \begin{matrix} \text{(limited)} \\ -3 \text{ ft/sec} \end{matrix}$$

Touchdown will normally occur within two seconds after the time wings level is commanded. The final touchdown command will not be given if:

$$\bar{v} \geq 2-3 \text{ ft/sec}$$

where $\bar{v} =$ lateral speed w. r. t. ground.

This will ensure that the sideload on the landing gear will not be excessive.

Go-Around

An additional consideration is the need for an automatic "go-around". A helicopter will have less need for a go-around than a conventional aircraft. With a helicopter, the approach speeds are much less, the deceleration capabilities are greater, and the required landing area is less. With a suitable presentation or display, the pilot should be able to perform instrument go-arounds.

The following information must be considered regardless of the method used to accomplish the go-around.

It will be assumed that the go-around will be initiated only during the approach, where the altitude will be 800 feet or less. The go-around maneuver should not apply to anything at an altitude more than the 800-foot approach. If something is necessary at 800 feet or more, a "loiter" or "standard turn" mode can be provided.

In the event of a go-around, a safe exit heading must be provided. This could take the form of "previously stored" obstructions with respect to the landing site or a clear heading provided by the ground. If the go-around is initiated because of some inertial difficulty, the location of obstructions with respect to the landing site would remain doubtful. If heading is provided, with update from the ground, the system is more reliable. In the go-around suggested, a safe exit heading is provided.

A safe climb angle must also be provided. This safe climb angle must be within the physical capabilities of the helicopter and also provide terrain clearance. It could be provided by the ground station at the same time as the safe heading information.

If a display is provided, the safe heading and climb angle should be shown with the present position of the helicopter. The pilot will be asked to fly above the safe climb angle consistent with the vehicle's potential rate of climb and forward speed. The amount of collective pitch required is dependent on weight, wind velocity, altitude, temperature, and rate of climb. Some of these parameters are related to the helicopter so that a universal solution is out of the question. Applicable performance charts are better stored in the computer with allowable rate of climb as the output. Typically, these charts take the form shown in Figure 6.

The gross weight must be known to determine the allowable rate of climb. Gross weight can be computed if the takeoff gross weight is recorded in the computer and fuel consumption is monitored. The computer could determine the performance via a table lookup or by direct solution of the equations represented by these charts.

As a result of these considerations, no automatic go-around computations are included as part of the baseline system definition. In addition, since a manual go-around probably can be provided with very little added system complexity, it is recommended that functional requirements be defined and mechanization be accomplished during the flight test program.

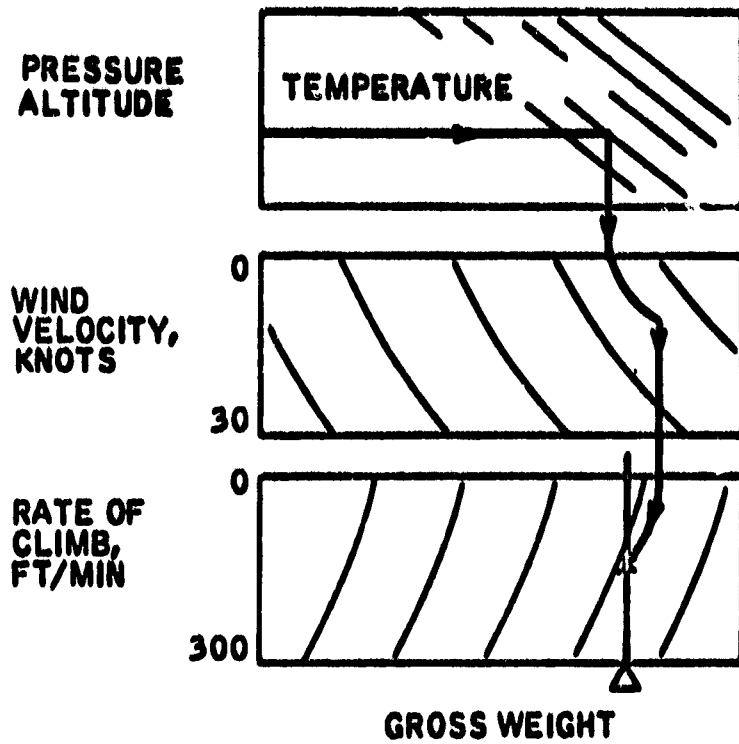


Figure 6. Typical Performance Chart

Block Diagrams

Some of the modes have been described in block diagram form (Figures 7 through 11.) These block diagrams are primarily used for sizing of the digital computer. The shaping networks and time constants will have to be determined from subsequent analysis. The block diagrams are intended to command velocities as required by the automatic flight control system. All of the functions shown in the block diagrams have been previously described in the text.

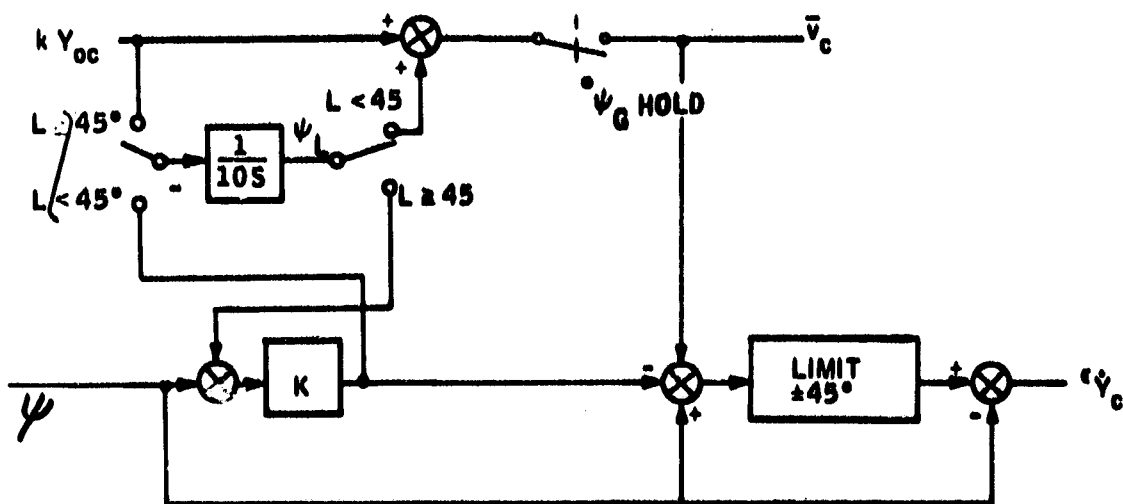


Figure 7. Heading

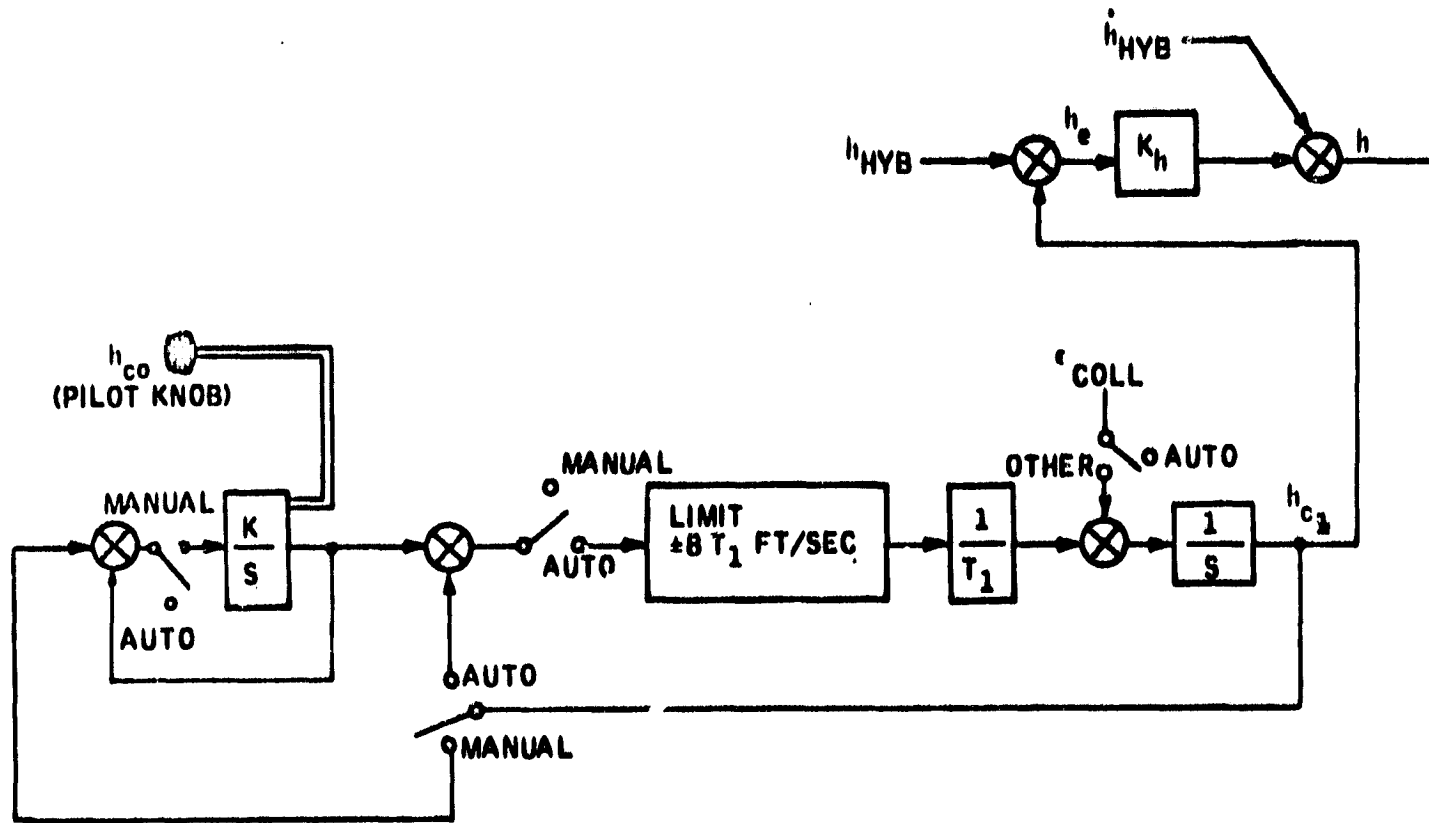


Figure 8. Altitude Control

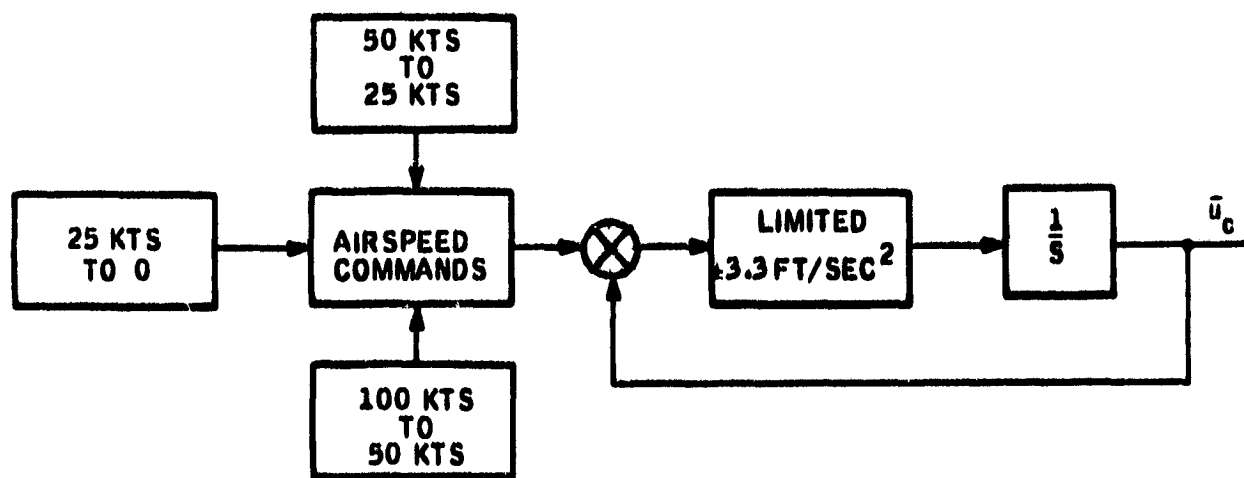


Figure 9. Airspeed Control

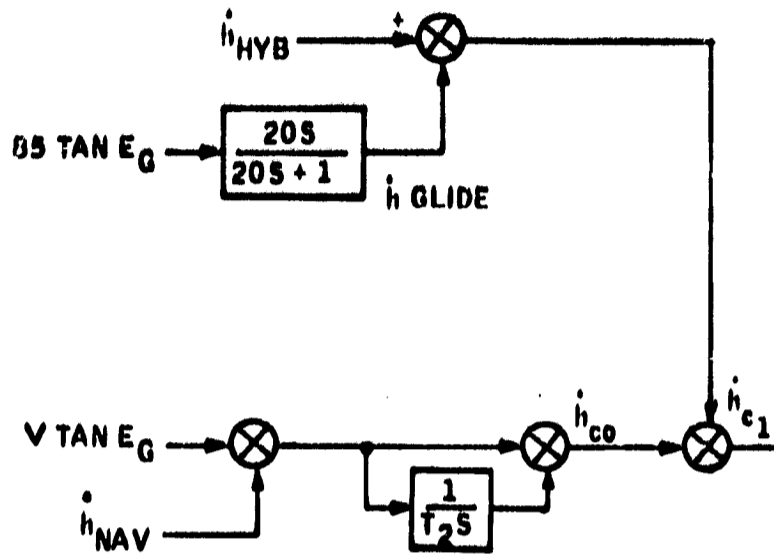


Figure 10. Glide Path

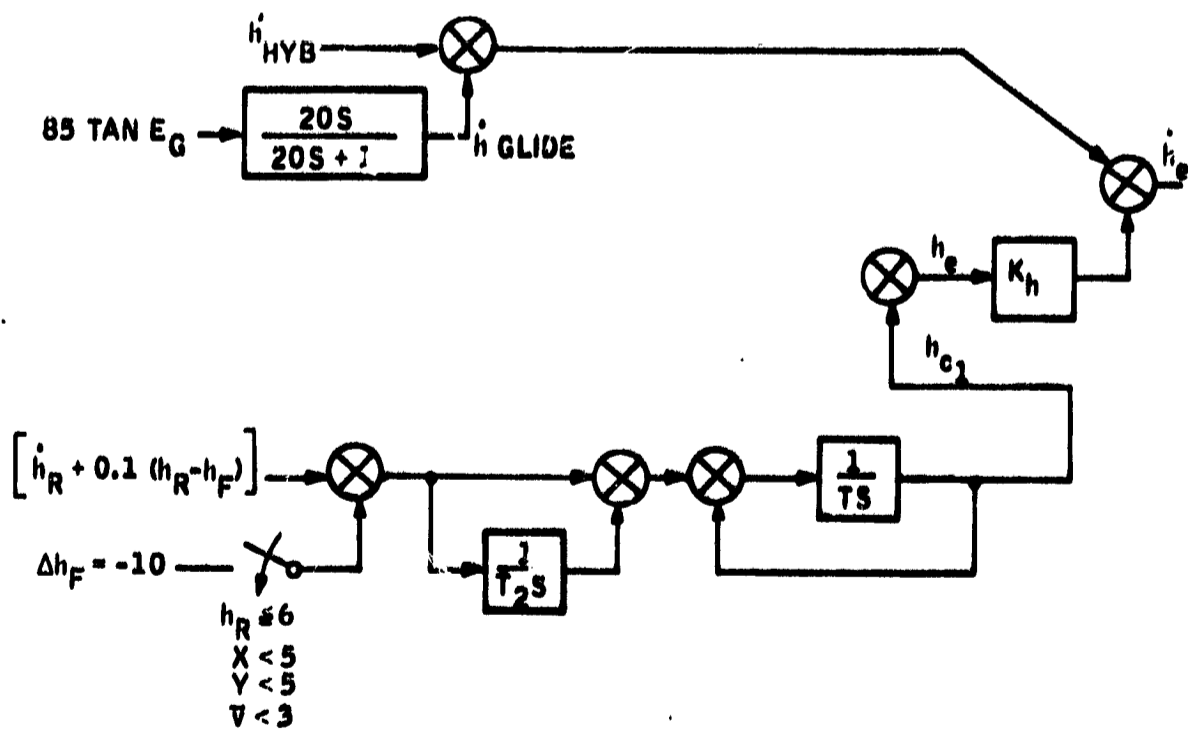


Figure 11. Flare

FLIGHT CONTROL

Scope

This section describes the baseline digital flight control system synthesized for the computer sizing task of the NASA-ERC AALS program.

The equations and diagrams in Appendix C describe the software for the baseline digital flight control system for the YHC-1A helicopter. This digital control system was "flown" on an SDS 9300/PACE 231R hybrid computer in all of its modes of operation. Results of typical flights are shown in Figures 12 and 13.

Underlying the synthesis of the digital controller was a concept of flexibility. To obtain this flexibility, four modes of flight control were synthesized: a rate damper, an attitude/heading hold, an altitude hold, and a velocity command or fully automatic guidance mode. Figures 14 and 15 show vehicle response in each of these modes for a specific input (pilot's pedal/stick or auto guidance command).

Additional studies were also performed in the areas of effects of quantization of sensor output signals, filtering requirements, sampling rates and multi-sample rate systems, and alternate mechanization of the system using analog rate gyros and an analog inner-loop stabilization system. The results of these studies are presented in the conclusions and recommendations and/or described in the discussion paragraphs.

System Description

The overall goal of the program is to develop concepts for an automatic approach and landing system for V/STOL aircraft which will utilize a strap-down inertial navigator with radar update and a central digital computer to perform digital flight control computations. The guidance output will be in the form of velocity commands to the flight control system.

The first task was to synthesize a digital flight control system which would enable the vehicle to respond to velocity commands and result in a plausible computer requirements estimate. In addition, an attempt was made to incorporate the greatest possible flight control system flexibility so that system development, ground checkout, and flight testing would be simplified. The overall goal of the system was envisioned as applied research, and therefore a need existed for a flight control system with wide capability.

Also, a goal was established that the automatic flight control system would be operable over the entire flight envelope of the NASA/LRC YHC-1A test vehicles.

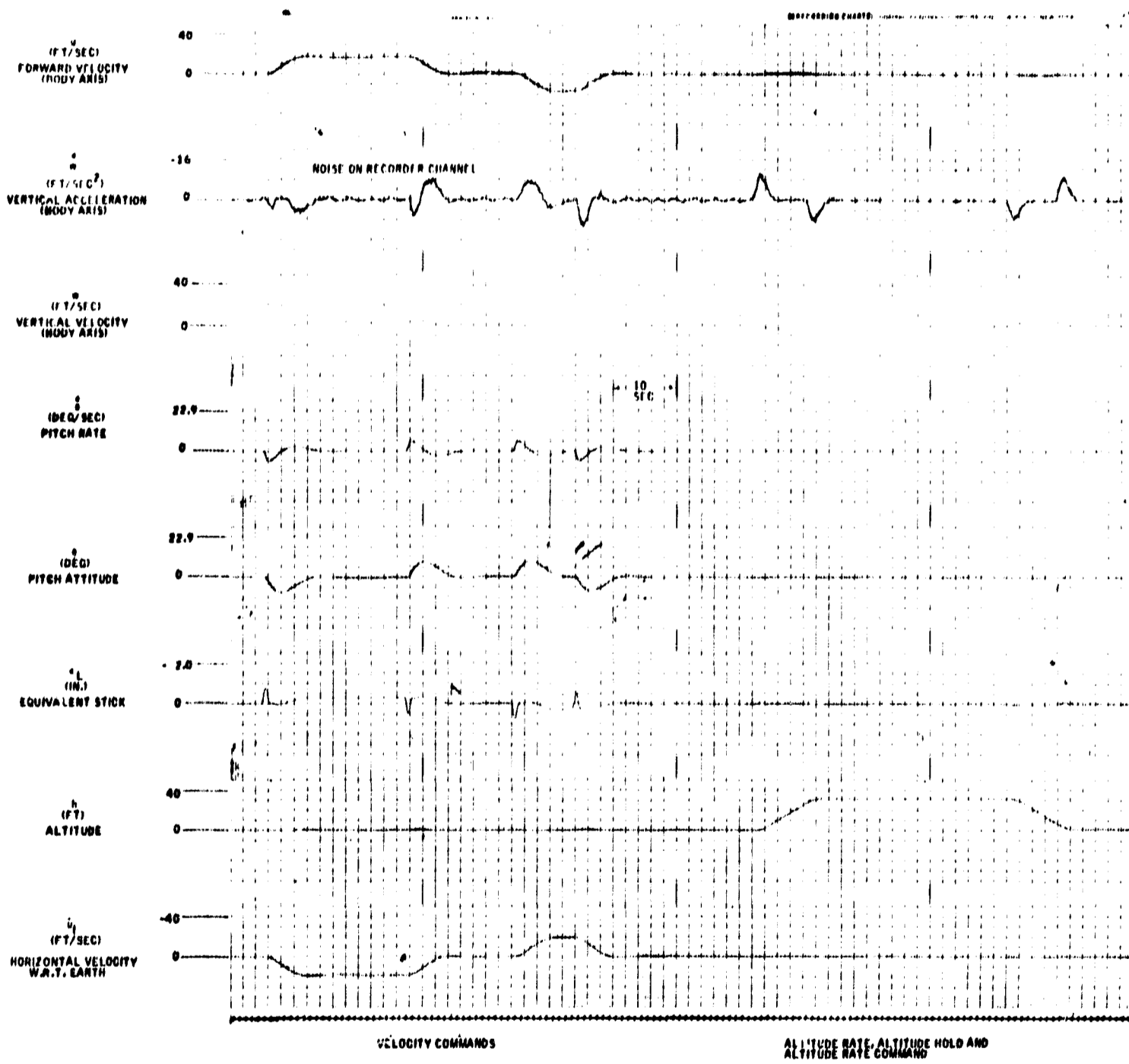


Figure 12. AFCS Pitch Axis - Hover

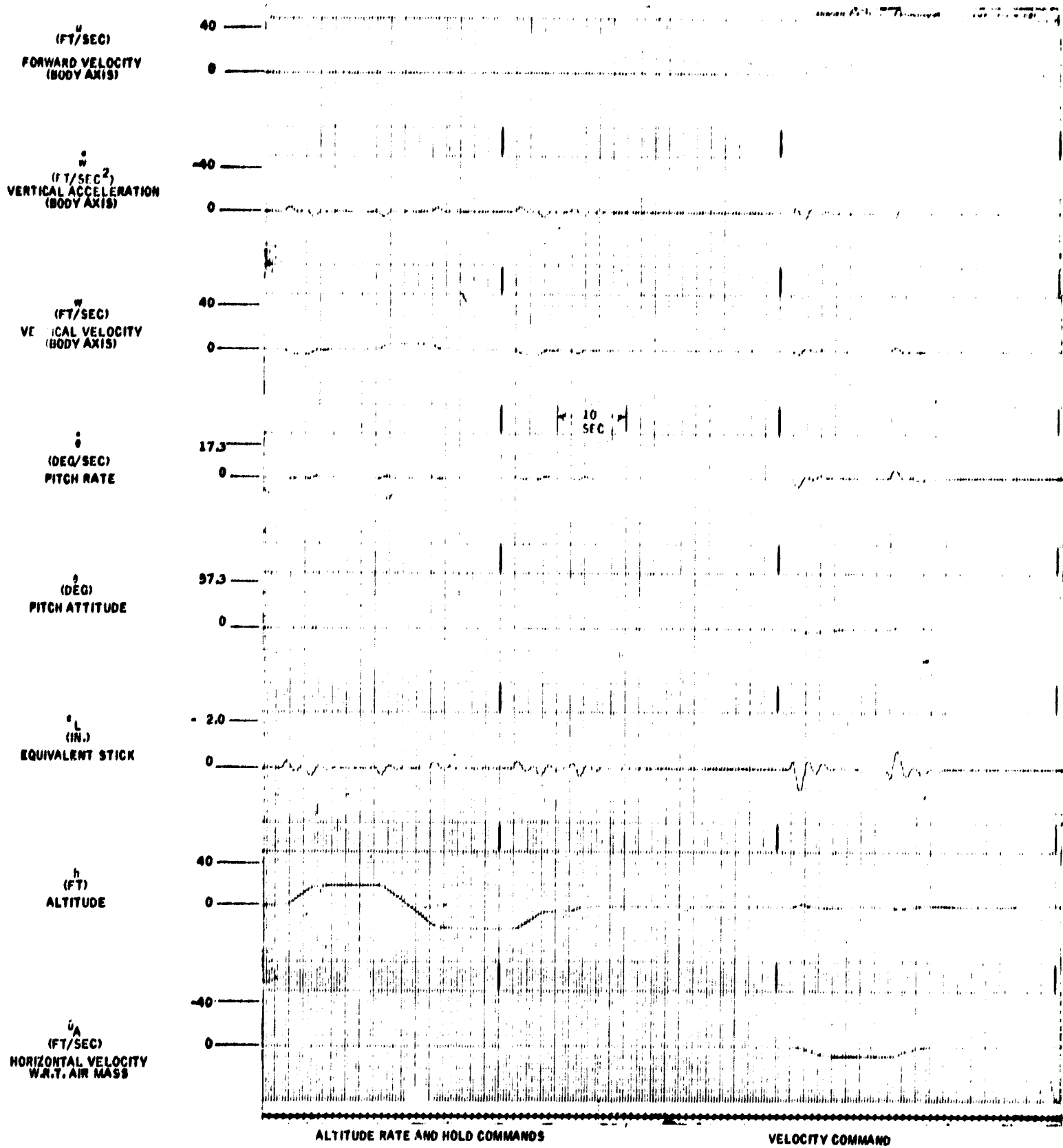


Figure 13. AFCS Pitch Axis - 100 Knots

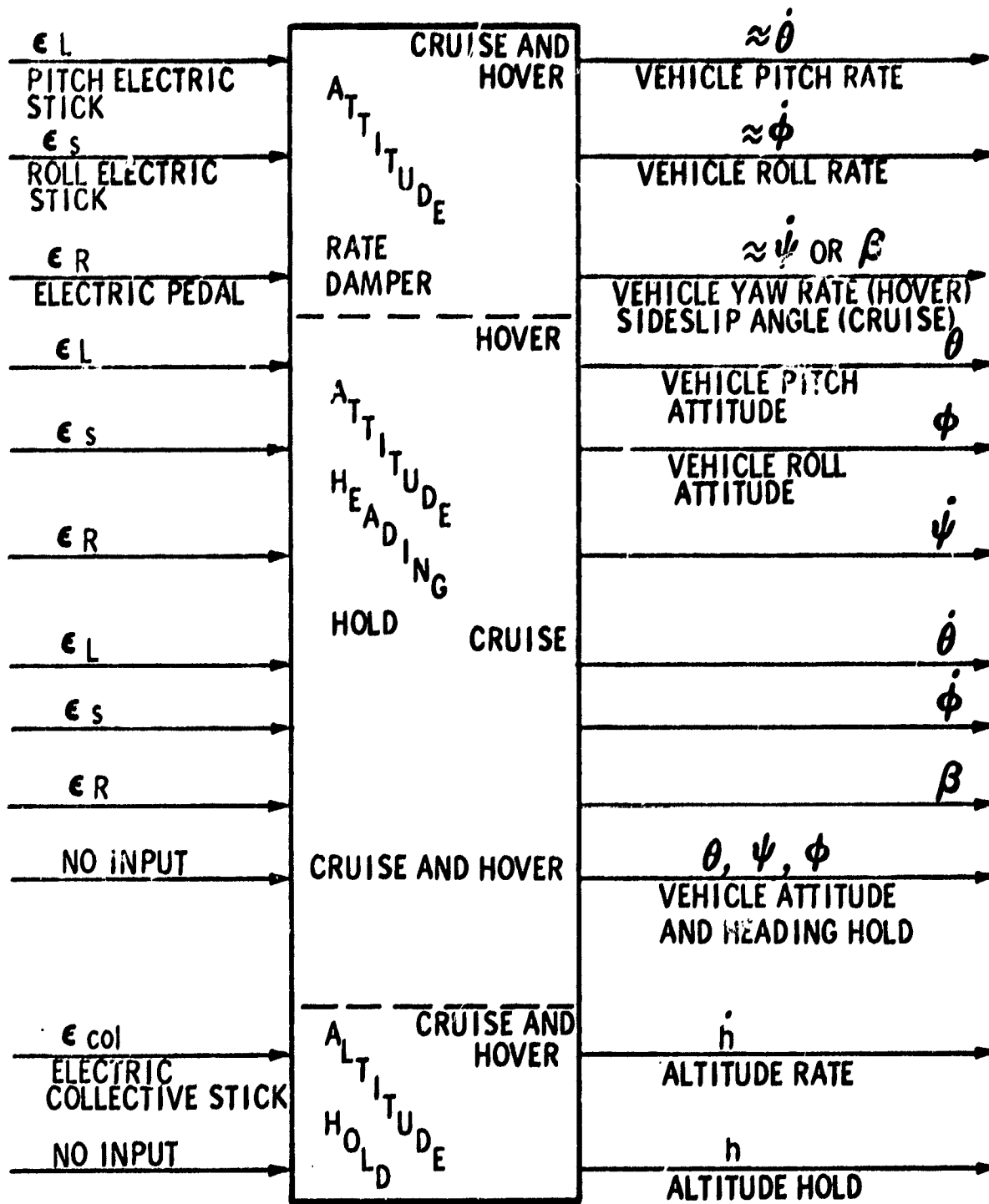


Figure 14. Input/Output, Attitude Rate Damper, and Attitude/Heading/Altitude Hold Modes

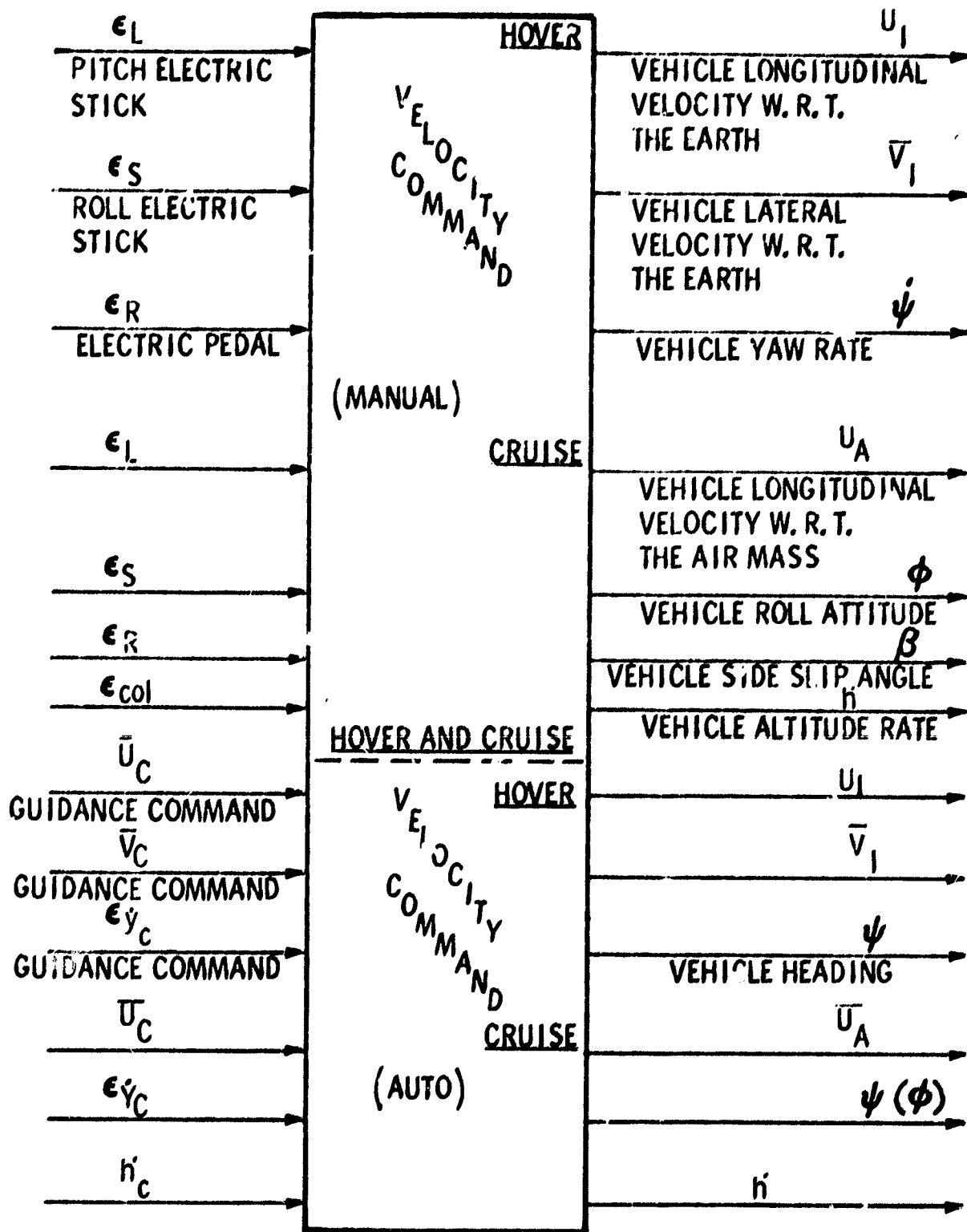


Figure 15. Input/Output Velocity Command Modes

The flight control system which evolved from this study was "flown" on the hybrid simulation. Figures 12 and 13 show typical vehicle responses for the specified inputs. Two flight conditions are shown, although a 60-knot flight condition was also examined. Note that vehicle response to commanded inputs is smooth and overshoots are acceptable.

The system involves four modes of control: rate damping, altitude hold, velocity command, and automatic guidance. Figures 14 and 15 show vehicle response for each of these modes for specified inputs. The rate damping mode is a stability augmentation system and would not be normally used other than to flight check the most basic elements of the system. The attitude/heading hold mode would normally be used for pitch control with or without altitude hold whenever the velocity command (or automatic guidance and navigation) system is not used. A unique feature of the attitude/heading hold mode is that, at hover, stick inputs result in a vehicle attitude, while, at cruise, stick inputs result in a vehicle attitude rate. This control feature has been used in other Honeywell VTOL systems, and test pilots have indicated that this type of response, particularly in gust conditions, is most desirable.

The altitude hold mode which is used in conjunction with the attitude/heading mode is self-explanatory. Stick inputs result in an altitude rate through use of an input integrator. Altitude control is obtained entirely through collective pitch. No use is made of the cyclic stick for controlling vehicle attitude to obtain altitude changes. This is in keeping with previous Honeywell helicopter studies which indicate that altitude is best controlled by collective at speeds up to about 100 knots. If other types of vehicles which will have speeds in excess of 100 knots are to be studied, then a blending of altitude to attitude control may need to be performed. However, this should not increase the complexity of the computations to any great degree.

The velocity command mode is used in conjunction with the attitude/heading hold mode and the altitude hold mode. Guidance commands in the form of velocity commands are generated by the guidance equations and input to the flight control system. Also, stick inputs result in a velocity command to the system. At the present time, stick inputs are superimposed upon velocity commands from the guidance equations. However, it may be desirable to inhibit the guidance signals whenever the stick is activated. This question of whether the stick signals should be superimposed upon or inhibit the guidance inputs should be resolved early in future studies.

The method by which various vehicle responses are obtained for various commands is obtained by logic equations and by adjusting certain gains. These gains and logic equations are described in Appendix C, which is a complete software description of the flight control system.

Difference Equations

The difference equations described in Appendix C were obtained through Tustin's method (Ref. 1). This method was used since it provides the flexibility desired in the system. With this method, the complete flight control system is divided into individual blocks. Difference equations are then

written for these individual blocks. The system can then be mathematically reassembled in any desired order simply by cascading the appropriate difference equations. Hence, logic equations may then be written to exclude or include those blocks which will give the desired response.

Sampling Frequency

The software description is based on sample rates of up to 30 samples/sec. This was determined by hybrid simulation of the flight control system. Vehicle attitude and attitude rate loops require 30 samples/sec. Honeywell, in the absence of vehicle bending data, has considered the fundamental rotor frequency (268 rpm) and the third harmonic (3 blade passages/revolution) to possess significant residues in the S domain. This would place underdamped poles at approximately 4, 5 and 13 Hz. Since half the sampling frequency should be greater than 13 Hz, the sampling frequency for the attitude control loops was chosen at 30 samples/sec.

The sampling rates of the altitude loop were highly dependent on flight condition. At hover, an altitude loop sample rate of 1 sample/sec would suffice (but not be satisfactory), while at 100 knots a sample rate of 5 samples/sec was required. Consequently, a sample rate of 10 samples/sec for the altitude control loop was selected.

For the velocity command loops, 1 sample/sec was adequate, but a smoother and more satisfactory performance was achieved with a sample rate of 2 samples/sec. In addition, it is envisioned, but not confirmed by computer results (the lateral guidance problem was not simulated), that heading guidance commands should be as high as 10 samples/sec since they would form part of the attitude hold loop. All other velocity command sample rates, as well as the altitude and attitude control system have been verified by hybrid computer simulation. Actual computer sizing was conducted for sample rates which are powers of 2. Thus, a simulation sample rate of 30/sec becomes 32/sec for the sizing model, 10/sec becomes 16/sec, and 2/sec remains the same.

Bit Weight

The baseline system for this study has no rate gyro signal. Instead, attitude rate is derived from the change of attitude signal by a first-past-difference equation in the software. The computation of this rate signal from quantized attitude signals has the same effect as that of resolution in a rate gyro in that it introduces a limit cycle oscillation. The limit cycle can be objectionable depending upon whether or not the pilot detects it. Pilot detection of the oscillation is a function of many factors including vehicle vibration, turbulence, frequency and amplitude of the oscillation and the individual pilot himself. The amplitude of the oscillation obtained in this hybrid study was on the borderline of being objectionable. As the bit weight (attitude change per pulse) is increased, so is the amplitude of the limit cycle. Currently, a bit weight of 0.0035 deg/pulse is used, although a bit weight of 0.00875 degree/pulse is desired.

Other analog signals quantized in this study were altitude, altitude rate, and velocity feedback. Bit weights of 0.25 feet (0.25 ft/sec) per pulse were used and performance was only acceptable. If the expected in-flight deterioration of these signals takes place, a bit weight of 0.1 feet (0.1 ft/sec) would be desired.

Alternate Inner-Loop Stabilization

In lieu of deriving an attitude rate signal, two alternate mechanizations were examined. These consist of using an analog rate gyro with a digital inner-loop stabilization system and an analog rate gyro with an analog inner-loop stabilization system.

The inner-loop stabilization system for the pitch and roll axes consists of the attitude rate signals which are shaped but do not pass through the integrators. For the yaw axis, the inner-loop stabilization system consists of the yaw attitude rate signal, sideslip signal, and roll rate-to-yaw signal. These signals are designated as δ_{LC_1} , δ_{SC_1} , δ_{RC_1} , δ_{RC_2} , and δ_{RC_3} on the

block diagrams in Appendix B. The rate gyro with digital inner loop reduced limit cycle oscillation by approximately a factor of five but did not reduce the minimum sample rate. With an analog inner-loop stabilization system and an analog rate gyro, the same improvement in limit cycle oscillation was noted as well as a reduction in minimum sampling of 25 percent.

Filters

The need for filtering was also examined. Previously it was stated that Honeywell, in the absence of vehicle bending data, was assuming significant residues associated with the main rotor frequency and the third harmonic. Based on this assumption, a notch filter at the main rotor frequency was included in the software. A second-order roll-off filter one octave below the third harmonic frequency was also incorporated in the software. This will reduce the gain of the system at the frequency of the third harmonic by 12 dB and in addition will serve as a noise filter.

Plant Dynamics

An examination of the analog portion of the plant was also conducted. This consisted of studying the math modeling of the servos and actuators on the CH-46 aircraft. Previous velocity command studies considered the actuators and the rotors as a 20-rad/sec lag plus a 14-rad/sec lag (see Ref. 2).

Previous studies at Honeywell on the CH-46D resulted in an actuator and rotor model of greater lag and complexity. Reference 3 states that the actuator/controls model is a 15-cycle, 0.6-damped, second-order lag. Since this value also seemed optimistic, it was agreed with NASA-ERC that an adequate model for the actuators plus control linkage would be a 15-rad/sec, 0.6-damped, second-order lag and that the rotor could be modeled by

a 27-rad/sec, 0.67-damped, second-order lag. This is the model which was used in this study.

Optimal Control

In addition to the baseline system definition studies, an independent control system synthesis was performed using optimal control techniques. This optimal control study is discussed in Appendix D.

Conclusions

As a result of the control study it was concluded that:

- 1) A digital autopilot can be synthesized for an unstable vehicle such as the YHC-1A and can control the vehicle for an automatic landing.
- 2) An analog rate gyro provides a negligible reduction in sample rate requirements. An analog inner-loop stabilization system reduces sample rate requirements by approximately 25 percent.
- 3) The effects of quantization of sensor output signals results in the general deterioration of the system in the form of introducing potentially objectionable limit cycle oscillations.
- 4) Tustin's method of mechanizing difference equations has been verified by induction.

Results obtained, however, should be treated as preliminary. Further studies are necessary to define a flightworthy system. In particular, the following should be done:

- 1) In lieu of reducing gyro and accelerometer pulse weight, methods of compensation suitable for software implementation should be studied as a means of minimizing limit cycles.
- 2) Filtering requirements are more stringent than ever with a sample data system due to the frequency folding (aliasing) phenomenon. Therefore, analysis including vehicle structural mode feedback is recommended.
- 3) It should be resolved whether, while in the velocity command mode, stick inputs should inhibit guidance command signals or whether they should be superimposed.
- 4) Optimal control studies should be conducted and the resulting control functions evaluated by simulation and flight test.

DISPLAYS

Included in the total effort for the definition of the baseline automatic approach and landing system is the task of defining relevant navigation/guidance/flight control parameters to be displayed to the aircraft crew. This task requires specification of parameters to be supplied by the AALS central computer to a display subsystem (display generator and displays). The listing of recommended parameters to be provided by the AALS central computer is fairly long. This is because of the need to retain flexibility of display design (which will depend upon final system design and operational characteristics and which should be developed analytically) at this phase of the AALS development program.

Design Considerations

Several system operational and design considerations influence the scope and size of the recommended set of parameters to be provided by the AALS central computer to the display subsystem as part of the baseline system. These considerations are discussed below.

Multi-regime operation of the aircraft. - The AALS is being developed for ultimate use in a V/STOL-type aircraft. This type of aircraft will operate in at least two different flight regimes. In one, it will operate like a conventional aircraft, with the aircraft/local-air-mass relationships being of prime importance. In the other, it will operate as a V/STOL aircraft, with the aircraft/ground relationships being of prime importance. In addition, there will be a transition zone in which the aircraft is changing from one regime to the other.

This multi-regime operational capability requires the aircraft to operate in different reference systems at different times. The relevant parameters for control will differ depending upon the current reference system. Since parameters for display must be compatible with those for control (if the displays are to be meaningful), they will also differ depending upon the current reference system.

Multiple flight-phase operation. - In addition to operating within several different reference frames for different flight regimes, the current reference frame will vary by flight phase. The total flight profile for the aircraft will consist of several phases (e.g., take-off and departure from an initial field, enroute navigation and flight management, initial approach into the landing pattern, final approach, and terminal landing operations). As the relevant reference frame changes, the appropriate parameters for display will also change.

Multiple flight control method. - The flight control method and laws used for the system could be of several types (e. g., command flight path, command attitude/airspeed, command velocity vector, etc.). For different methods of flight control, the resulting reference frame and appropriate parameters for display will vary.

Human operator functions. - Under nominal operating conditions, the pilot's functions may consist primarily of updating and adjusting automatic subsystems, selecting automatic operating modes and functions, and monitoring automatic system operation. However, in the event of automatic system failures or performance degradations, the pilot may be required to assume manual control over one or more functions. In addition, the pilot may desire to operate the system manually even if fully automatic operation is possible. To permit the pilot to "get into the loop" for manual control, he must be provided with sufficient, relevant information regarding system operation and its responses to his control inputs. This information will not necessarily be the same as that he will need for monitoring automatic system operations. For this reason, the capability to provide different displays of information for the manual control and the monitoring of automatic operation may be required.

Basic parameters. - In addition to the special navigation/guidance/flight control parameters which should be displayed for different flight regimes, flight phases, flight control methods, and human operator functions, certain parameters are considered basic by pilots and must be available for display if the system is to be considered adequate. Such parameters as attitude, altitude, altitude rate, and heading fall into the "basic" category.

Special signal conditioning. - Depending upon the flight regime, flight phase, flight control method, human operator functions, and aircraft dynamics existing at a particular time, it may be necessary to provide special conditioning of certain parameters prior to their presentation via displays. Such special conditioning would be required for quickened or predictor displays to provide a "lead" on system responses for the pilot. In general, efficient manual control of high-order control systems is not possible without some "lead". For example, for a V/STOL aircraft, the commanded pitch rate may be proportional to fore-aft stick displacements. If the pilot is attempting to control the aircraft X-position via a pitch rate control, he is operating a fourth-order control system. Unless certain related parameter derivatives (e. g., \dot{X} , \ddot{X} , θ) are added to the display of position, it is unlikely that the pilot will be able to control aircraft position. Thus, these parameter derivatives (which would perhaps never be displayed in their "raw" form) need to be combined, with appropriate relative gains, and added to position information.

Display Formats

Two example display formats are discussed below to illustrate the use of quickened or predictor displays. Both displays are of a plan position indicator (PPI) form. However, related information could be presented via vertical situation indicators or head-up displays.

Figure 16 presents a PPI format referenced to aircraft heading. It displays actual aircraft position (X_{Λ} , Y_{Λ}) as a fixed symbol (triangle). Quickened aircraft position (X_0 , Y_0) is presented as a moving symbol (asterisk). Actual landing site location (X_o , Y_o) is presented as a moving symbol (diamond). Command track is presented as a moving symbol (line intersecting the landing site in this case). Points of interest on the command flight path (e. g., glideslope intercept) are presented as tic marks on the command track. Altitude and altitude error can be presented on the linear scale and pointers at the left margin of the display. It should be noted that the diamond, command track, and tic-mark symbols could represent elements of the approach landing pattern other than landing site location, final approach command track and glideslope intercept location.

Equations for calculating the quickened aircraft position symbol parameters are given below the display drawing.

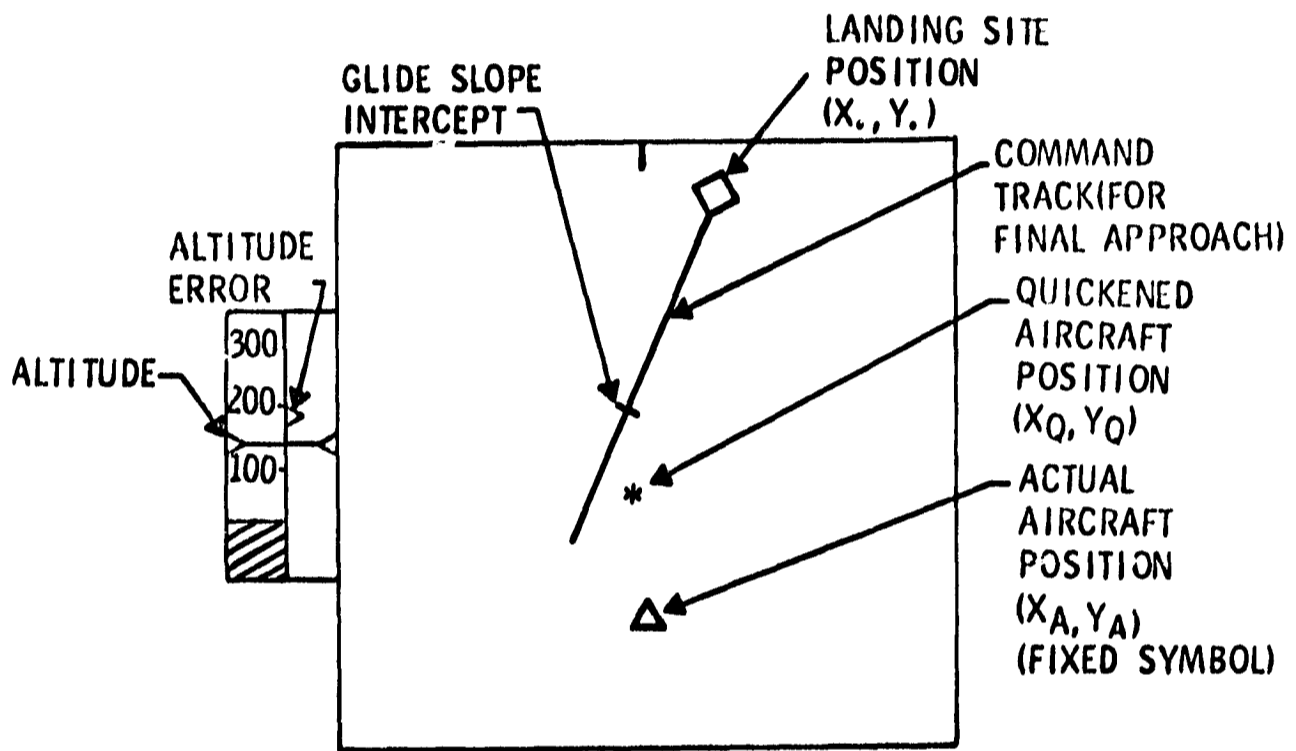
Figure 17 presents a PPI format which uses prediction. Again, the fixed diamond symbol presents actual aircraft position. The "string" of dots extending from the actual aircraft position represents the predicted X, Y path for the aircraft under present pitch, roll, wind velocity and direction, heading and airspeed conditions. The solid line represents a selected command path (e. g., the base leg of the landing pattern). The display indicates that an overshoot to command path acquisition will occur if aircraft flight conditions remain unchanged.

The equations under the figure define the terms used in calculations. These equations are integrated ahead for differing amounts of time to present the predicted path data on the display. The incremental prediction interval τ and the number of intervals n can be varied as a function of range to the selected reference point, altitude, etc.

Helicopter dynamics are assumed in each display such that airspeed is varied by pitch attitude variations and heading is varied by bank angle changes.

Candidate Parameters

It is recommended that the following navigation/guidance/flight control parameters be provided by the AALS central computer for display. This preliminary selection of recommended parameters is based on the consid-



$$X_Q = X_A + K_{\bar{u}}(R) \bar{u} + K_{\theta}(R) \theta + K_{\dot{\theta}} \dot{\theta}$$

$$Y_Q = Y_A + K_y \dot{Y}_A + K_{\phi} \phi + K_{\dot{\phi}} \dot{\phi}$$

\bar{u} = AIRCRAFT GROUND SPEED ALONG TRACK

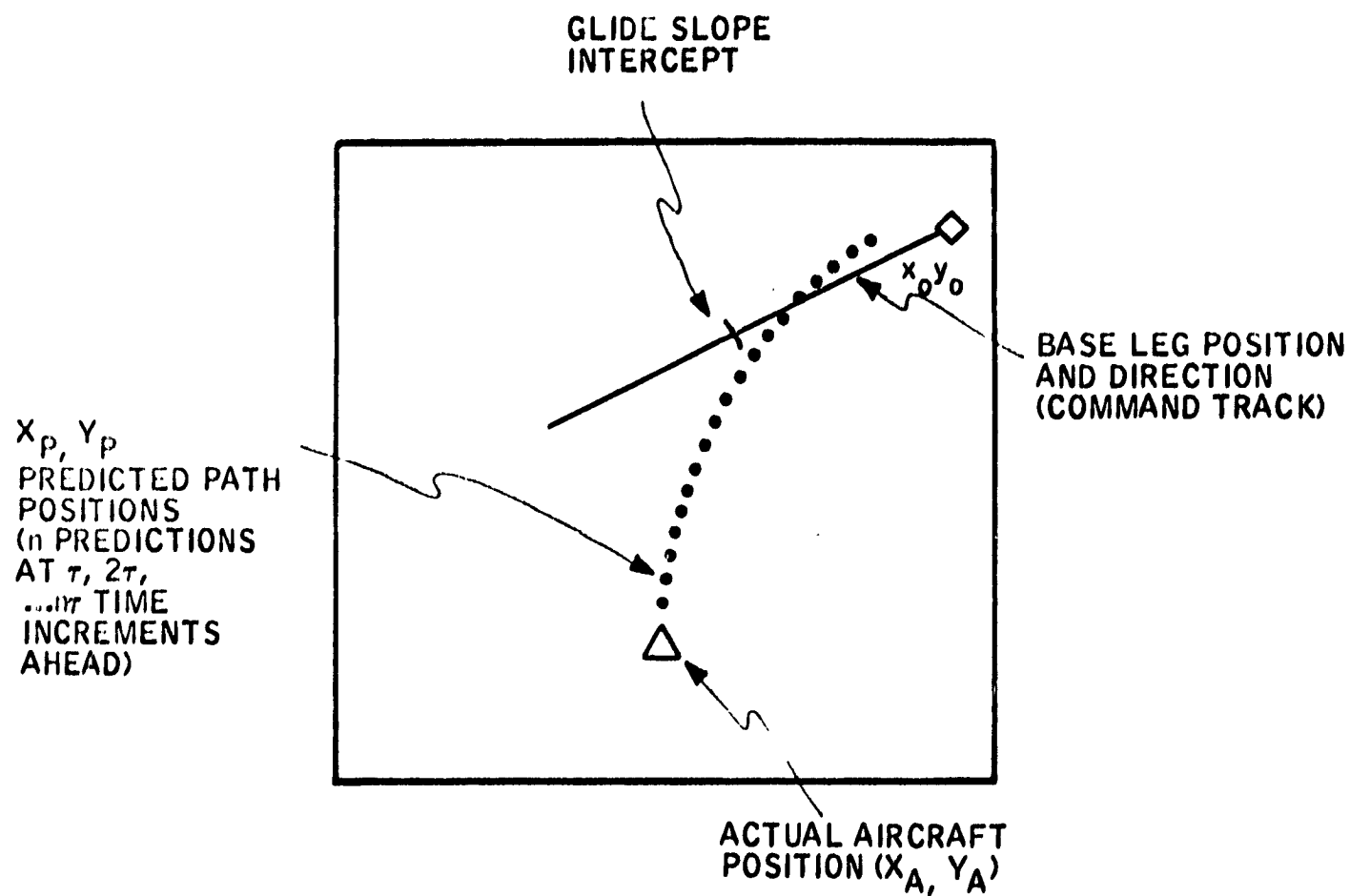
θ = AIRCRAFT PITCH ATTITUDE

ϕ = AIRCRAFT ROLL ATTITUDE

$K_{\bar{u}}, K_{\theta},$ ETC = GAINS SCHEDULED WITH RANGE TO LANDING SITE

$X_A =$
 $Y_A =$ } POSITION OF AIRCRAFT W.R.T. LANDING SITE

Figure 16. Example Quickened PPI Format



ASSUME SMALL ANGLES AND CONSTANT PITCH AND ROLL OVER THE PREDICTION TIME

$$\dot{u} + D = -g\theta$$

$$\Delta\dot{\psi} = g\phi/u$$

$$\dot{X}_p = u + V_w \cos(\psi_0 - \gamma)$$

$$\dot{Y}_p = u\Delta\psi + V_w \sin(\psi_0 - \gamma)$$

u = AIRCRAFT VELOCITY

D = AIRCRAFT DRAG

g = ACCELERATION OF GRAVITY

θ = PITCH ATTITUDE

ϕ = ROLL ATTITUDE

ψ_0 = PRESENT AIRCRAFT HEADING

X_A, Y_A = PRESENT AIRCRAFT POSITION

V_w = WIND VELOCITY

γ = WIND DIRECTION

Figure 17. Example Predictor PPI Format

erations discussed above and on the desire to retain display design flexibility at this stage of the AALS development program. Final decisions regarding the appropriate parameters for display will depend upon actual system operational and design characteristics.

The candidate parameters are categorized by the system functions to which they relate:

- 1) AALS operation parameters
 - a. Output to cyclic and differential collective control servos
 - b. Output to collective thrust control servo
- 2) Flight condition parameters
 - a. Heading
 - b. Elevation angle
 - c. Roll angle
 - d. Altitude
 - e. Altitude rate
 - f. Airspeed
- 3) Command error parameters
 - a. Longitudinal velocity error in horizontal plane
 - b. Velocity error normal to command ground track
 - c. Altitude rate error
 - d. Heading error (w. r. t. command course)
- 4) Situation parameters
 - a. Longitudinal velocity command
 - b. Lateral velocity command
 - c. Lateral velocity command (w. r. t. command course)
 - d. Command heading
 - e. Command altitude
 - f. Command altitude rate
 - g. Landing site location
 - h. Present aircraft location
 - i. Command course intersection locations
 - j. Horizontal range to specified location

- k. Ground speed
- l. Bearing to specified location
- m. Local cross-track wind velocity
- n. Final approach heading
- o. Predicted aircraft position

"Eight-Ball" Display

For early AALS evaluation flights it is anticipated that an "eight-ball" display be used to present relevant navigation/guidance/flight control information to the pilot. It is assumed that the "eight-ball" display used will be the Gemini flight director/attitude indicator. This indicator has the following display elements:

- Three-axis ball (used to display vehicle orientation Euler angles for Gemini)
- Roll needle (used to display vehicle roll angle for Gemini)
- Two cross-pointers (used to present pitch and yaw attitude errors or angular rates about the three vehicle axes for Gemini)

At the present time, it is uncertain how the Gemini indicator will be configured to display relevant AALS information for various flight phases. Because of the limited number of display elements available on the Gemini indicator, additional instruments may be required to display sufficient navigation/guidance/flight control information for adequate performance monitoring or manual control.

Also, the particular physical location and orientation of the several display elements on the Gemini indicator, and their resultant direction-of-motion characteristics, may not be suitable for the display of certain parameters (e. g., displaying altitude error on a horizontally moving cross-pointer).

For the reasons stated above, the Gemini indicator above may not be fully adequate (or fully appropriate) as the display device to be used with the AALS.

The preliminary suggested parameters for display for the initial approach, final approach, and terminal landing phases are presented below. It should be noted that, whereas basic parameters are listed, they may have to be presented in combined, quickened, or predictor form to ensure good performance with man-in-the-loop.

The parameters listed are in addition to the following basic parameters which should be displayed at all times (or be available for display at the pilot's discretion):

- Actual heading
- Actual elevation angle
- Actual roll angle
- Actual altitude
- Actual altitude rate
- Actual airspeed

Initial approach phase. - For initial approach (i. e., all operations including acquisition of the initial command track up to the turn onto the final approach), the following parameters should be displayed (or be available for display at the pilot's discretion):

- a. X-deviation from the selected command path (e. g., downwind leg or base leg)
- b. Y-deviation from the selected command path
- c. X-deviation rate
- d. Y-deviation rate
- e. Range to selected command path intersections
- f. Relative bearing to selected command path intersections.
- g. Heading error
- h. Altitude error
- i. Altitude rate error

Final approach phase. - For final approach (i. e., all operations from the turn onto the final approach to near touchdown), the following parameters should be displayed (or be available for display at the pilot's discretion):

- a. X-deviation from the commanded path
- b. Y-deviation from the commanded path
- c. X-deviation rate
- d. Y-deviation rate
- e. Range to "glideslope" intercept
- f. Range to landing site
- g. Altitude error
- h. Altitude rate error

- i. Heading error
- j. Local wind direction
- k. Local wind velocity

Terminal landing phase. - For terminal landing (i. e., operations just prior to touchdown) the following parameters should be displayed:

- a. X-deviation from the commanded path
- b. Y-deviation from the commanded path
- c. X-deviation rate
- d. Y-deviation rate
- e. Range to landing site
- f. Range rate to landing site
- g. Altitude error
- h. Altitude rate error
- i. Heading error
- j. Local wind direction
- k. Local wind velocity

Baseline System

Baseline system display functions as defined are intended to be suitable for use with an "eight-ball"-type display, with expansion to a CRT situation-type display as a goal. As such, all functions potentially useful to both the "eight-ball" and the CRT display are defined.

The form of each display function is estimated. Firm quantitative expressions require detailed analysis which is not within the scope of the present effort. It is assumed that normal flight condition information such as airspeed, sideslip, servo command, etc., will be supplied to the pilot in conventional displays. Airspeed, and other appropriate data, may also be incorporated in the CRT display. However, there will be no need for central computer involvement in this type display function.

It is anticipated that all displays will require an analog signal. Therefore, a digital-to-analog converter will be needed for display function outputs. In addition, a display generator (impedance matching, filtering for smoothing sampling ripple, symbol generation for the CRT display, etc.) will be required. The display functions which must be obtained from the central computer or computed digitally are discussed in Appendix E.

DOWN LINK

Instrumentation provisions include a "down link" (or telemetry system) to the ground. NASA/ERC intends to use modified Gemini equipment for the down link. A description of the equipment and a list of quantities for transmission has been provided by NASA/ERC. Appendix F is based on NASA-supplied information. It can be expected that the quantities transmitted on the down link will change with the purpose of specific flights. The baseline system definition includes the list given in Appendix E. However, instrumentation needs are not specifically included in the design description such as the AALS input/output signals description of Table I.

ENDING PAGE BLANK NOT FILMED.

APPENDIX A

ANALOG RATE GYRO RECOMMENDATION

Mechanization of the alternate analog inner-loop stabilization function requires an analog output attitude rate gyro. The Gemini rate gyro package (Honeywell device GG246B) should be usable in the mechanization. However, there are two areas in which care must be used. They are range available and vibration sensitivity.

Full-scale gyro output occurs at 35 deg/sec minimum. This rate may be marginal in roll and possibly in yaw. Effects should be apparent only when maneuvering at high attitude rates when in the stability augmentation mode. It is not expected that full-scale output would be reached during automatic guidance. If it does occur, it would mean only that some damping would be momentarily lost in most cases. No problem exists for manual control maneuvering, since the gyros can withstand 500-deg/sec inputs.

Vibration tests made on the Gemini rate gyro package (RGP), which NASA-ERC intends to use for instrumentation purposes, disclosed that the gyros have resonant points near the rotor frequencies. (See Honeywell report 20987-TR1, "CH-46 Attitude Control System Design Recommendation and Analysis Summary" dated 20 March 1968.) When output traces from the NASA/LRC YHC-1A test vehicle become available, they should be examined for evidence of resonant responses. The required inner-loop compensation networks will need filters for the resonances if the resonances are present as expected. The one-per-revolution frequency would be the most severe problem. A notch filter probably would be required. Roll-off filters would be satisfactory for the higher frequencies. Whether or not the gyros are usable depends on the amplitude of peaking obtained (and degree of filtering required). Whether or not it is practical to use the gyros will depend on the wear induced by the resonant response and the added complexity needed in the inner-loop compensation circuits.

Substitution of a different rate gyro is an alternate solution. Again, however, particular attention would have to be paid to vibration characteristics. It would be well to impose a vibration acceptance test in the procurement of a substitute gyro. This test should consist of base motion input vibration of ± 0.05 inch amplitude from 4.0 to 20 Hz and ± 2 g's amplitude from 20 to 500 Hz. Input should be a 15-minute scan in each axis. No resonances should be permitted at rotor or blade frequencies or harmonics of the blade frequencies or at helicopter structural frequencies. (It is assumed that any gyro procured would be qualified to MIL-E-5400 or equivalent.)

As a result of the above considerations, it is recommended that:

- 1) The Gemini rate gyro package be flight tested on the NASA/LRC YHC-1A helicopter. Gyro output in all three axes should be continuously monitored during start-up, take-off, cruise, maneuvering, let-down, hover, and shut-down.

- 2) A preliminary analog inner-loop stabilization design be made based on in-flight gyro output characteristics.
- 3) If a complex filter is needed, then the ability of alternate off-the-shelf "autopilot grade" rate gyros to meet the vibration requirements should be established. (Most available rate gyros will meet the functional requirements needed.)
- 4) If an acceptable alternate gyro(s) is found, then a decision can be made for the preferred mechanization: complex filtering versus new gyros.

APPENDIX B
NAVIGATION UPDATE INTERFACES

VORTAC INTERFACE

The VORTAC radio navigation system is a combination of the VOR (Very High Frequency Omnidirectional Range) system operating in the vhf band (around 100 MHz) and the TACAN (Tactical Air Navigation) system operating in the uhf band (around 1000 MHz).

In the VORTAC system, a TACAN station is erected to supplement an existing VOR station. The VOR station provides bearing information using a phase-difference technique, and the TACAN station provides distance information using travel time of radio waves (propagation delay). This system, when interfaced with a central airborne guidance computer, could provide range and bearing information of the aircraft from any of the many VORTAC stations located throughout the world. This will provide bearing information within two degrees and range information to about 0.1 nautical mile. This information could be used either for updating position or application to overall guidance for steering to the target station.

INTERFACE INFORMATION

The following information can be received from the VORTAC system:

- Range
- Bearing
- Station identification

Range information on the TACAN airborne system is displayed on a Veeder counter. This is a motor-driven device, and a potentiometer, encoder, or synchro could be added to the shaft to give analog, digital, or synchro information to the computer.

The present system has a variable resistor which might be used to provide a variable dc signal to go into an A/D converter of the computer.

The bearing indicator is also a motor-driven output and could easily be adapted to the outputs listed under the range information. The existing system has a synchro output which could be put into a synchro-to-digital converter of the computer. This would give 360-degree bearing information through one rotation of the synchro. In addition, an output is available in the form of a discrete level which tells whether the aircraft is heading away or toward the VORTAC transmitter. If needed, this signal could be a discrete input to the computer.

Station identification is in international morse code transmitted along with distance information. With special equipment, station identification could be converted into an address code and interfaced with the computer. With this input the entire system could be automated to provide nonambiguous position information based on VORTAC inputs.

GSN-5 INTERFACE

This section is concerned mainly with the airborne digital command system (DCS) interface with the system computer. There is no direct interface of the GSN-5 with the computer; however, the GSN-5 interface with the overall system does have a bearing on the computer interface. Therefore, in this discussion those overall characteristics of the system interface which affect the computer interface will be considered.

Inputs

DCS ready (DCS to computer). - This is a discrete signal which sets "true" after the DCS receives a set of up-link data. The total duration will not exceed 110 msec. If the computer fails to reply to this signal within the first 100 msec, the DCS will automatically reset in preparation for receipt of the next transmission.

If the computer does reply to this signal stimulation, the "true" state will prevail for the subsequent transmission of data from DCS to computer. Therefore, in this situation, the duration of "DCS ready" at the computer interface is greater than 5 and less than 10 msec subsequent to receipt by the DCS of the first data clock pulse from the computer.

Data input (DCS to computer). - Data from DCS to computer is transmitted on a serial binary line. One serial word will consist of 24 bits in an NRZ format. Frequency of transmission is 500 kHz, with a bit duration of 2 μ sec.

The data is transmitted only if a data clock is presented to the DCS, which event is contingent upon computer acceptance of the "DCS ready" discrete described above.

Outputs

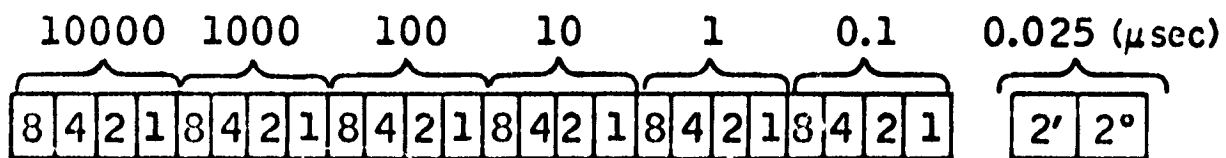
Data clock (computer to DCS). - If a "DCS ready" discrete is received and accepted by the computer, the computer will issue 24 clocking pulses to the DCS to allow clocking of data into the computer. The clock repetition rate is 500 kHz; pulse duration is 1.0 μ sec. The computer must provide the first clock pulse to the DCS within 100 msec after receipt of a "DCS ready," or else the "DCS ready" will go low, and a new transmission from the ground will occur.

LORAN C INTERFACE

This section describes typical interface signals with a Loran C receiver. It is assumed that the receiver processes the rf input and provides to the computer the applicable data in a digital format, and that the computer provides data and control to the receiver in a digital format. The signals and their associated characteristics are described below.

Inputs

Time difference (from receiver). - The 10,000- μ sec-to-0.1- μ sec time difference information is transmitted in a BCD code on 24 parallel wires. The 0.025- μ sec time difference information is sent in a standard binary code on two wires. Format is as follows:



This data is available to the computer for the "A" and "B" slaves (assuming a Loran triad consisting of a master and two slaves) in accordance with the receiver-computer timing diagram, Figure B-1.

Time difference identification (from receiver). - The "A Gate" and "B Gate" waveforms are used to gate the time-difference information as shown on the timing diagram, Figure B-1. These signals are pulse format and require two wires.

Velocity advance (from receiver). - This is a trigger pulse which instructs the computer to transmit the next word of velocity aid information to the receiver. The velocity aid information is transmitted sequentially in order: Master, Slave A, Slave B. Timing is shown in Figure B-1. This signal requires one wire.

Supply initial M velocity (from receiver). - This discrete signal instructs the computer to insert the M initial velocity information into the receiver. When this data is desired, the signal will switch to the "true" state. When the signal returns to the "false" state, normal M acceleration data is supplied to the receiver. This signal requires one wire.

Loran status (from receiver). - Four alarm signals are generated in the receiver to indicate Loran status. Typical status indications are:

- Transmitter malfunction
- Jammed receiver
- Ground wave available
- Receiver searching

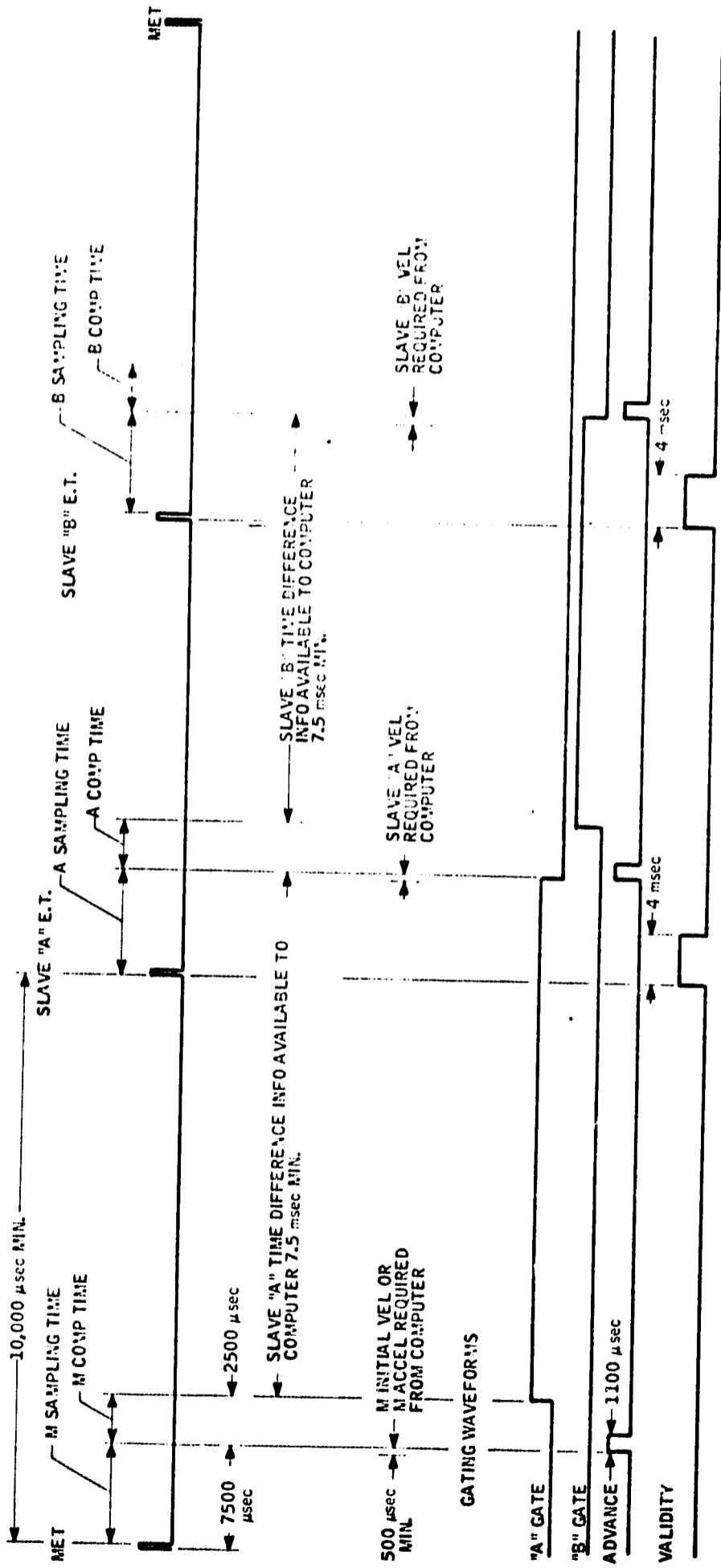


Figure B-1. Receiver - Computer Timing

In the application with which we are familiar, each indication is transmitted on an individual line, requiring a total of four wires. However, the number of indications could be increased or the number of wires decreased by coding the discrettes, if desired.

Control inputs (from control panel). - Because of the variety of modes in which the system is expected to be operated, and to allow versatility in selection of Loran station pairs, allowance should be made for control inputs from the main system control point. These signals would most likely be in the form of coded discrete levels which assume either a "true" or "false" logic state depending on operator preference. Acceptance of these discrettes at the computer could efficiently be accomplished on the "sense switch" inputs using an STE- or SKS-type instruction, as typified in the ALERT and SIGN-III computers. Approximately 10 to 15 input discrettes should be reserved for these functions. Among the functions to be handled by these discrettes are:

- PRR basic select
- PRR specific select
- Slave A or B coding delay select
- Search mode select
- Power control

Outputs

Basic rate (computer to receiver). - Provision should be made to allow selection of the basic PRR. These are switched discrete outputs changing under operator control. There are six basic rates possible; therefore, three coded discrete output lines should be reserved for this purpose.

Specific rate (computer to receiver). - Provision should be made to allow selection of the specific PRR. These are switched discrete outputs changing under operator control. There are eight specific rates possible; therefore, three coded discrete output lines should be reserved for this purpose.

Coding delay (computer to receiver). - The coding-delay information is transferred to the receiver on 16 wires in a BCD code. These signals will define the 10,000- μ sec and 1000- μ sec time difference for slaves A and B. Levels of these signals will be unchanging during the time that a particular station group is being tracked.

Velocity aid (computer to receiver). - Three kinds of velocity aid information are supplied to the receiver: slave time difference velocity aid, master acceleration aid, and master initial velocity. The information is computed from non-Loran sensors and passed to the receiver on 12 parallel lines in a binary code. The most significant bit is sign, true being positive and false being negative.

Normally, these signals are transmitted sequentially to the receiver in a master acceleration aid, slave A velocity aid, and slave B velocity aid order as instructed by the "velocity advance" waveform. During master lock-on, the receiver will request the "master initial velocity" information (see Figure B-1):

- Slave time difference velocity aid - The LSB (least significant bit) will have dimension $0.025 \mu\text{sec}/(32)$ (PRR) with accuracy to one bit.
- Master acceleration aid - The LSB will have dimensions $10 \mu\text{sec}/\text{sec}/(1024)(128)$ (PRR) with accuracy of ± 5 percent.
- Master initial velocity - The LSB will be weighted at $0.0098 \mu\text{sec}/\text{sec}$ with accuracy of ± 5 percent. This information is supplied to the receiver when requested by the "supply initial M velocity" signal.

Velocity identification (computer to receiver). - Velocity identification information should be supplied to the receiver indicating which velocity aid information is being provided. This function could be part of the parallel bus output and would require two lines. Rate of occurrence would be in accordance with the timing diagram of Figure B-1.

Start search (computer to receiver). - Three discretes (output or two coded output discrete lines) should be made available to allow the receiver to initiate master, slave A, or slave B search.

Summary

The following summarizes the expected interface requirements for Loran C:

- 26-bit parallel input bus
- 14-bit parallel output bus
- 4 pulsed discretes (input)
- 20 switched discretes (input)
- 22 switched discretes (output)
- 2 pulsed discretes (output)

DECCA INTERFACE

The DECCA radio navigation system uses hyperbolic LOPs (lines of position) to determine position fixes. In certain respects, DECCA combines features of both Loran and Omega; however, the application of these features differs in the two cited systems. Very little, if any, applications have been made where DECCA was interfaced with automatic navigation. Normally, the end output is either three visual indicators or a strip-chart-type flight log. For the application under consideration the input from receiver will have to be buffered in the input/output (I/O) to produce digital data for computer processing.

Inputs

Phase difference. - These ac inputs will be processed in pairs. Since there are three pairs, a total of six wires will be required. The pairs are designated red, green, and purple. The difference in phase between two wires of a pair represents the position within a lane, and is generated as a result of comparison between transmissions from the master and one of the slaves; i. e., red, green, or purple. One line of each of the pairs is the reference for that pair.

Input frequencies are:

- Green = 255 kHz
- Red = 340 kHz
- Purple = 425 kHz

The phase difference will vary from 0 degree to 360 degrees for each of the pairs as a lane is traversed.

The I/O should be capable of converting this ac phase difference into a digital signal for computer processing. The input to the computer central processor could then be either a serial or parallel binary interface.

Lane identification. - Three input discrettes from the receiver are required for lane identification. These discrettes occur at the rate of one per minute in the following order (L. I. = lane identification):

- Red L. I. occurs every whole minute
- Green L. I. occurs 15 seconds after red L. I.
- Purple L. I. occurs 15 seconds after green L. I.

Control inputs (from control panel). - Provision should be made for selection of mode of operation of DECCA. These would be in the form of coded discrettes and would operate in conjunction with the control inputs described in the Loran C discussion. Among the functions of these discrettes would be:

- Entry into DECCA mode
- DECCA test mode
- Reset DECCA oscillator

Outputs

Mode discrettes. - These discrettes are outputs to the receiver and are used to control the DECCA receiver as necessary to conform with the input controls described above.

APPENDIX C
BASELINE AALS AUTOMATIC FLIGHT
CONTROL SYSTEM EQUATIONS

- 1) Initialization of the difference equations is implied.
- 2) Bookkeeping terms for the difference equations are implied.
- 3) Two fader subroutines are to be included:
 - a) $\frac{s + 1}{s(2s + 1)}$
 - b) $\frac{1}{2S + 1}$
- 4) If a stick signal inhibits velocity commands from the guidance system, two velocity synchronizers will be required.

Function:

Input to AFCS

Term	Description	Units	Accuracy	Range	Resolution	Sample Rate
V_{IAS}	Indicated Air Speed from Air Data System	ft/sec			.1 ft/sec	30/sec
β	Side slip Angle from Air Data System	Rad			.00174 rad	30/sec
h_{BARO}	BARO Altitude from Air Data System	ft			.1 ft	10/sec
E_L	Pitch Electric Stick	IN			.012 IN	30/sec
E_R	Roll Electric Stick	IN			.013 IN	30/sec
E_P	Electric Pedal	IN			.005 IN	30/sec
E_{COL}	Collective Electric Stick	IN			.014 IN	10/sec
\dot{V}_{IC}	Longitudinal Velocity Command from Guidance	ft/sec			.1 ft/sec	2/sec
\dot{h}_{IC}	Altitude Rate Command from Guidance	ft/sec			.1 ft/sec	10/sec
\dot{h}_{GLIDE}	Glide Path Rate Command from Guidance	ft/sec			.1 ft/sec	10/sec
\dot{V}_C	Vehicle Side Velocity Command From Guidance	ft/sec			.1 ft/sec	2/sec
E_{Y_C}	Cross Course Velocity Command From Guidance	ft/sec			.1 ft/sec	10/sec

Function:

Input To AFCS

Term	Description	Units	Accuracy	Range	Resolution	Sample Rate
\bar{U}_I	Inertial measurement of component of Vehicle Forward Velocity in the plane parallel to earth's surface from Nav System	ft/sec			.1 ft/sec	2/sec
θ_I	Vehicle Elevation Angle (Earth Axis) from Nav System	Rad			.001 Rad	30/sec
$\phi_{R(i)}$	vehicle body angle from some arbitrary reference from Nav System where $i = 0 \rightarrow 7$	Rad			.0000145 Rad	30/sec
\dot{h}_I	Inertial Altitude Rate from Nav System	ft/sec			.1 ft/sec	10/sec
\bar{V}_I	Inertial Component of Vehicle Lateral Velocity in the plane parallel to the earth's surface from Nav System	ft/sec			.1 ft/sec	2/sec
Φ	Vehicle Roll Angle (Earth Axis) from Nav System	Rad			.001 Rad	30/sec
$\phi_{R(i)}$	Vehicle Roll Body Angle from some arbitrary reference from Nav System where $i = 0 \rightarrow 7$	Rad			.0000145 Rad	30/sec

Function:

Input To AFCS

Term	Description	Units	Accuracy	Range	Resolution	Sample Rate
$\bar{\Psi}$	Vehicle Heading Angle (Earth Axis) from Nav System	Rad			.001 Rad	30/sec
$\Psi_{(n-i)}$	Vehicle yaw body angle from an arbitrary reference from Nav System where $i=0 \rightarrow 7$	Rad			.0000145 Rad	30/sec

Function:

Output from AFCS

Term	Description	Units	Accuracy	Range	Resolution	Sample Rate
δ_{LC}	Differential Collective (Pitch) Command to Pitch EISS	IN			.00025 _{IN}	30/sec
θ_{colc}	Collective Command to Collective EISS	IN			.00025 _{IN}	10/sec
	Autopilot Altitude Command Feedback Signal to Guidance	ft			.1 ft	10/sec
δ_{RC}	Differential Cyclic (Yaw) Command to Rudder EISS	IN			.00025 _{IN}	30/sec
δ_{sc}	Cyclic (Roll) Command to Roll EISS	IN			.00025 _{IN}	30/sec

Function:

Pitch Axis A/p

Math Description:

$$G_{\dot{\epsilon}} = \text{constant}$$

$$K_{\dot{\epsilon}} = \text{constant}$$

$$K_{\epsilon_R} = \text{constant}, V_{IAS} < 50.7 \text{ ft/sec}$$

$$= \text{constant} - (V_{IAS} - 50.7) \cdot 0.355, 50.7 < V_{IAS} < 101.4 \text{ ft/sec}$$

$$= \text{constant}, V_{IAS} > 101.4 \text{ ft/sec}$$

$$K_{\epsilon_S} = \text{constant}, V_{IAS} < 50.7 \text{ ft/sec}$$

$$= \text{constant} + (V_{IAS} - 50.7) \cdot 0.355, 50.7 < V_{IAS} < 101.4 \text{ ft/sec}$$

$$= \text{constant}, V_{IAS} > 101.4 \text{ ft/sec}$$

Term	Description	Units	Accuracy	Range	Resolution	Sample Rate
$G_{\dot{\epsilon}}$	Pitch Rate damper Gain	$\frac{100 \text{ Stick}}{\text{Rad/sec}}$	—	—	—	—
$K_{\dot{\epsilon}}$	Autopilot Rate damper Gain	$\frac{100 \text{ Stick}}{\text{Rad/sec}}$	—	—	—	—
K_{ϵ_R}	Altitude Reference Gain	$\frac{100 \text{ Stick}}{\text{Rad}}$	—	—	—	30/sec
K_{ϵ_S}	Altitude Slewrate Gain	$\frac{100 \text{ Stick}}{\text{Rad}}$	—	—	—	30/sec

Function:

Pitch Axis A/P

Math Description:

$$K_{\theta c} = \text{Constant}$$

$$K_{\delta_L} = \text{Constant} \quad V_{IAS} < 50.7 \text{ ft/sec}$$

$$= \text{Constant} - (V_{IAS} - 50.7) \cdot 0.38 \quad 50.7 < V_{IAS} < 101.4 \text{ ft/sec}$$

$$= \text{Constant} \quad V_{IAS} > 101.4 \text{ ft/sec}$$

$$K_h = \text{Constant}$$

$$K_h' = \text{Constant}$$

Term	Description	Units	Accuracy	Range	Resolution	Sample Rate
$K_{\theta c}$	Velocity Command Gain	$\frac{\text{in. Stick}}{\text{ft/sec}}$	—	—	—	—
K_{δ_L}	Stick Command Gain	$\frac{\text{in. Stick}}{\text{in. Stick}}$	—	—	—	30/sec
K_h	Altitude Rate Command per Altitude Error Gain	$\frac{\text{ft/sec}}{\text{ft}}$	—	—	—	—
K_h'	Collective per Altitude Rate Error Gain	$\frac{\text{in}}{\text{ft/sec}}$	—	—	—	—

Function:

Fit to Axis F/P

Math Description:

χ = constant

$K_{\bar{u}} = 1.0 \quad V_{IAS} < 67.6 \text{ ft/sec}$

$K_{\bar{u}} = 2.0 - \frac{V_{IAS}}{500} \quad 67.6 < V_{IAS} < 135.2 \text{ ft/sec}$

$K_{\bar{u}} = 0.0 \quad 135.2 \text{ ft/sec} \leq V_{IAS}$

$K_{\text{col}} = \text{constant}$

$K_{\text{col}} = \text{constant}$

Term	Description	Units	Accuracy	Range	Resolution	Sample Rate
χ	Stick to Stick position Feedback Loop Offset	in	—	—	—	—
V_{IAS}	Indicated Airspeed	ft/sec	—	—	0.1 ft/sec	30/sec
$K_{\bar{u}}$	Velocity Reference Select Loop Gain	—	—	—	0.1 ft/sec	2/sec
K_{col}^i	Collection Gain per pitch rate	$\frac{IN}{\text{Pitch/sec}}$	—	—	—	—
K_{col}^j	Collection Gain per roll rate	$\frac{IN}{\text{Roll/sec}}$	—	—	—	—

Function:

Switch from \bar{u}_I to \bar{u}_A

Math Description:

$$\bar{u}_A = V_{TAS} \cos \theta \cos \beta$$

$$\bar{u} = K_u \bar{u}_I + (1.0 - K_u) \bar{u}_A$$

If [Navigation Switch ON] - No $\Rightarrow \Theta_c = 0.0$ (Go To Next Page)

Yes

$$\Theta_c = \bar{u} + \bar{u}_c$$

Term	Description	Units	Accuracy	Range	Resolution	Sample Rate
\bar{u}_I	Inertial measurement of component of vehicle Forward Velocity (x body axis) in the plane parallel to the earth's surface (from Nav System)	ft/sec	-	-	0.1 ft/sec	2/sec
\bar{u}_A	Air Mass measurement of component of vehicle Forward Velocity (x body axis) in the plane parallel to the earth's surface	ft/sec			0.1 ft/sec	2/sec

Function:

Pitch Axis F/P

Term	Description	Units	Accuracy	Range	Resolution	Sample Rate
θ	Vehicle Elevation Angle from Nav System	Rad	--	--	.0001 Rad	30/sec
β	Vehicle Sideslip Angle	Rad	--	--	.0017 rad	30/sec
$\dot{\theta}_c$	Angular Command	ft/sec	--	--	.1 ft/sec	2/sec
\dot{u}_c	Velocity Command from Guidance	ft/sec	--	--	.1 ft/sec	2/sec
\dot{u}	Velocity Feedback	ft/sec	--	--	.1 ft/sec	2/sec

Function:

Pitch Error 1/s

Math Description:

$$\Delta \theta_R^{(N)} = \theta_R^{(N)} - \theta_R^{(N-1)}$$

$$\dot{\theta} = \Delta \theta_R^{(N)} / T$$

$$\dot{h}_{hyb} = \dot{h}_I$$

$$h_{hyb}^{(N)} = \left\{ h_{Baro}^{(N)} \left[b + a \frac{2}{T} \right] + h_{Baro}^{(N-1)} \left[2b - a \frac{2}{T} \right] + h_{hyb}^{(N)} \left[\frac{2}{T} \right] - h_{hyb}^{(N-2)} \left[\frac{2}{T} \right] - h_{hyb}^{(N-1)} \left[2b - 2 \frac{4}{T} \right] - h_{hyb}^{(N-2)} \left[\frac{4}{T^2} - a \frac{2}{T} + b \right] \right\} / \left[\frac{4}{T^2} + a \frac{2}{T} + b \right]$$

Term	Description	Units	Accuracy	Range	Resolution	Sample Rate
θ_R	Vehicle Pitch Attitude (Arbitrary body axis) From Nav System	Rad	-	-	.00006 rad	10/sec
$\Delta \theta_R$	Incremental Vehicle Pitch Attitude	Rad	-	-	.00006 Rad	10/sec
T	Sample Period (Constant)	Sec	-	-	.0001 Sec	10/sec
\dot{h}_{hyb}	Altitude Rate From Altitude Sensing System	ft/sec	-	-	.1 ft/sec	10/sec
\dot{h}_I	Altitude Rate From Inertial Sensing System	ft/sec	-	-	.1 ft/sec	10/sec
h_{Baro}	Barometric Altitude	ft	-	-	.1 ft	10/sec
h_{hyb}	Altitude From Altitude Sensing System	ft	-	-	.1 ft	10/sec

Function:

Pitch Axis A/P

Term	Description	Units	Accuracy	Range	Resolution	Sample Rate
b	constant	-	-	-	-	-
a	constant	-	-	-	-	-
$\dot{\theta}$	Vehicle Rate (body axis)	Rad/sec	-	-	.001 Rad/sec	30/sec

Function:

Pitch Error f/p

Math Description:

$$f_1(n) = \left\{ \dot{\theta}(n) [z^{-\frac{2}{T}} + 1.0] + \dot{\theta}(n-1) [1.0 - z^{-\frac{2}{T}}] - f_1(n-1) [1.0 - z^{-\frac{2}{T}}] \right\} / [z^{-\frac{2}{T}} + 1.0]$$

$$f_2(n) = \left\{ f_1(n) [z^{-\frac{2}{T}} + 1.0] + f_1(n-1) [1.0 - z^{-\frac{2}{T}}] - f_2(n-1) [1.0 - z^{-\frac{2}{T}}] \right\} / [z^{-\frac{2}{T}} + 1.0]$$

$$f_3(n) = \left\{ 101(n) [z^{-\frac{2}{T}} + 1.0] + 101(n-1) [1.0 - z^{-\frac{2}{T}}] - f_3(n-1) [1.0 - z^{-\frac{2}{T}}] \right\} / [z^{-\frac{2}{T}} + 1.0]$$

$$|f_2| = \text{ABS}[f_2]$$

Term	Description	Units	Accuracy	Range	Resolution	Sample Rate
f_1	First Filtered Function of $\dot{\theta}$	Rad/sec	-	-	.001 Rad/sec	30/sec
f_2	Second Filtered Function of $\dot{\theta}$	Rad/sec	-	-	.001 Rad/sec	30/sec
f_3	Filtered Function of 101	Rad	-	-	.0001 Rad	30/sec
$z_5 \rightarrow z_{10}$	Constants	-	-	-	-	-
$ f_2 $	Magnitude of f_2	Rad/sec	-	-	.001 Rad/sec	10/sec

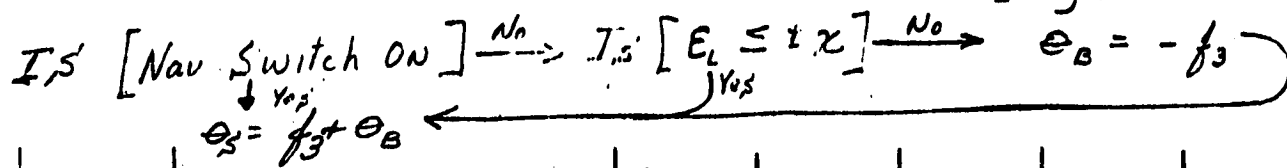
Function:

Pitch Axis A/p

Math Description:

$$\delta_{LC1}^{(N)} = \left\{ G_0 \left[\left(1.0 + 1.455 \frac{z}{T}\right) f_2(N) + \left(1.0 - 1.455 \frac{z}{T}\right) f_2(N-1) \right] - \left(1.0 - 1.59 \frac{z}{T}\right) \delta_{LC1}^{(N-1)} \right\} / \left[1.0 + 1.59 \frac{z}{T} \right]$$

$$\delta_{LC2}^{(N)} = \left\{ K_{\theta} \left[\left(1.0 + \frac{z}{T}\right) f_2(N) + \left(1.0 - \frac{z}{T}\right) f_2(N-1) \right] + K_{\theta R} \left[\left(1.0 + \frac{z}{T}\right) f_3(N) + \left(1.0 - \frac{z}{T}\right) f_3(N-1) \right] - K_{\theta L} \left[\left(1.0 + \frac{z}{T}\right) E_L(N) + \left(1.0 - \frac{z}{T}\right) E_L(N-1) \right] + \frac{z}{T} \delta_{LC2}^{(N-1)} \right\} / \frac{z}{T}$$



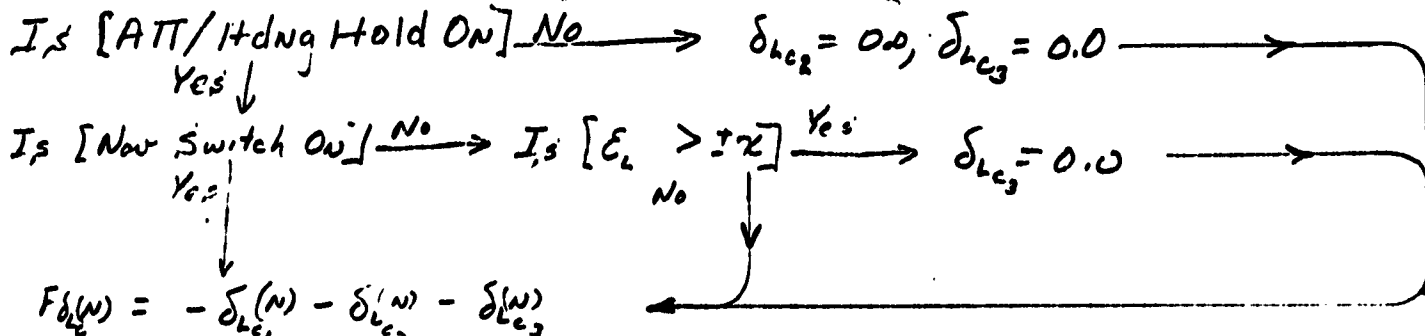
Term	Description	Units	Accuracy	Range	Resolution	Sample Rate
δ_{LC1}	Differential Collective for Pitch Rate Dampers Loop	IN	—	—	.00025 IN	30/sec
E_L	Electro Stick Input	IN	—	—	.012 IN	30/sec
θ_B	Synchronizer Bias	Rad	—	—	.0001 Rad	30/sec
θ_S	Synchronizer Output	Rad	—	—	.0001 Rad	30/sec
δ_{LC2}	Differential Collective for Autopilot Rate Dampers Loop Stick Input	IN	—	—	.00025 IN	30/sec

Function:

Pitch Axis A/P

Math Description:

$$\delta_{lc_3}^{(N)} = \left\{ K_{a_1} \left[\left(1.0 - \frac{4}{72} + 1.0 \right) \delta_{lc_1}^{(N)} + (2.0 - \frac{4}{72}) \theta_1^{(N-1)} + \left(1.5 \frac{4}{72} - 1.5 \frac{2}{7} + 1.0 \right) \theta_1^{(N-2)} \right] \right. \\ \left. - K_{a_2} \left[(1.0 + \frac{2}{7}) \theta_1 + (2.0) \theta_1^{(N-1)} + (1.0 - \frac{2}{7}) \theta_1^{(N-2)} \right] + \frac{4}{72} \delta_{lc_1}^{(N-1)} \right. \\ \left. - \left(1.5 \frac{4}{72} - \frac{2}{7} \right) \delta_{lc_1}^{(N-2)} \right\} \cdot \left[1.0 - \frac{4}{72} + \frac{2}{7} \right]$$



$$F_{\delta_{lc}}^{(N)} = -\delta_{lc_1}^{(N)} - \delta_{lc_2}^{(N)} - \delta_{lc_3}^{(N)}$$

Term	Description	Units	Accuracy	Range	Resolution	Sample Rate
δ_{lc_3}	... Velocity Command ...	IN	—	—	0.00025 IN	30/sec
$F_{\delta_{lc}}$	Total Difference ...	IN	—	—	0.00025 IN	30/sec

Function:

Pitch Axis A/p

Math Description:

$$G_{\delta_{LC}}^{(N)} = \left\{ F_{\delta_{LC}}^{(N)} \left[.001375 \frac{4}{T_c} + .0037 \frac{2}{T_c} + 1.0 \right] + F_{\delta_{LC}}^{(N-1)} \left[2.0 - .00275 \frac{4}{T_c} \right] + F_{\delta_{LC}}^{(N-2)} \left[.001375 \frac{4}{T_c} - .0037 \frac{2}{T_c} + 1.0 \right] - G_{\delta_{LC}}^{(N-1)} \left[2.0 - .00275 \frac{4}{T_c} \right] - G_{\delta_{LC}}^{(N-2)} \left[.001375 \frac{4}{T_c} - .0037 \frac{2}{T_c} + 1.0 \right] \right\} / \left[.001375 \frac{4}{T_c} + .0037 \frac{2}{T_c} + 1.0 \right]$$

$$\delta_{LC}^{(N)} = \left\{ G_{\delta_{LC}}^{(N)} + 2.0 G_{\delta_{LC}}^{(N-1)} + G_{\delta_{LC}}^{(N-2)} - \delta_{LC}^{(N-1)} \left[2.0 - .00275 \frac{4}{T_c} \right] - \delta_{LC}^{(N-2)} \left[.001375 \frac{4}{T_c} - .0037 \frac{2}{T_c} + 1.0 \right] \right\} / \left[.000595 \frac{4}{T_c} + .0244 \frac{2}{T_c} + 1.0 \right]$$

Term	Description	Units	Accuracy	Range	Resolution	Sample Rate
$G_{\delta_{LC}}$	First Filtered Function of Total Differential Collective	IN	-	-	.00025 IN	30/sec
δ_{LC}	Second Filtered Function of Total Differential Collective	IN	-	-	.00025 IN	30/sec

Function:

Collective Axis

Math Description:

$$f_5(n) = \left\{ K_{S_{col}} \left[\frac{1}{z} f_4(n) \left[z_1 \frac{z}{T} + 1.0 \right] + f_4(n-1) \left[1.0 - z_1 \frac{z}{T} \right] - f_5(n-1) \left[1.0 - z_2 \frac{z}{T} \right] \right\} / \left[z_2 \frac{z}{T} + 1.0 \right]$$

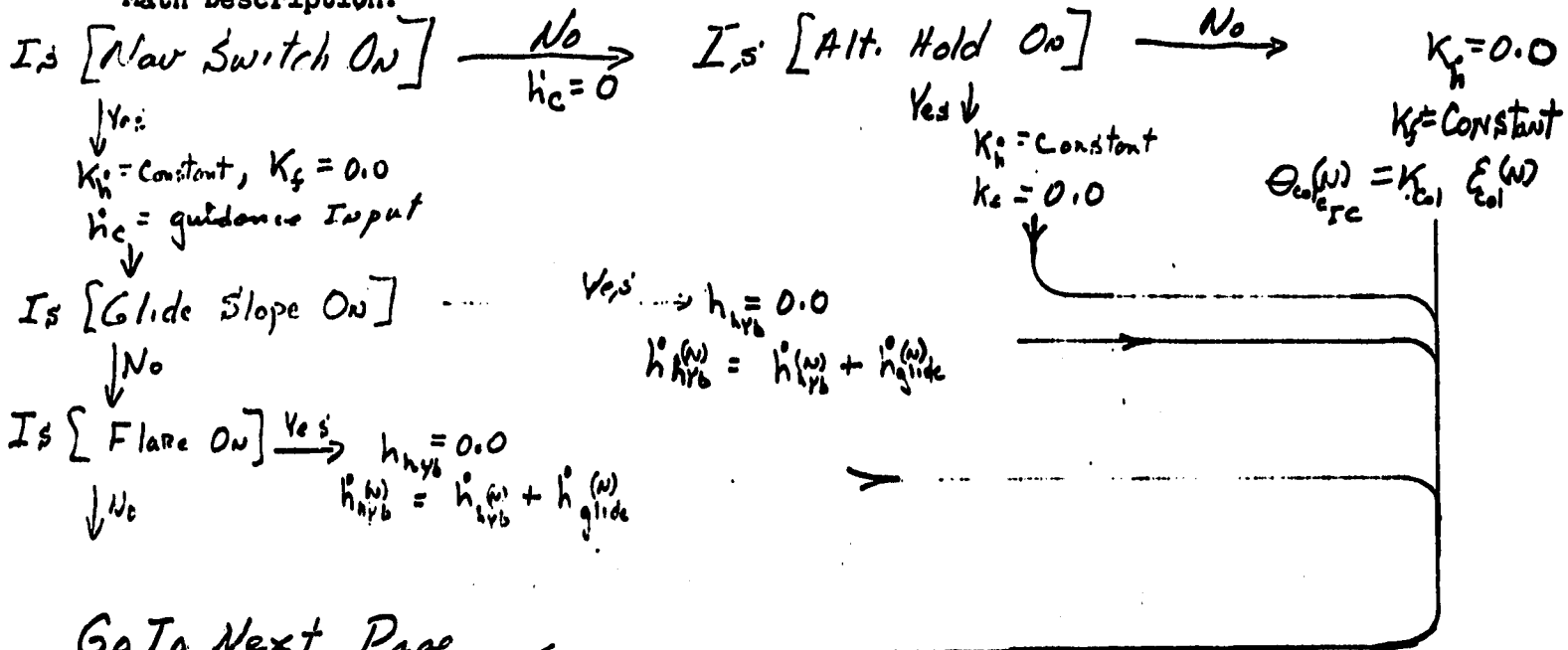
$$f_6(n) = \left\{ K_{S_{col}} \left[\frac{1}{z} f_5(n) \left[z_3 \frac{z}{T} + 1.0 \right] + f_5(n-1) \left[1.0 - z_3 \frac{z}{T} \right] - f_6(n-1) \left[1.0 - z_4 \frac{z}{T} \right] \right\} / \left[z_4 \frac{z}{T} + 1.0 \right]$$

Term	Description	Units	Accuracy	Range	Resolution	Sample Rate
$z_1 \rightarrow z_4$	Constants	—	—	—	—	—
$ f_4 $	2 nd filtered Function of $\dot{\phi}$ (Absolute Value)	Rad/sec	—	—	.001 Rad/sec	30/sec
f_5	3 rd Filtered Function of $\dot{\phi}$	Rad/sec	—	—	.001 Rad/sec	30/sec
f_6	3 rd Filtered Function of $\dot{\phi}$	Rad/sec	—	—	.001 Rad/sec	30/sec

Function:

Collective Axis

Math Description:



Go To Next Page ←

Term	Description	Units	Accuracy	Range	Resolution	Sample Rate
K_f	Feedback Gain of h_e	$\frac{ft}{sec}$	—	—	—	—
θ_{colc}	Initial Condition of θ_{colc}	IN	—	—	.014 IN	10/sec
h_{glide}	Glide Path Rate Command From Guidance	ft/sec	—	—	.1 ft/sec	10/sec
h_c	Altitude Rate Command	ft/sec	—	—	.1 ft/sec	10/sec
E_{col}	Electric Collective Stick	IN	—	—	.014 IN	10/sec

Function:

Collective Axis

Math Description:

$$h_e^{(n)} = \left\{ \frac{2}{T} h_{hyb}^{(n)} - \frac{2}{T} h_{hyb}^{(n-1)} - \dot{h}_c^{(n)} - \dot{h}_c^{(n-1)} - \epsilon_{col}^{(n)} - \epsilon_{col}^{(n-1)} - [K_f - \frac{2}{T}] h_e^{(n-1)} \right\} / \left[\frac{2}{T} + K_f \right]$$

$$\dot{h}_e^{(n)} = f_s^{(n)} + f_c^{(n)} + \dot{h}_{hyb}^{(n)} + K_h h_e^{(n)} + \theta_{col_c}^{(n)}$$

$$\theta_{col_c}^{(n)} = -K_h \dot{h}_e^{(n)}$$

$$h_{\epsilon_1}^{(n)} = \left\{ \epsilon_{col}^{(n)} + \epsilon_{col}^{(n-1)} + \dot{h}_e^{(n)} + \dot{h}_e^{(n-1)} + \frac{2}{T} h_e^{(n-1)} \right\} / \frac{2}{T}$$

Term	Description	Units	Accuracy	Range	Resolution	Sample Rate
h_e	Altitude Error Signal	ft.	—	—	.1 ft	10/sec
\dot{h}_e	Altitude Rate ERROR Signal	ft/sec	—	—	.1 ft/sec	10/sec
θ_{col_c}	Collective Command to EISS	IN	—	—	.00025 IN	10/sec

Function:

Lateral A/P

Math Description:

$$K_{\phi_R} = \text{Constant}$$

$$V_{IAS} < 50.7 \text{ ft/sec}$$

$$K_{\phi_R} = \text{Constant} - .435(V_{IAS} - 50.7)$$

$$50.7 \leq V_{IAS} \leq 101.4 \text{ ft/sec}$$

$$K_{\phi_R} = \text{Constant}$$

$$V_{IAS} > 101.4 \text{ ft/sec}$$

$$K_{\phi_S} = \text{Constant}$$

$$V_{IAS} < 50.7 \text{ ft/sec}$$

$$K_{\phi_S} = \text{Constant} + .435(V_{IAS} - 50.7)$$

$$50.7 \leq V_{IAS} \leq 101.4 \text{ ft/sec}$$

$$K_{\phi_S} = \text{Constant}$$

$$V > 101.4 \text{ ft/sec}$$

$$G_{\dot{\phi}_R} = \text{Constant}$$

Term	Description	Units	Accuracy	Range	Resolution	Sample Rate
K_{ϕ_R}	Roll Attitude Reference Gain	$\frac{\text{IN stick}}{\text{Rad}}$	—	—	—	30/sec
K_{ϕ_S}	Roll Attitude Synchronization Gain	$\frac{\text{IN stick}}{\text{Rad}}$	—	—	—	30/sec
$G_{\dot{\phi}_R}$	Roll Rate to differential cyclic (Rudder) Gain	$\frac{\text{on Pedal}}{\text{Rad/sec}}$	—	—	—	—

Function:

Lateral A/P

Math Description:

$$G_{\dot{\phi}} = \text{Constant}$$

$$K_{\dot{\phi}} = \text{Constant}$$

$$K_{\delta_s} = \text{Constant}$$

$$V_{IAS} < 50.7 \text{ ft/sec}$$

$$= \text{Constant} - .0277 (V_{IAS} - 50.7)$$

$$50.7 \leq V_{IAS} \leq 101.4 \text{ ft/sec}$$

$$= \text{Constant}$$

$$V_{IAS} > 101.4 \text{ ft/sec}$$

$$G_{\dot{\psi}} = \text{Constant}$$

Term	Description	Units	Accuracy	Range	Resolution	Sample Rate
$G_{\dot{\phi}}$	Roll Rate Damper Gain	<u>IN stick</u> Rad/sec	—	—	—	—
$K_{\dot{\phi}}$	Autopilot Roll Rate Gain	<u>IN stick</u> Rad/sec	—	—	—	—
K_{δ_s}	Roll stick Command Gain	<u>IN stick</u> <u>IN stick</u>	—	—	—	30/sec
$G_{\dot{\psi}}$	Yaw Rate Damper Gain	<u>IN Pedal</u> Rad/sec	—	—	—	—

Function:

External A/p

Math Description:

$K_{Vz} = \text{Constant}$

$V_{z0} < 200 \text{ ft/sec}$

$K_{Vz} = \text{Constant} - 0.028(V_{z0}^2)$

$V_{z0} > 200 \text{ ft/sec}$

$K_{Vz} = 0.0$

$V_{z0} > 200 \text{ ft/sec}$

$K_{Vz} = 0.0$

$V_{z0} < 200 \text{ ft/sec}$

$K_{Vz} = .37 V_{z0}$

$V_{z0} > 200 \text{ ft/sec}$

$G_z = 0.0$

$V_{z0} < 200 \text{ ft/sec}$

$G_z = .124 V_{z0}$

$V_{z0} > 200 \text{ ft/sec}$

Term	Description	Units	Accuracy	Range	Resolution	Sample Rate
K_{Vz}	Velocity Command Gain	1/ft/sec	-	-	-	2/sec
K_{Vz}	Heading Error Gain	1/ft/sec	-	-	-	-
G_z	Heading Error Gain	1/ft/sec	-	-	-	-

Function:

Lateral A/P

Math Description:

$K_{V_c} = 0.0$ $V_{IAS} < 50.7 \text{ ft/sec}$

$K_{V_c} = k V_{IAS}$ $V_{IAS} \geq 50.7 \text{ ft/sec}$

K_{S_R} - Constant

$K_{H_L} = \text{Constant}$ $V_{IAS} < 50.7 \text{ ft/sec}$

$K_{H_L} = 0.0$ $V_{IAS} \geq 50.7 \text{ ft/sec}$

$K_{V_c} = \text{Constant}$ $V_{IAS} < 50.7 \text{ ft/sec}$

$K_{V_c} = 0.0$ $V_{IAS} \geq 50.7 \text{ ft/sec}$

XX = Constant

XXX = Constant

Y = Constant

Term	Description	Units	Accuracy	Range	Resolution	Sample Rate
K_{V_c}	Velocity Command Gain	$\frac{\text{IN Stick}}{\text{ft/sec}}$	—	—	—	10/sec
K_{S_R}	Pedal to differential Collective (Rudder) Gain	$\frac{\text{IN Pedal}}{\text{IN Pedal}}$	—	—	—	30/sec
K_{H_L}	Heading to differential Collective Gain	$\frac{\text{IN Pedal}}{\text{Rad}}$	—	—	—	30/sec
K_{V_c}	Heading Command to differential Collective Gain	$\frac{\text{IN Pedal}}{\text{Rad}}$	—	—	—	10/sec
XX	Roll Stick to Synchronizer Breakout Logic Deadband	IN	—	—	—	—
XXX	Pedal to Synchronizer Breakout Logic Deadband	IN	—	—	—	—
Y	Roll Synchro Deadband	Rad	—	—	—	—

Function:

Lateral A/P

Math Description:

$$\Delta \phi_R(N) = \phi_R(N) - \phi_R(N-1)$$

If [New System] $\xrightarrow{\text{No}}$ $\phi_c = 0.0, \epsilon_{\dot{y}_c} = 0.0$
 (goto next Para.)
 \downarrow Yes

$$\phi_c = \bar{v}_I - \bar{v}_c$$

Term	Description	Units	Accuracy	Range	Resolution	Sample Rate
$\Delta \phi_R$	Incremental Vehicle Roll Angle (Body Axis)	Rad	—	—	.00006 Rad	30/sec
ϕ_R	Vehicle Roll Angle (Arbitrary Initial Phase) From New System	Rad	—	—	.00006 Rad	30/sec
\bar{v}_I	Vehicle Side Velocity W.R.T. earth from Nav System	ft/sec	—	—	.1 ft/sec	2/sec
\bar{v}_c	Vehicle Side Velocity command from Guidance	ft/sec	—	—	.1 ft/sec	2/sec
$\dot{\phi}_c$	Vehicle Roll Command	ft/sec	—	—	.1 ft/sec	2/sec
$\epsilon_{\dot{y}_c}$	Cross Course Velocity Error Command	ft/sec	—	—	.1 ft/sec	10/sec

Function:

Lateral A/P

Math Description:

$$\dot{\phi}(N) = \Delta \phi(N) / T$$

$$\Delta \psi_R(N) = \psi_R(N) - \psi_R(N-1)$$

$$\dot{\psi}_R(N) = \Delta \psi_R(N) / T$$

Term	Description	Units	Accuracy	Range	Resolution	Sample Rate
$\dot{\phi}$	Vehicle Roll Rate	Rad/sec	---	---	.001 Rad/sec	30/sec
$\dot{\psi}$	Vehicle Yaw Rate	Rad/sec	---	---	.001 Rad/sec	30/sec
$\Delta \psi_R$	incremental Heading Angle	Rad	---	---	.00006 rad	30/sec
ψ_R	Vehicle Yaw Angle from Nav System	Rad	---	---	.00006 rad	30/sec

Function:

Lateral A/p

Math Description:

$$L_1(n) = \left\{ \left[\frac{\tau_{10}}{T} + 1 \right] L_1^{(n)} + \left[1.0 - \frac{\tau_{10}}{T} \right] L_1^{(n-1)} - \left[1.0 - \frac{\tau_{18}}{T} \right] L_1^{(n-2)} \right\} / \left[1.0 + \frac{\tau_{18}}{T} \right]$$

$$L_4(n) = \left\{ \left[\frac{\tau_{19}}{T} + 1.0 \right] L_4^{(n)} + \left[1.0 - \frac{\tau_{19}}{T} \right] L_4^{(n-1)} - \left[1.0 - \frac{\tau_{20}}{T} \right] L_4^{(n-2)} \right\} / \left[1.0 + \frac{\tau_{20}}{T} \right]$$

$$L_{11}(n) = \left\{ \left[\frac{\tau_{21}}{T} + 1.0 \right] \Phi^{(n)} + \left[1.0 - \frac{\tau_{21}}{T} \right] \Phi^{(n-1)} - \left[1.0 - \frac{\tau_{22}}{T} \right] \Phi^{(n-2)} \right\} / \left[1.0 + \frac{\tau_{22}}{T} \right]$$

$$L_9(n) = \left\{ \left[\frac{\tau_{16}}{T} + 1.0 \right] \Psi^{(n)} + \left[1.0 - \frac{\tau_{16}}{T} \right] \Psi^{(n-1)} - \left[1.0 - \frac{\tau_{16}}{T} \right] \Psi^{(n-2)} \right\} / \left[1.0 + \frac{\tau_{16}}{T} \right]$$

Term	Description	Units	Accuracy	Range	Resolution	Sample Rate
$\tau_{10} - \tau_{22}$	Constants	—	—	—	—	—
L_1	First Filtered Function of $\dot{\phi}$	Rad/sec	—	—	.0001 Rad/sec	30/sec
L_4	Second Filtered Function of $\dot{\phi}$	Rad/sec	—	—	.0001 Rad/sec	30/sec
L_{11}	Filtered Function of ϕ	Rad	—	—	.0001 Rad	30/sec
L_9	Filtered Function of ψ	Rad	—	—	.0001 Rad	30/sec
Φ	Vehicle Roll Angle (Earth Axis) From Nav System	Rad	—	—	.0001 Rad	30/sec
Ψ	Vehicle Heading Angle (Earth Axis) From Nav System	Rad	—	—	.0001 Rad	30/sec

REPRODUCIBILITY OF THE ORIGINAL PAGE IS POOR.

Function:

Lateral A/p

Math Description:

$$\delta_{sc_1}^{(N)} = \left\{ G \phi \left[f_{sc_1}^{(N)} \left[\frac{2}{T} + 1.0 \right] + \frac{1}{4} (N-1) \left[1.0 - \frac{2}{T} \right] \right] - \delta_{sc_1}^{(N-1)} \left[1.0 - \frac{2}{T} \right] \right\} / \left[\frac{2}{T} + 1.0 \right]$$

$$\delta_{sc_2}^{(N)} = \left\{ K_{\phi} \left[f_{sc_2}^{(N)} \left[\frac{2}{T} + 1.0 \right] + \frac{1}{4} (N-1) \left[1.0 - \frac{2}{T} \right] \right] - K_{\phi} \left[f_{sc_2}^{(N-1)} \left[\frac{2}{T} + 1.0 \right] + \frac{1}{4} (N-1) \left[1.0 - \frac{2}{T} \right] \right] \right. \\ \left. - K_{\delta} \left[\epsilon_s^{(N)} \left[\frac{2}{T} + 1.0 \right] + \epsilon_s^{(N-1)} \left[1.0 - \frac{2}{T} \right] \right] + \delta_{sc_2}^{(N-1)} \frac{2}{T} \right\} / \left[\frac{2}{T} \right]$$

Term	Description	Units	Accuracy	Range	Resolution	Sample Rate
δ_{sc_1}	Roll Cyclic per Roll Rate Dampen	IN	-	-	.00025 IN	30/Sec
δ_{sc_2}	Roll Cyclic per Roll Attitude and Stick Input	IN	-	-	.00025 IN	30/Sec
ϵ_s	Elevator Stick Limit (Roll)	IN	-	-	.013 IN	30/Sec

Function:

Lateral A/p

Math Description:

$$f_7^{(N)} = \left\{ \left[z_{11} \frac{z}{T} + 1.0 \right] \dot{\psi}(N) + \left[1.0 - z_{11} \frac{z}{T} \right] \dot{\psi}^{(N-1)} - \left[1.0 - z_{12} \frac{z}{T} \right] f_7^{(N-1)} \right\} / \left[1.0 + z_{12} \frac{z}{T} \right]$$

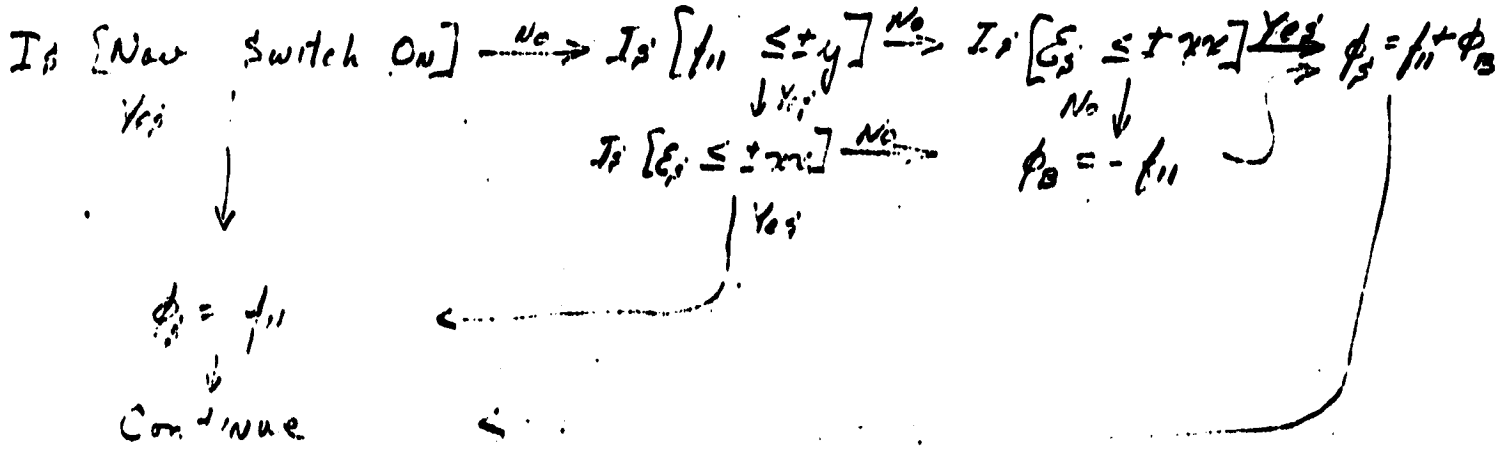
$$f_8^{(N)} = \left\{ \left[z_{13} \frac{z}{T} + 1.0 \right] f_7^{(N)} + \left[1.0 - z_{13} \frac{z}{T} \right] f_7^{(N-1)} - \left[1.0 - z_{14} \frac{z}{T} \right] f_8^{(N-1)} \right\} / \left[1.0 + z_{14} \frac{z}{T} \right]$$

Term	Description	Units	Accuracy	Range	Resolution	Sample Rate
$z_{11} \rightarrow z_{14}$	Constants	—	—	—	—	—
f_7	First Filtered Function of $\dot{\psi}$	Rad/sec	—	—	.001 Rad/sec	30/sec
f_8	Second Filtered Function of $\dot{\psi}$	Rad/sec	—	—	.001 Rad/sec	30/sec

Functions:

Lateral A/P

Math Descriptions:



Term	Description	Units	Accuracy	Range	Resolution	Sample Rate
ϕ_B	Synchronizer Roll Bias	Rad	—	—	.0001 Rad	30/sec
ϕ_s	Synchronizer Output Roll	Rad	—	—	.0001 Rad	30/sec

REPRODUCIBILITY OF THE ORIGINAL PAGE IS POOR.

Functions:

Lateral Flip

Math Description:

$$I = \text{[New Function Data]} \quad \text{---} \quad T_0 \text{ [} \epsilon_0 \leq \text{true and } \epsilon_R \leq \text{true]} \text{---} \quad \text{No. } \psi_B = -f_9$$

$$\downarrow \text{Yes} \quad \text{Yes}$$

$$\psi_B = -f_9$$

$$\downarrow$$

$$\psi_2 = f_9 + \psi_{12}$$

Term	Description	Units	Accuracy	Range	Resolution	Sample Rate
ψ_B	Heading Synthesizer Bias	Rad	-	-	.0001 Rad	30/sec
ψ_{12}	Heading Synthesizer Output	Rad	-	-	.0001 Rad	30/sec
ϵ_R	Electric Pedal Input (Yaw)	IN	-	-	.005IN	30/sec

Function:

Lateral A/P

Math Description:

$$\delta_{sc3}(\omega) = \left\{ K_{\phi_s} \left[\phi_s(\omega) \left[.5 \frac{4}{7^2} + 1.5 \frac{2}{7} + 1.0 \right] + \phi_s(\omega-1) \left[2.0 - \frac{4}{7^2} \right] + \phi_s(\omega-2) \left[1.0 - 1.5 \frac{2}{7} + .5 \frac{4}{7^2} \right] \right. \right. \\ \left. \left. + K_{\phi_c} \left[\phi_c(\omega) \left[\frac{2}{7} + 1.0 \right] + \phi_c(\omega-1) \left[2.0 \right] + \phi_c(\omega-2) \left[1.0 - \frac{2}{7} \right] \right] + \delta_{sc1}(\omega-1) \left[\frac{4}{7^2} \right] \right. \right. \\ \left. \left. - \delta_{sc3}(\omega-2) \left[.5 \frac{4}{7^2} - \frac{2}{7} \right] \right\} / \left[.5 \frac{4}{7^2} + \frac{2}{7} \right]$$

$$\delta_{scy}(\omega) = \left\{ K_{\psi_s} \left[\psi_s(\omega) \left[.5 \frac{4}{7^2} + 1.5 \frac{2}{7} + 1.0 \right] + \psi_s(\omega-1) \left[2.0 - \frac{4}{7^2} \right] + \psi_s(\omega-2) \left[1.0 - 1.5 \frac{2}{7} + .5 \frac{4}{7^2} \right] \right. \right. \\ \left. \left. - K_{\psi_c} \left[\psi_c(\omega) \left[\frac{2}{7} + 1.0 \right] + \psi_c(\omega-1) \left[2.0 \right] + \psi_c(\omega-2) \left[1.0 - \frac{2}{7} \right] \right] + \delta_{scy}(\omega-1) \left[\frac{4}{7^2} \right] \right. \right. \\ \left. \left. - \delta_{scy}(\omega-2) \left[.5 \frac{4}{7^2} - \frac{2}{7} \right] \right\} / \left[.5 \frac{4}{7^2} + \frac{2}{7} \right]$$

Term	Description	Units	Accuracy	Range	Resolution	Sample Rate
δ_{scy}	Roll Cyclic per Heading Synchronizer and Velocity Command (cross course)	IN	—	—	.0025 IN	30/sec
δ_{sc3}	Roll Cyclic per Roll Synchronizer and Velocity Command (body axis 'ij')	IN	—	—	.0025 IN	30/sec

Function:

Lateral A/P

Math Description:

$$\delta_{RC_1}^{(N)} = \left\{ G_{RC_1} [f_y^{(N)} + f_y^{(N-1)}] - \delta_{RC_1}^{(N-1)} [1.0 - 3 \frac{2}{7}] \right\} / [1.0 + 3 \frac{2}{7}]$$

$$\delta_{RC_2}^{(N)} = \left\{ G_{RC_2} [f_y^{(N)} [2.41 \frac{4}{7}] - \delta_{RC_2}^{(N-1)} [2.41 \frac{4}{7}]] - \delta_{RC_2}^{(N-1)} [2.0 - .482 \frac{4}{7}] - \delta_{RC_2}^{(N-2)} [2.41 \frac{4}{7} - 2.51 \frac{2}{7} + 1.0] \right\} / [2.41 \frac{4}{7} + 2.51 \frac{2}{7} + 1.0]$$

$$\delta_{RC_3}^{(N)} = \left\{ G_{RC_3} [R^{(N)} + R^{(N-1)}] - [1.0 - .3 \frac{2}{7}] \delta_{RC_3}^{(N-1)} \right\} / [1.0 + .3 \frac{2}{7}]$$

$$\delta_{RC_4}^{(N)} = \delta_R^{(N)}$$

Term	Description	Units	Accuracy	Range	Resolution	Sample Rate
δ_{RC_1}	Yaw Cyclic per roll rate	IN	-	-	.00025 IN	30/sec
δ_{RC_2}	Yaw Cyclic per Yaw Rate	IN	-	-	.00025 IN	30/sec
δ_{RC_3}	Yaw Cyclic per Side Slip	IN	-	-	.00025 IN	30/sec
δ_{RC_4}	Yaw Cyclic per Pedal Input	IN	-	-	.00025 IN	30/sec

Function:

Lateral A/P

Math Description:

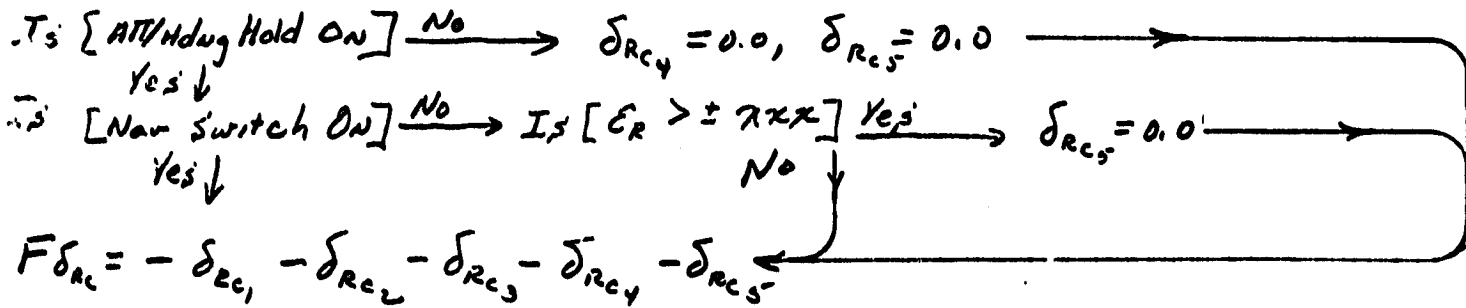
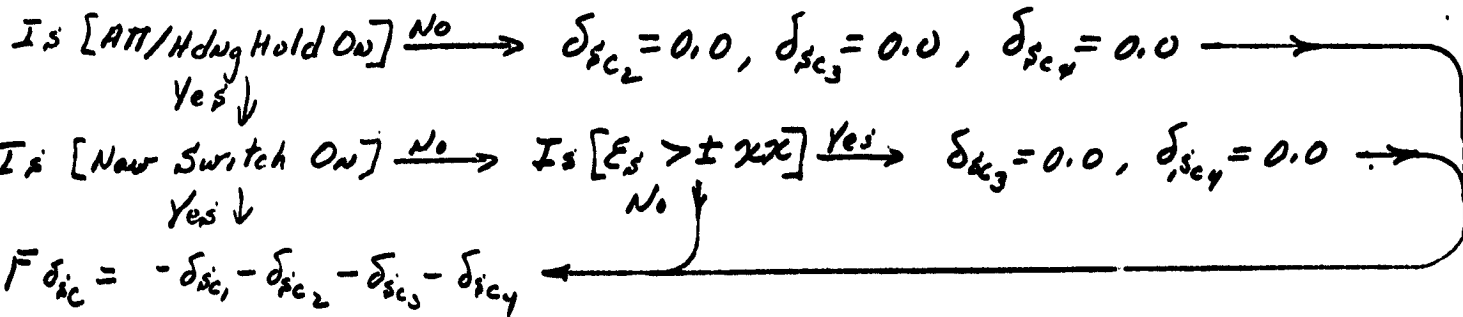
$$\delta_{RC5}^{(N)} = \left\{ K_{\psi} \left[\psi_{\delta}^{(N)} \left[.5 \frac{2}{T} + 1.0 \right] + \psi_{\delta}^{(N-1)} \left[1.0 - .5 \frac{2}{T} \right] \right] - K_{\psi} \left[\epsilon_{\psi}^{(N)} + \epsilon_{\psi}^{(N-1)} \right] - \delta_{\psi}^{(N-1)} \left[1.0 - .5 \frac{2}{T} \right] \right\} / \left[.5 \frac{2}{T} + 1.0 \right]$$

Term	Description	Units	Accuracy	Range	Resolution	Sample Rate
δ_{RC5}	Yaw Cyclic per Heading Synchronizer and Heading Command Input	IN	-	-	.00025 IN	30/Sec

Function:

Lateral A/P

Math Description:



Term	Description	Units	Accuracy	Range	Resolution	Sample Rate
$\bar{F}\delta_{ic}$	Total Roll Cyclic Command	IN	—	—	.00025 IN	30/sec
$\bar{F}\delta_{rc}$	Total Yaw Cyclic Command	IN	—	—	.00025 IN	30/sec

Function:

Lateral A/P

Math Description:

$$G_{\delta_{sc}}^{(N)} = \left\{ F_{\delta_{sc}}^{(N)} \left[.001375 \frac{4}{72} + .0037 \frac{2}{7} + 1.0 \right] + F_{\delta_{sc}}^{(N-1)} \left[2.0 - .00275 \frac{4}{72} \right] \right. \\ \left. + F_{\delta_{sc}}^{(N-2)} \left[.001375 \frac{4}{72} - .0037 \frac{2}{7} + 1.0 \right] - G_{\delta_{sc}}^{(N-1)} \left[2.0 - .00275 \frac{4}{72} \right] \right. \\ \left. - G_{\delta_{sc}}^{(N-2)} \left[.001375 \frac{4}{72} - .037 \frac{2}{7} + 1.0 \right] \right\} / \left[.001375 \frac{4}{72} + .037 \frac{2}{7} + 1.0 \right]$$

$$G_{\delta_{rc}}^{(N)} = \left\{ F_{\delta_{rc}}^{(N)} \left[.001375 \frac{4}{72} + .0037 \frac{2}{7} + 1.0 \right] + F_{\delta_{rc}}^{(N-1)} \left[2.0 - .00275 \frac{4}{72} \right] \right. \\ \left. + F_{\delta_{rc}}^{(N-2)} \left[.001375 \frac{4}{72} - .0037 \frac{2}{7} + 1.0 \right] - G_{\delta_{rc}}^{(N-1)} \left[2.0 - .00275 \frac{4}{72} \right] \right. \\ \left. - G_{\delta_{rc}}^{(N-2)} \left[.001375 \frac{4}{72} - .037 \frac{2}{7} + 1.0 \right] \right\} / \left[.001375 \frac{4}{72} + .037 \frac{2}{7} + 1.0 \right]$$

Term	Description	Units	Accuracy	Range	Resolution	Sample Rate
$G_{\delta_{sc}}$	First Filtered Function of Roll Cyclic	IN	—	—	.00025 IN	30/sec
$G_{\delta_{rc}}$	First Filtered Function of Yaw Cyclic	IN	—	—	.00025 IN	30/sec

Function:

Lateral A/P

Math Description:

$$\delta_{S_c}^{(N)} = \left\{ G_{\delta_{S_c}}^{(N)} + 2.0 G_{\delta_{S_c}}^{(N-1)} + G_{\delta_{S_c}}^{(N-2)} - \delta_{S_c}^{(N-1)} \left[2.0 - .00119 \frac{4}{T} \right] - \delta_{S_c}^{(N-2)} \left[.000595 \frac{4}{T} - .0244 \frac{2}{T} + 1.0 \right] \right\} / \left[.000595 \frac{4}{T} + .0244 \frac{2}{T} + 1.0 \right]$$

$$\delta_{R_c}^{(N)} = \left\{ G_{\delta_{R_c}}^{(N)} + 2.0 G_{\delta_{R_c}}^{(N-1)} + G_{\delta_{R_c}}^{(N-2)} - \delta_{R_c}^{(N-1)} \left[2.0 - .00119 \frac{4}{T} \right] - \delta_{R_c}^{(N-2)} \left[.000595 \frac{4}{T} - .0244 \frac{2}{T} + 1.0 \right] \right\} / \left[.000595 \frac{4}{T} + .0244 \frac{2}{T} + 1.0 \right]$$

Term	Description	Units	Accuracy	Range	Resolution	Sample Rate
δ_{S_c}	Second Filtered Function of Roll Cyclic	IN	—	—	.00025 IN	30/sec
δ_{R_c}	Second Filtered Function of Yaw Cyclic	IN	—	—	.00025 IN	30/sec

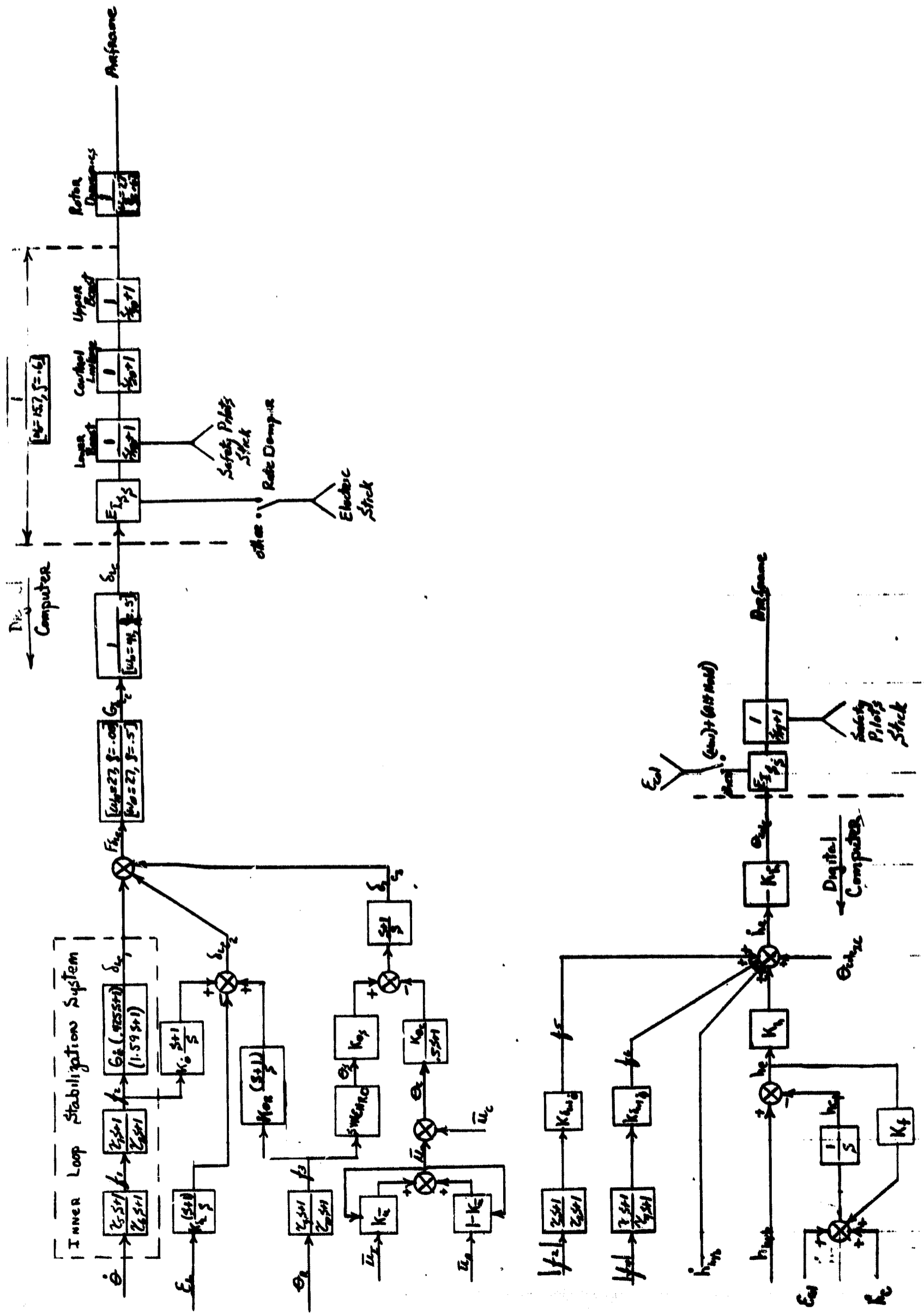


Figure C-1. AFCS Pitch Axis Mechanization Block Diagram

Fold out

4

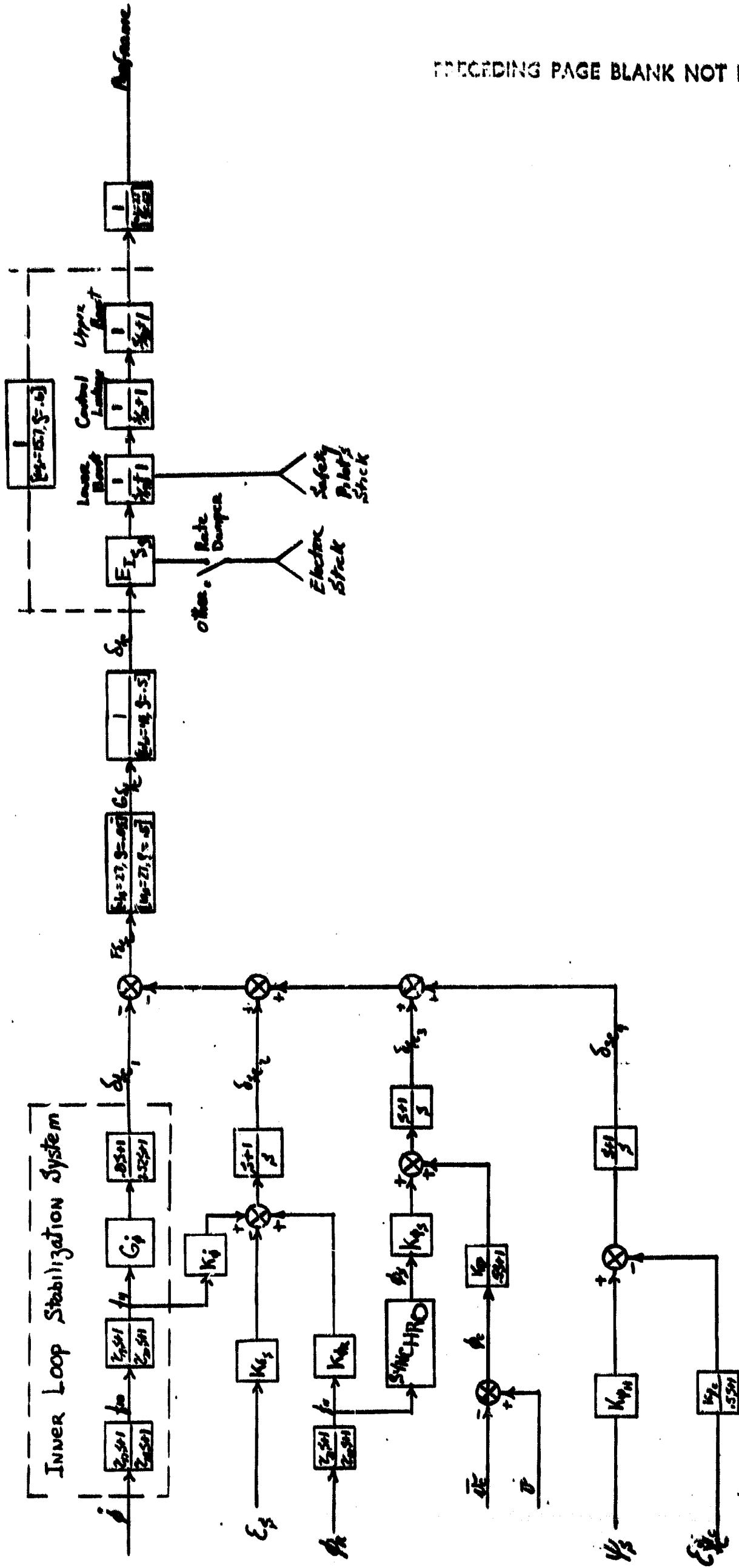


Figure C-2. AFCS Roll Axis Mechanization Block Diagram

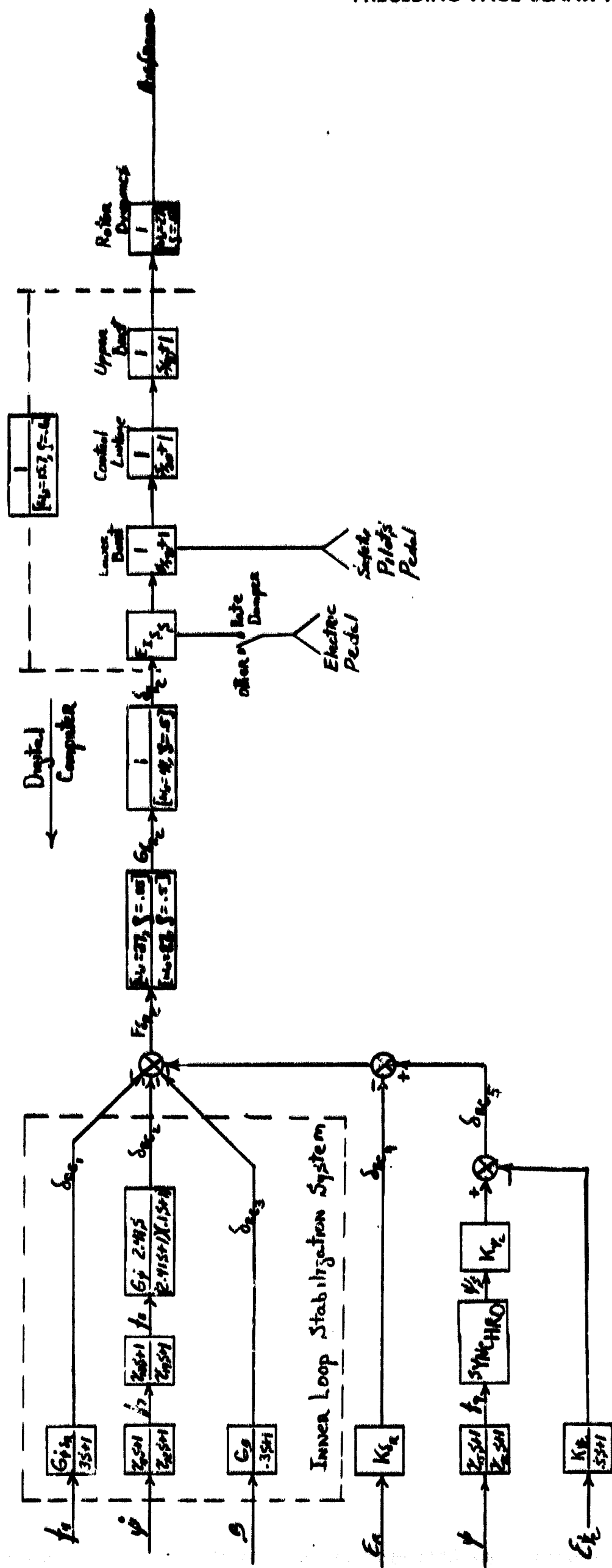


Figure C-3. AFCS Yaw Axis Mechanization Block Diagram

PRECEDING PAGE BLANK NOT FILMED.

APPENDIX D
QUADRATIC OPTIMAL CONTROL FOR THE
NASA LRC YHC-1A HELICOPTER

SUMMARY

Quadratic optimization methods were applied to synthesize a velocity control system for the YHC-1A helicopter. The resulting system was found to be tolerant of errors introduced by quantizing pitch angle and velocity signals which simulate measurements from a strapped-down inertial platform with pulse-rebalanced instruments.

Equations of Motion

The computer program (RAOPT) used to calculate the quadratic-optimal feedback gains accepts the equations of motion as a system of first-order equations written in the form

$$\dot{X} = F X + G_1 U + G_2 N \quad (D-1)$$

The feedback control U is found to be linear in the state so that $U = KX$. The program calculates the gain matrix K . The term $G_2 N$ represents a white-noise disturbance input. It is not used in the problem at hand so we put $G_2 = 0$. The response of the system is defined to be

$$R = H X + D U \quad (D-2)$$

The matrices H and D must be chosen to give proper meaning to the optimization of the quadratic integral

$$J = \int_0^{\infty} R' Q R dt \quad (D-3)$$

with suitable choices for elements in the weighting matrix Q . (Note that we may change H , D , and Q in ways which will not alter the performance index J .)

The simplest procedure is to consider the actuators as integrators, and hence their outputs are variables of the state of the system. The method then puts feedbacks around these integrators and converts them into simple lags. Whether the actual actuator dynamics alters the performance in an essential manner must then be determined on the simulation.

The vectors for the system state and the system response for the helicopter were taken as

$$X = \begin{bmatrix} u \\ w \\ \dot{\theta} \\ \theta \\ \delta_L \\ \theta_C \end{bmatrix}, \quad R = \begin{bmatrix} \dot{\theta} \\ \theta \\ \dot{x} \\ \dot{h} \\ \delta_{LF} + \delta_{LA} \\ \theta_{CF} + \theta_{CA} \end{bmatrix} \quad (D-4)$$

where

$$\begin{cases} \dot{x} = u + \theta_0 w \\ \dot{h} = \theta_0 u - w \end{cases} \quad (D-5)$$

and $\delta_{LF} + \delta_{LA}$, $\theta_{CF} + \theta_{CA}$ represent the total feedbacks split into two parts to isolate the contributions of the dynamical variables u , w , $\dot{\theta}$, θ from those of the actuator outputs δ_L and θ_C . In detail, the equations of motion are:

$$\frac{d}{dt} \begin{bmatrix} u \\ w \\ \dot{\theta} \\ \theta \\ \delta_L \\ \theta_C \end{bmatrix} = \begin{bmatrix} X_u/m & X_w/m & X_{\dot{\theta}}/m - U_0 & -g & X_{\delta_L}/m & X_{\theta_C}/m \\ Z_u/m & Z_w/m & Z_{\dot{\theta}}/m + U_0 & -\theta_0 g & Z_{\delta_L}/m & Z_{\theta_C}/m \\ M_u/l_{yy} & M_w/l_{yy} & M_{\dot{\theta}}/l_{yy} & 0 & M_{\delta_L}/l_{yy} & M_{\theta_C}/l_{yy} \\ 0 & 0 & 1.0 & 0 & 0 & 0 \\ 0 & 0 & 0 & 0 & \delta & 0 \\ 0 & 0 & 0 & 0 & 0 & 0 \end{bmatrix} \begin{bmatrix} u \\ w \\ \dot{\theta} \\ \theta \\ \delta_L \\ \theta_C \end{bmatrix} + \begin{bmatrix} 0 & 0 \\ 0 & 0 \\ 0 & 0 \\ 0 & 0 \\ 1 & 0 \\ 0 & 1 \end{bmatrix} \begin{bmatrix} \delta_{LF} + \delta_{LA} \\ \theta_{CF} + \theta_{CA} \end{bmatrix} \quad (D-6)$$

The feedback-control vector is then

$$U = \begin{bmatrix} \theta_{LF} \\ \theta_{CF} \end{bmatrix} + \begin{bmatrix} \theta_{LA} \\ \theta_{CA} \end{bmatrix} \cdot \begin{bmatrix} DU & DW & DTD & DT \\ TV & TW & TTD & TT \end{bmatrix} \begin{bmatrix} u \\ w \\ \delta \\ \theta \end{bmatrix} + \begin{bmatrix} DDL & DTC \\ TDL & TTC \end{bmatrix} \begin{bmatrix} \theta_L \\ \theta_C \end{bmatrix} \quad (D-7)$$

The expressions DU, DW, DTD, etc., are FORTRAN symbols for the gain constants computed by the optimization program. Matrices F and G₁ are displayed in equation (D-6). To get the response vector R, H, and D are taken as

$$H = \begin{bmatrix} 0 & 0 & 1 & 0 & 0 & 0 \\ 0 & 0 & 0 & 1 & 0 & 0 \\ 1 & \theta_0 & 0 & 0 & 0 & 0 \\ \theta_0 & -1 & 0 & 0 & 0 & 0 \\ 0 & 0 & 0 & 0 & 0 & 0 \\ 0 & 0 & 0 & 0 & 0 & 0 \end{bmatrix}, \quad D = \begin{bmatrix} 0 & 0 \\ 0 & 0 \\ 0 & 0 \\ 0 & 0 \\ 1 & 0 \\ 0 & 1 \end{bmatrix}$$

and then Q may be the diagonal matrix:

$$Q = \begin{bmatrix} QTD & & & & & 0 \\ & QT & & & & \\ & & QXD & & & \\ & & & QDL & & \\ 0 & & & & & QTC \end{bmatrix}$$

Control Configuration:

The resulting system is diagrammed in Figure D-1. Two notch filters of the form

$$\frac{s^2 + (30)^2}{s^2 + 2(0.3)30s + (30)^2}$$

were added as shown to see if they reduced the system performance. (They did not.)

For simplicity it was decided to command u and w rather than \dot{x} and \dot{h} as called for in the response vector R . This introduced a small discrepancy and it should be removed on further study. Feed-forward terms DWC and TUC shown in Figure D-1 were added to re-establish the proper steady-state values. In spite of this, qualitative conclusions of the study are valid.

Optimal Gains:

Gains computed for various choices of the elements of the weighting matrix Q are listed in Table D-1. It takes between 10 and 20 seconds for RAOPT to compute a set of gains for this sixth-order system on the Honeywell H1800 computer.

The step size for the difference equation corresponding to equation (D-1) was taken as 0.05 or 20 steps a second. The simulation was run at 30 steps a second. It was found that the gains computed at 10, 20 and 50 steps did not differ greatly, so this inconsistency is ignored.

The basic weighting of the variables, Cases 1, 9 and 12 in Table D-1, were chosen from the analog scalings (Figure D-2) which seemed to give uniform signal levels in the analog simulation. The gains of these cases were found to be satisfactory. The assumption leading to this choice is that the optimal gains will make all terms of the performance index of the same order of magnitude.

The Simulation:

The aircraft was simulated on an analog computer and the control computation was performed on the SDS 9300. Figure D-2, Table D-2 and Figure D-3 record the analog diagram, potentiometer settings used, and the digital FORTRAN program.

The pitch angle was quantized to 0.0035 degree of arc, horizontal and vertical velocities to 0.25 feet per second. Pitch rate, when quantization on pitch was used, was computed as the change in pitch divided by the time for a cycle. In a separate study, Lagrangian polynomials of second, third and fourth orders were used to calculate the derivative of pitch angle. The FORTRAN formulas

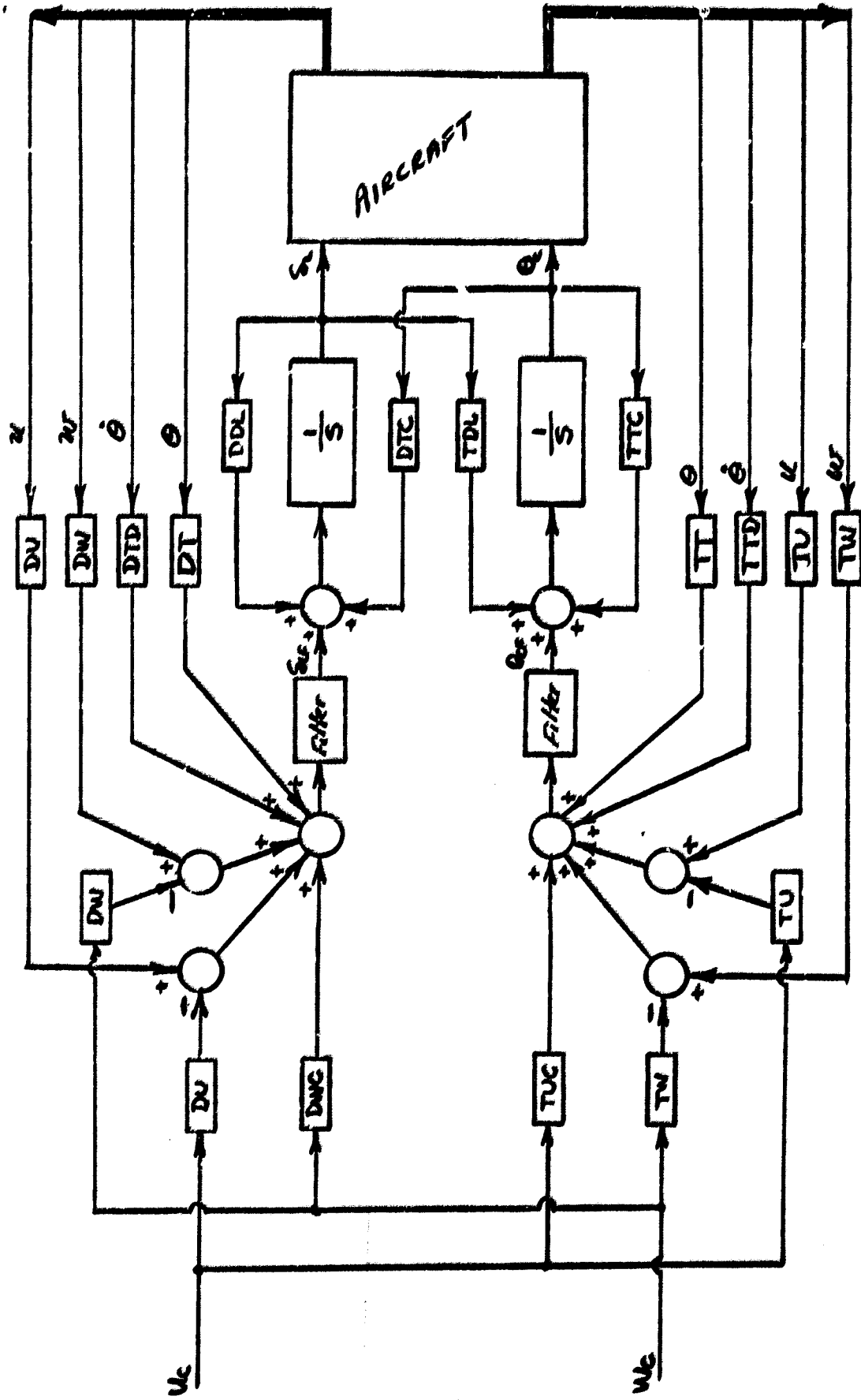


Figure D-1. Control Configuration

TABLE D-1
FEEDBACK GAINS

Case	FC	Step	PTD	PT	QXD	QHD	QDL	QTC	DJ	DW	DTD	DT	DDL	DTC	TU	TW	TTD	TT	TPL	TTC
1	100K	.05	1000	1000	1	.04	1	1000	.59	-.23	-37.	-42.	-5.0	-54.	.018	.0007	-.60	-1.5	-.05	-2.3
2	100K		1000	1000	1	.04	5	1000	.17	-.13	-15.7	-10.9	-3.0	-24.	.024	-.0025	-1.1	-2.0	-.12	-3.2
3	100K		1000	1000	1	.04	10	1000	.082	-.10	-10.1	-9.4	-2.3	-15.	.026	-.0025	-1.3	-2.1	-.15	-3.5
4	100K		1000	1000	1	.01	1	1000	.64	-.17	-35.	-45.	-4.7	-62.	.016	-.0010	-.65	-1.3	-.065	-2.0
5	100K		1000	1000	1	1	1	1000	.50	-.74	-51.	-35.	-6.7	-27.	.021	.013	-.14	-1.7	-.023	-3.0
6	100K		1000	1000	1	1	10	1000	.087	-.34	-30.	-10.	-4.3	-20.	.022	-.0010	-2.3	-3.5	-.19	-5.3
7	100K		1000	1000	1	1	10	1000	.094	-.34	-29.	-6.5	-4.3	-19.	.024	-.0025	-2.5	-2.5	-.19	-5.0
8	100K		1000	1000	1	1	10	1000	.086	-.33	-35.	-4.9	-4.1	-15.	.026	.0022	-1.1	-2.2	-.14	-3.8
9	60K		1000	1000	1	.04	1	1000	.67	-.22	-36.6	-15.6	-4.7	-18.	.018	.0014	-.53	-1.3	-.019	-2.2
10	60K		1000	1000	1	.04	5	1000	.23	-.14	-15.6	-14.5	-2.9	-21.	.025	-.0025	-1.0	-1.8	-.10	-3.8
11	60K		1000	1000	1	.04	10	1000	.12	-.11	-10.3	-7.7	-2.3	-13.	.027	-.0025	-1.2	-2.0	-.13	-3.1
12	100V		1000	1000	1	.04	1	1000	.76	.085	-44.	-62.	-5.0	-17.	.0027	.0018	-.20	-2.3	-.017	-1.6
13	100V		1000	1000	1	.04	5	1000	.33	.021	-23.	-30.	-3.6	-9.9	.0065	.0052	-.46	-.63	-.017	-1.7
14	100V		1000	1000	1	.04	10	1000	.21	.0077	-17.	-21.	-3.1	-7.6	.0083	.0052	-.64	-.86	-.07	-1.8
15	100K		Compressed Gains						.7	-.2	-40	-50	-5	-40	.005	.005	-.6	-1.5	0	-2.0
16	100V								.7	-.2	-40	-50	-5	-40	.005	.005	-.6	-1.7	0	-2.0

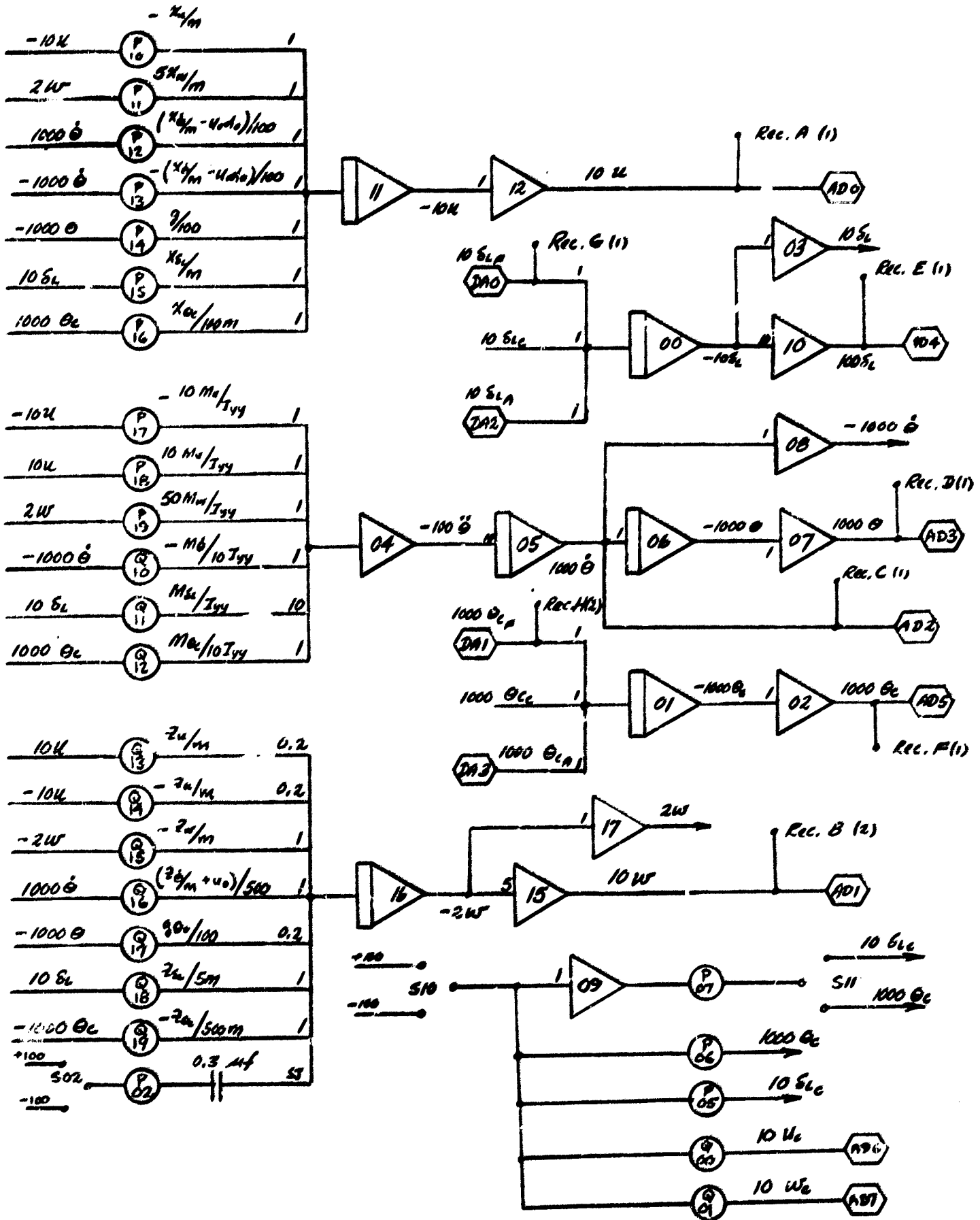


Figure D-2. Analog Diagram

TABLE D-2
POTENTIOMETER SETTINGS

Quantity	Pot	60K	100K	100K
$-x_u/m$	P10	0252	0325	0152
$5x_u/m$	P11	2135	3205	3185
$(x_b/m - u_s)/100$	P12	0105	0000	0000
$-(x_b/m - u_s)/100$	P13	0000	0160	0535
$g/100$	P14	3220	3220	3220
x_{su}/m	P15	1750	2130	1810
$x_{sc}/100m$	P16	4361	2507	2047
$-10M_u/I_{yy}$	P17	0000	0511	0299
$10 M_u/I_{yy}$	P18	0437	0000	0000
$50 M_u/I_{yy}$	P19	0888	9000	9100
$-M_b/10I_{yy}$	Q10	0590	1093	1175
M_b/I_{yy}	Q11	2950	3440	3805
$M_{sc}/10I_{yy}$	Q12	1520	6260	7290
z_u/m	Q13	0457	0000	0338
$-z_u/m$	Q14	0000	0283	0000
$-z_w/m$	Q15	2830	5790	7120
$(z_b/m + u_s)/500$	Q16	0007	2027	3372
$g\theta/100$	Q17	0526	0282	0134
$z_{su}/5m$	Q18	0101	0738	0420
$-z_{sc}/500m$	Q19	5176	5614	6490

ΔFORTRAN LS.G0.

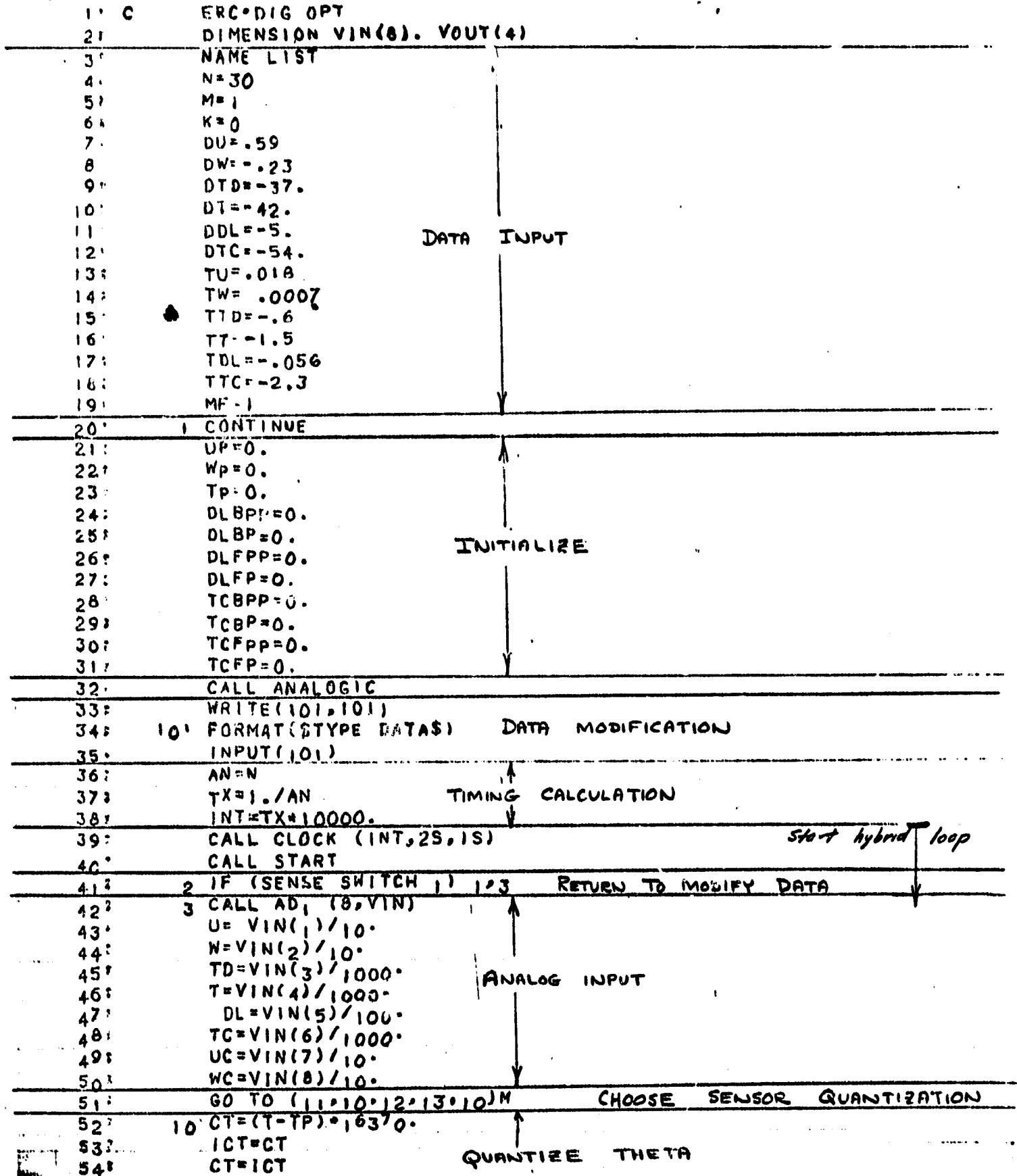


Figure D-3. Digital Program

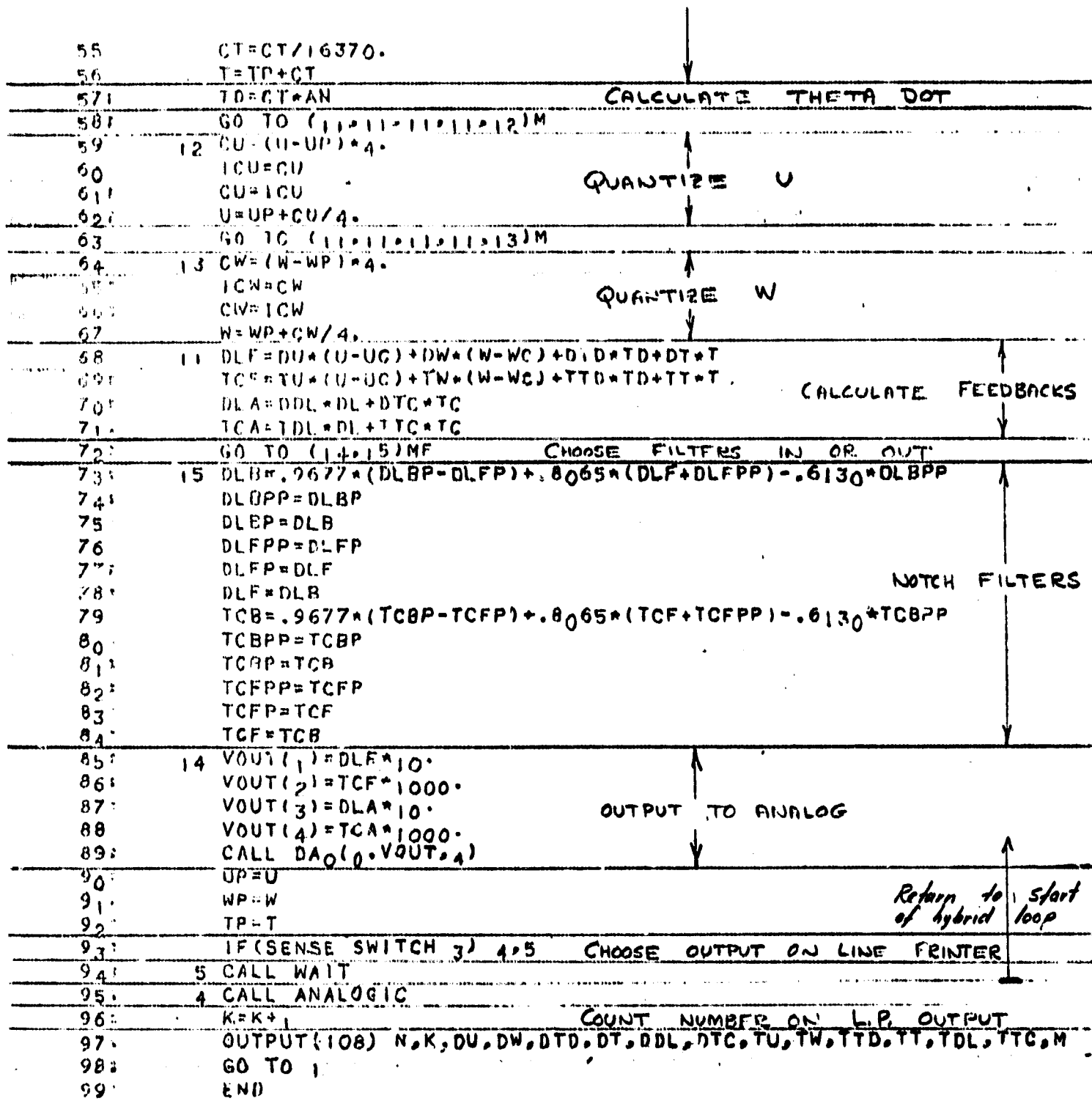


Figure D-3. Digital Program (Concluded)

compared were:

$$TD = CT * AN \text{ (difference)}$$

$$TD = (3. * CT - CTP) * AN/2. \text{ (second)}$$

$$TD = (11. * CT - 7. * CTP + 2. * CTPP) * AN/6. \text{ (third)}$$

$$TD = (25. * CT - 23. * CTP + 12. * CTPP - 3. * CTPPP) * AN/12. \text{ (fourth)}$$

(CT, CTP, etc., represent changes in theta in the current and past cycles. AN is the frequency in cycles per second.)

The higher-order formulas did not improve the performance of the system.

Results:

Computer traces are shown in Figures D-4, D-5, and D-6. The system with optimal gains from Case 12 at hover is represented in Figure D-4. The effect of the quantization of all three signals and of the notch filters may be seen by comparing the first and third traces with the second and fourth. The response to a step vertical gust is shown in the fifth trace. The optimal gains of Case 1 were found to give satisfactory results at the 100-knot flight condition. The corresponding traces are omitted.

In Figures D-5 and D-6, the performances of the system with the gains of Case 16 at hover and with the gains of Case 15 at 100 knots are represented. Again, the system without or with quantization and filters may be studied. These gains were found by slightly modifying the 100-knot optimal and then trying to make the gains at hover as close as possible to the 100-knot case. As can be seen from the traces, the 100-knot case has been favored. Only two gains change. These are DTC and TT. The change of DTC most likely can be eliminated on another iteration of the study, and it is possible that the change in TT may be removed, also. However, the transient coupling of the u- and w-commands is somewhat high, particularly at hover, and this may be improved at the expense of more gain changing.

The system is tolerant to the effects of the signal quantization used in the study. It may be too slow in its response to step commands, and a further study with different Q-weightings may be necessary to achieve the system desired.

REPRODUCIBILITY OF THE ORIGINAL PAGE IS POOR.

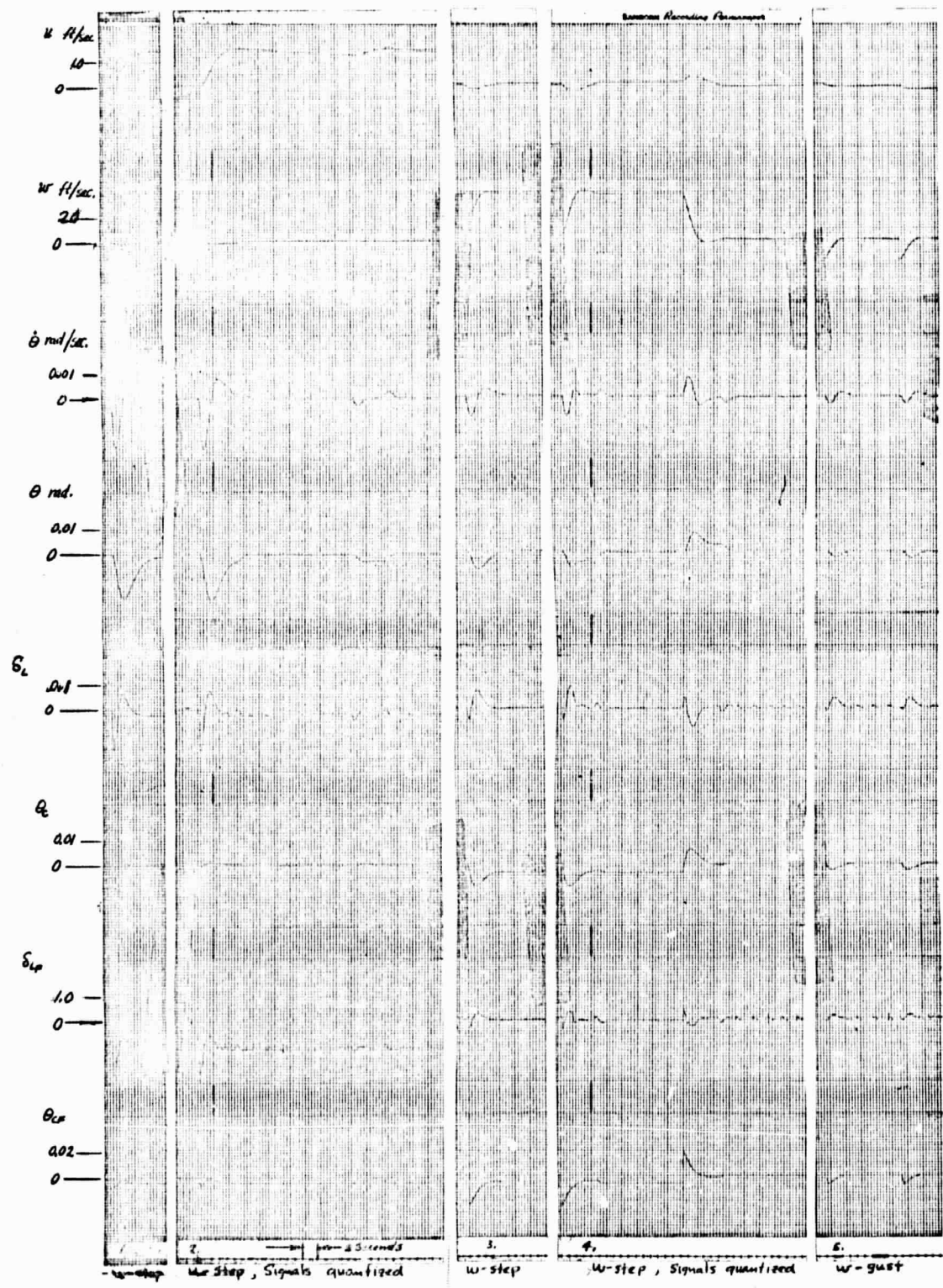


Figure D-4. Optimal Control No. 12 at Hover

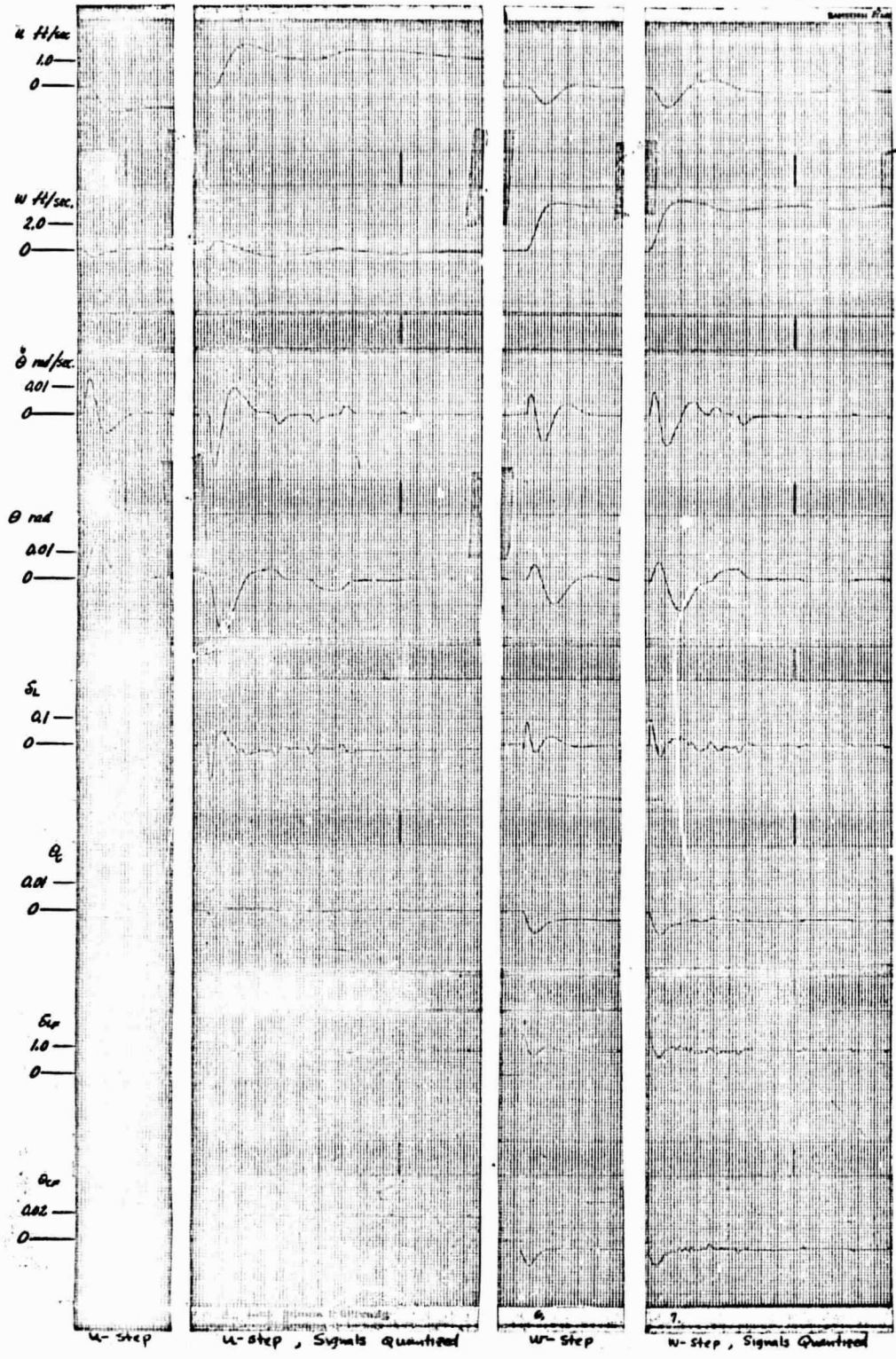


Figure D-5. Compromised Control No. 16 at Hover

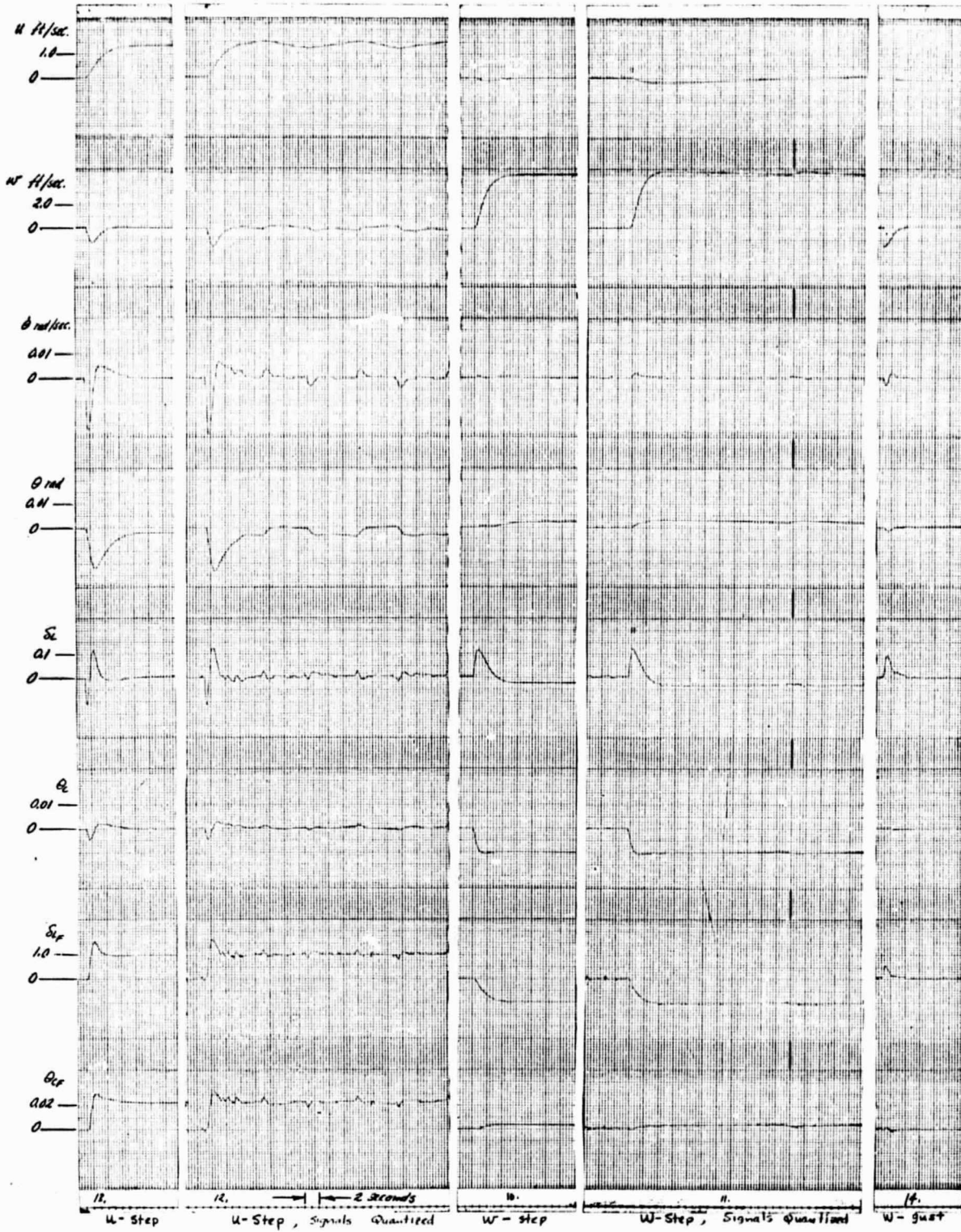


Figure D-6. Compromised Control No. 15 at 100 Knots

APPENDIX E
BASELINE DISPLAY EQUATIONS ^{1, 2}

Function: **Displays**

Math Description:

Quantities listed are obtained from navigation, guidance, or AFCS computations.

Term	Description	Units	Accuracy	Range	Resolution	Sample Rate
\bar{U}_c	Longitudinal Velocity Command	Knots				8 Hz
\bar{V}_c	Lateral Velocity Command	knots				↓
E_{jc}	Lat. Vel. error w.r.t. Course	knots				
\dot{h}_c	Altitude rate Command	ft/sec				
N_A	Aircraft Position-North	feet				
E_A	Aircraft Position-East	feet				
N_i E_i	} North & East Coord. of Command Course Intersections	feet				

¹ Accuracy, range, and resolution are per navigation, guidance, and control requirements.

² All outputs are read out at 64 Hz.

Function: Displays

Quantities listed are obtained from navigation, guidance, or AFCS computations.


Term	Description	Units	Accuracy	Range	Resolution	Sample Rate
ψ	Actual Heading	deg				8 Hz
θ	Elevation Angle	deg				16 Hz
ϕ	Roll Angle	deg				16 Hz
h_a	Altitude	ft				8 Hz
\dot{h}_a	Altitude Rate	ft/sec				16 Hz
h_R	Altitude - Radar	ft				8 Hz
\dot{h}_R	Altitude Rate - Radar	ft/sec				16 Hz
h_D	Altitude Commanded	ft				8 Hz
β_i	Decaying	deg				
V_G	Ground Speed	knots				
ψ_f	Final Approach Hdg	deg				
R_{S0}	Range to start turn	ft				
t_{S0}	Time to start turn	sec				
δ	Landing Site Wind	deg				
\bar{u}_{AP}	Pilot selected airspeed	knots				
h_{c0}	Pilot selected approach alt.	feet				
E_G	Pilot selected glide angle	deg				
h_F	Pilot selected hover alt.	feet				
β_{cp}	Pilot selected checkpt. bearing	deg				
ψ_c	Pilot selected heading Com.	deg				

REPRODUCIBILITY OF THE ORIGINAL PAGE IS POOR

Function: Forward velocity error

Math Description:

$$\begin{aligned} (\Delta \bar{u})_m = & \frac{(T+2\tau_1)(\bar{u}_c - \bar{u}_n) + (T-2\tau_1)(\bar{u}_c - \bar{u}_{n-1}) - (T-2\tau_1)(\Delta \bar{u}_D)_{n-1}}{T+2\tau_1} \\ & - K \frac{T(\dot{\theta}_n + \dot{\theta}_{n-1}) - (T-2\tau_1)(\Delta \bar{u}_D)_{n-1}}{T+2\tau_1} \end{aligned}$$

Term	Description	Units	Accuracy	Range	Resolution	Sample Rate
\bar{u}_c	Command velocity	ft/sec				8 Hz 
T	Sample period	sec				
N	Constant	None				
τ_1	Constant	sec				
τ_2	Constant	sec				
\bar{u}	Horizontal velocity - either \bar{u}_A or \bar{u}_I	ft/sec				
$\dot{\theta}$	AFC's Pitch Rate	deg/sec				

Function: Lateral velocity error

Math Description:

$$E_{y_{err}} = \frac{(k_1 T_1 + k_2 T_2) V_{err} - (T_1 T_2) \dot{\phi}}{T_1 T_2}$$

$$- k_1 \frac{V_{err} + \dot{\phi} T_1 - (T_1 T_2) \dot{\phi}}{T_1 T_2}$$

$$- k_2 \frac{V_{err} + \dot{\phi} T_2 - (T_1 T_2) \dot{\phi}}{T_1 T_2}$$

V_{err}	N	T_1	K_1	K_2
$\dot{\phi}$	N	T_1	0	(K_1)
Lateral Velocity Error	Knots	$K_1 V_{err}$	$K_2 V_{err}$	$K_2 V_{err}$
Yaw Rate	N	(T_1)	(K_1)	0

Term	Description	Units	Accuracy	Range	Resolution	Sample Rate
$E_{y_{err}}$	Lateral Velocity Error	ft/sec				8 Hz
T	Sample Period	sec				
N	Scheduled Count	count				
K_1	↓	ft/sec/deg				
K_2		ft/sec/deg				
T_1		sec				
T_2		sec				
V_{err}	airspeed	ft/sec				
$\dot{\phi}$	Roll Rate	deg/sec				
$\ddot{\phi}$	APCS Roll Rate	deg/sec				

Function: Altitude rate error

Math Description:

$$e_{alt} = \frac{(T - T_{int}) (h_c - h_{i-1}) - (T - T) (h_0)_{i-1}}{T_{int}}$$

Term	Description	Units	Accuracy	Range	Resolution	Sample Rate
h_c	Altitude Command	ft/sec				16 Hz
h_i	Altitude Actual Alt.	ft/sec				↓
T	Sample Period	sec				
n	Count	none				
T	Interval	sec				

Function: Heading error

Math Description:

$$\psi_n = \frac{(T+2\tau_1)(\psi_c - \psi) + (T-2\tau_1)(\psi_c - \psi) - (T-2\tau_1)(\Delta\psi_D)_{n-1}}{T+2\tau_1}$$

$$-K_1 \frac{T(\dot{\psi}_n + \dot{\psi}_{n-1}) - (T-2\tau_2)(\Delta\psi_D)_{n-1}}{T+2\tau_2}$$

V_{IAS}	N	K_1
$< (V_{IAS})_1$	N_1	$(K_1)_1$
$(V_{IAS})_1 \pm V_{IAS} \pm (V_{IAS})_2$	$K_N V_{IAS}$	$K_N V_{IAS}$
$> (V_{IAS})_2$	N_2	\sim

Term	Description	Units	Accuracy	Range	Resolution	Sample Rate
ψ_c	Heading Command	deg				8 Hz
ψ	Actual Heading	deg				
T	Sample Period	sec				
N	Scheduled Constant	none				
K_1	Scheduled Constant	sec				
V_{IAS}	Airspeed	ft/sec				↓


Function: Range to course intersection/landing site

Math Description:

$$\Delta N = N_A - N_i \quad \Delta E = E_A - E_i$$

$$\Delta h = h_{CO} - h_{NAV}$$

$$R_H = \sqrt{(\Delta N)^2 + (\Delta E)^2}$$

Term	Description	Units	Accuracy	Range	Resolution	Sample Rate
N_A	Airc. Position - N					$8' \text{ Hg}$ 
E_A	Airc. Position - E					
h_{NAV}	Airc. Altitude					
N_i	Check point Pos. - N					
E_i	Check point Pos. - E					
h_{CO}	Pilot set altitude					

Function: Local wind

Math Description:

$$V_{w_{c,t}} = - \bar{U}_A \sin(\Psi_A - \Psi_G)$$

$$V_{w_x} = V_G - \bar{U}_A \cos(\Psi_A - \Psi_G)$$

$$V_w = \sqrt{(V_{w_{c,t}})^2 + (V_{w_x})^2}$$

$$\Delta \psi_w = 2\pi \cdot \frac{V_{w_{c,t}}}{V_{w_x}}$$

$$\psi_w = \psi_A - \psi_G$$

Term	Description	Units	Accuracy	Range	Resolution	Sample Rate
\bar{U}_A	Airc. Horiz. Velocity	knots				8-Hz
Ψ_A	Aircraft Heading	deg				↓
Ψ_G	Ground Track Hdq	deg				
V_G	Ground Speed	knots				

Function: Predicted position

Math Description:

$$\Delta X = + K_{\bar{u}_s} \bar{u}_s + K_{\theta} \theta + K_{\dot{\theta}} \dot{\theta}$$

$$\Delta Y = + K_{\dot{Y}_A} \dot{Y}_A + K_{\Phi} \Phi + K_{\dot{\Phi}} \dot{\Phi}$$

$$N_{\phi} = N_A + \Delta X \cos \Psi - \Delta Y \sin \Psi$$

$$E_{\phi} = E_A + \Delta X \sin \Psi + \Delta Y \cos \Psi$$

R_H	$K_{\bar{u}_s}$	$K_{\dot{Y}_A}$	K_{θ}
$< (R_H)_1$	$K_1 \times R_H$	$K_2 \times R_H$	0
$(R_H)_1 \leq R_H \leq (R_H)_2$	$K_1 \times R_H$	$K_2 \times R_H$	$K_3 \times R_H$
$> (R_H)_2$	$(K_{3,1})$	$(K_{3,2})$	$(K_{3,3})$

Term	Description	Units	Accuracy	Range	Resolution	Sample Rate
N_A	Aircraft Position-North					16 Hz ↓
E_A	Aircraft Position-East					
\bar{u}_s	Aircraft Ground speed					
θ	Elevation Angle					
$\dot{\theta}$	Pitch Rate					
Φ	Roll Angle					
\dot{Y}_A	Aircraft cross course velocity					
$\dot{\Psi}_A$	Aircraft Heading					
R_H	Horizontal Range to or landing site					
$K_{\bar{u}_s}$	Scheduled Constants					
$K_{\dot{Y}_A}$	↓					
K_{θ}						
$K_{\dot{\theta}}$						

PRECEDING PAGE BLANK NOT FILMED.

APPENDIX F DOWN LINK DESCRIPTION

The baseline AALS is defined as using the Gemini PCM programmer as the link with the computer subsystem. It has the capability for operating as a self-contained data-handling unit. Internally it provides the functions of analog data multiplexing, analog-to-digital conversion, and digital-data multiplexing, including the required timing to perform these functions. The outputs of this programmer consist of two PCM data signals: 51.2 kilobits/second (kbps) data in NRZ-C form and 5.12 kbps data in RZ form. A frame of data from the PCM programmer consists of the following channels:

<u>No. of channels</u>	<u>Type of signal</u>	<u>Sample rate, samples/sec</u>	<u>Bits per sample</u>
6	0-20 mV	640	8
6	0-20 mV	160	8
9	0-20 mV	80	8
3	0-5 V	40	8
3	0-5 V	20	8
6	0-5 V	10	8
32	0-5 V	1.25	8
40 (corr. to 5 ea. 8-bit words)	Bilevel	10	1
24	Digital (computer)	0.416	24
1	Time	10	8

The basic sample rate of the commutator is 40 samples per second. The main frame consists of 160 word slots with 8 bits per word. Six of the 160 words are used for frame synchronization; thus 154 word slots are available for data. The complete Gemini DTS system provided for over 300 input channels by using low-speed subcommutation.

The airborne computer and time reference system (TRS) supply the digital data inputs to the programmer. The Gemini computer output is 21 words of 24 bits length each, and the TRS output is 3 words of 24 bits each. These digital data words are transferred serially from the computer into a buffer storage register internal to the programmer. This serial transfer is accomplished as follows. At the proper time for sampling the computer data, the PCM programmer sends a request pulse to the computer for a data word. The computer provides 24 clock pulses to the programmer to transfer into the buffer storage register the 24-bit computer data word available to the programmer. The Gemini computer clocks this data into the programmer at

a 500-kHz rate. The programmer unloads the buffer storage register in 8-bit groups at a 51.2-kbps rate. The programmer sends request pulses to the computer for a 24-bit word every 75 milliseconds until 21 computer words have been read into the programmer. The computer clock and data output lines are isolated from the programmer by transformers located in the computer.

The Gemini PCM programmer has some flexibility in the areas of increasing the number of digital channels, increasing the frequency of sampling the digital channels, or increasing the length of the digital words. There are some basic constraints which are applicable to any PCM system used in a vhf transmit link. The most severe limitation is the bit rate for an NRZ code which is 150 kbps maximum. This means the present frame format could be increased by a factor of 3 either in number of word slots or in sampling speed. If the length of the computer words is increased above 24 bits, then the buffer storage register will require additional shift registers, and the format will be changed to 32 bits per digital word (the next multiple of 8). As an example, if the computer word were increased from 24 to 28 bits, the number of computer words were increased from 21 to 40, and the sample rate were increased from 0.416 sample/sec to 40 samples/sec, the computer data words alone would require 160 main frame word slots. This exceeds the 154 words available at 40 samples/sec in the present PCM system. Thus, it is apparent that the number of words in a frame would have to be increased or some other tradeoff between sample rate and the number of computer words read out would be necessary. Another consideration in the computer/PCM programmer interface is the rate at which the computer must clock data into the programmer storage register. The present clock rate of 500 kHz can be increased to 1.0 MHz.

Based on data requirements known at this time (Table F-1), it does not appear feasible to modify the existing Gemini PCM programmer to satisfy these requirements. The digital and analog data requirements must be defined in light of the constraints cited above. Consideration should be given to supplying the digital data signals to the programmer in serial form rather than parallel form.

**TABLE F-1
DIGITAL SIGNALS FOR DATA TRANSMISSION
FROM CENTRAL COMPUTER**

Signal	No. of words	Transmissions per second
Direction cosine matrix	9	computation rate
Sum of XYZ accelerometer counts	3	$1/\Delta t$
Sum of XYZ gyro counts	3	$1/\Delta t$
Flight time	1	$1/\Delta t$
Computation cycle time	1	computation rate
XYZ position and velocity (radar frame)	6	1
XYZ position and velocity (IMU frame)	6	1
XYZ position and velocity (estimator frame)	6	1
Latitude and longitude	2	1
Gyro scaling (bilevel)	1	$1/\Delta t$
Altimeter output	1	5
XY area/navigation (Z sources)	4	1
Euler angles	3	5
Body-axis angular rates	3	5
Guidance velocity commands	3	5

RECORDING PAGE BLANK NOT FILMED.

**APPENDIX G
NEW TECHNOLOGY**

After a diligent review of the work performed under this contract, no new innovation, discovery, improvement, or invention was made.

MISSING PAGE BLANK NOT FILMED.

REFERENCES

- 1) Fryer, W. D. and Schultz, W. C. : A Survey of Method for Digital Simulation of Control Systems. Cornell Aero. Lab. No. XA-1681-E-1, July 1964.
- 2) Anon. : Advanced Flight Control System Concepts for VTOL Aircraft. Phase I Technical Report, TRECOM TR 64-50, October 1964.
- 3) Garren, Jr., J. F. and Kelly, J. R. : Description of an Analog Computer Approach to V/STOL Simulations Employing a Variable Stability Helicopter, NASA TN D-1970, January 1964.